Final Report

Contract No. NASr-65(02)
IITRI Project No. M272

STUDIES OF LUNAR SOIL MECHANICS

by

E. Vey and J. D. Nelson

for

National Aeronautics and Space Administration
Washington 25, D.C.

July, 1963

IIT RESEARCH INSTITUTE
Technology Center - Chicago, Illinois

4247300

Final Report

(NASA Contract No. NASr-65(02);
IITRI Project No. M272)

STUDIES OF LUNAR SOIL MECHANICS

by

E. Vey and J. D. Nelson

for

National Aeronautics and Space Administration
Structures and Operations Problem Group
Space Vehicles Division
Washington 25, D.C.

July, 1963

100 pp ~ 7 refs

(NASA CR-50930) OTS: $ 8.60 ph, $3.20 mf

PREFACE

This report represents the final report on Phase I of IIT Research Institute (formerly Armour Research Foundation of Illinois Institute of Technology) project no. M272, sponsored by National Aeronautics and Space Administration under contract no. NASr-65(02). The work reported was performed during the period June 15, 1962 to June 15, 1963. Persons who contributed materially to this work are: A. Ketterer, R. J. Larson, J. D. Nelson, E. Vey, N. A. Weil and R. Yong.

Respectfully submitted,
IIT RESEARCH INSTITUTE

E. Vey
Project Engineer

APPROVED:

J. W. Dally
Assistant Director

ABSTRACT

21044

To provide basic engineering data on the behavior of soils under lunar environmental conditions, experiments were performed to determine the properties of soils under atmospheric pressures and vacuum levels up to the 10^{-10} torr range. Three different soil samples were used, 1) silica flour having 90 per cent of the particles between 2 and 26μ, 2) ground olivine having 90 per cent of the particles between 2 and 60μ, 3) ground olivine having 90 per cent of the particles between 0.7 and 15μ.

Experiments consisted primarily of the determination of the vacuum in soil pores in relation to chamber vacuum, the porosity attained by deposited soil, shear strength parameters and load-settlement relationships on small loaded areas.

It was observed that the vacuum in the soil pores was considerably less than that recorded in the chamber. Porosities attained by soil deposited under low vacuums (1 to 10^{-3} torr) were less than those attained in atmosphere but at higher vacuum levels the porosity increased with an increase in vacuum, and in the case of silica flour for vacuums of 10^{-7} torr or higher it was greater than when deposited in atmosphere. Direct shear tests showed that the apparent cohesion and the internal friction of the silica flour increased under vacuum. This was also evidenced by increased bearing capacity. The internal friction of the olivine also increased under vacuum but its apparent cohesion appeared to decrease.

The increase in porosity in both soils and the effects on the apparent cohesion were attributed to the development of interparticle forces. These forces may be either attractive or repulsive depending on the mineralogical composition of the soil and the vacuum level.

TABLE OF CONTENTS

Section		Page
I.	INTRODUCTION	1
II.	THE NATURE OF THE LUNAR SURFACE	2
III.	PREVIOUS STUDIES OF LUNAR SOIL MECHANICS	9
IV.	DESCRIPTION OF REPRESENTATIVE LUNAR SOIL	12
V.	VACUUM IN SOIL PORES IN RELATION TO CHAMBER VACUUM	15
VI.	CHARACTERISTICS OF SOIL DEPOSITED UNDER VACUUM	21
	A. Porosity Attained by Silica Flour	24
	B. Porosity Attained by Coarse Grained Olivine	27
	C. Porosity Attained by Fine Grained Olivine	30
	D. Effect of Grain Size on Porosity	30
	E. Angle of Repose of Material Deposited Under Vacuum	33
	F. General Behavior of Soil Under Vacuum	35
VII.	DETERMINATION OF SHEAR STRENGTH PARAMETERS UNDER VACUUM	39
	A. Results of Direct Shear Tests on Silica Flour	46
	B. Results of Direct Shear Tests on Olivine	46
	C. General Observations in Direct Shear Tests	51
VIII.	BEARING CAPACITY OF SMALL FOOTINGS	55
IX.	IRREVERSIBLE EFFECTS OF VACUUM	68
X.	DISCUSSION OF RESULTS	73
	A. Interparticle Forces	73
	B. Intergranular Friction	76
	C. Temperature Effects	77
	D. Bearing Capacity	77
XI.	CONCLUSIONS	78
	BIBLIOGRAPHY	81
	APPENDIX - VACUUM FACILITIES	A-1

LIST OF ILLUSTRATIONS

Figure		Page
1	PHOTOGRAPH OF CRATER ARISTILLUS (6)	4
2	GRAIN SIZE ACCUMULATION CURVES FOR REPRESENTATIVE LUNAR SOILS	13
3	TEST ARRANGEMENT FOR PORE AIR PRESSURE MEASUREMENTS	16
4	CHAMBER PRESSURE AND PORE AIR PRESSURE AS A FUNCTION OF DRAWDOWN TIME	17
5	PRESSURE NEAR SOIL AS A FUNCTION OF CHAMBER PRESSURE AND TIME	19
6	SOIL IN APPARATUS PRIOR TO DEPOSITION UNDER HARD VACUUM	22
7	SOIL AFTER DEPOSITION UNDER HARD VACUUM	22
8	VACUUM ACHIEVED IN CHAMBER AS A FUNCTION OF DRAWDOWN TIME BEFORE, DURING AND AFTER DEPOSITION OF SILICA FLOUR	23
9	POROSITY OF SILICA FLOUR DEPOSITED UNDER VACUUM AS A FUNCTION OF PRESSURE	25
10	SILICA FLOUR DEPOSITED IN ATMOSPHERE	26
11	SILICA FLOUR DEPOSITED IN ULTRA-HIGH VACUUM	26
12	POROSITY OF COARSE OLIVINE FLOUR DEPOSITED UNDER VACUUM AS A FUNCTION OF PRESSURE	28
13	COARSE GRAINED OLIVINE DEPOSITED IN ATMOSPHERE	29
14	COARSE GRAINED OLIVINE DEPOSITED IN ULTRA-HIGH VACUUM	29
15	INDIVIDUAL OLIVINE GRAINS	31
16	CLUSTER OF OLIVINE GRAINS FORMED DURING DEPOSITION IN VACUUM	31

List of Illustrations (con't)

Figure		Page
17	POROSITY OF FINE OLIVINE FLOUR DEPOSITED UNDER VACUUM AS A FUNCTION OF PRESSURE	32
18	POROSITY AS A FUNCTION OF GRAIN SIZE FOR SILICA DEPOSITED IN ATMOSPHERE.....	34
19	ANGLE OF REPOSE OF SILICA FLOUR AS A FUNCTION OF PRESSURE	36
20	ANGLE OF REPOSE OF COARSE GRAINED OLIVINE AS A FUNCTION OF PRESSURE	37
21	ANGLE OF REPOSE OF FINE GRAINED OLIVINE AS A FUNCTION OF PRESSURE	38
22	STATE OF STRESS IN DIRECT SHEAR TEST.....	40
23	FAILURE OF SOIL IN THE DIRECT SHEAR TEST	42
24	DIRECT SHEAR BOX FOR USE IN VACUUM.....	43
25	DIRECT SHEAR APPARATUS IN VACUUM CHAMBER.....	43
26	SCHEMATIC DIAGRAM OF DIRECT SHEAR APPARATUS..	44
27	SHEAR STRESS AS A FUNCTION OF DISPLACEMENT IN SILICA FLOUR FROM DIRECT SHEAR TESTS.....	47
28	MOHR'S RUPTURE DIAGRAMS FOR SILICA FLOUR AT VARIOUS VACUUM LEVELS.....	48
29	APPARENT COHESION AND INTERNAL FRICTION OF SILICA FLOUR AS A FUNCTION OF VACUUM.....	49
30	SHEAR STRESS AS A FUNCTION OF DISPLACEMENT OF OLIVINE IN DIRECT SHEAR TESTS	50
31	MOHR'S RUPTURE DIAGRAM FOR FINE GRAINED OLIVINE AT VARIOUS VACUUM LEVELS	52
32	APPARENT COHESION AND INTERNAL FRICTION OF FINE GRAINED OLIVINE AS A FUNCTION OF VACUUM.....	53
33	S/B AS A FUNCTION OF $q/B\gamma$ IN ATMOSPHERE	56

List of Illustrations (con't)

Figure		Page
34	AVERAGE BEARING PRESSURE UNDER FOOTING AS A FUNCTION OF PENETRATION FOR VARIOUS RATIOS OF Z/B AND W/B	58
35	RELATIONSHIP BETWEEN $\frac{ZW^3n}{B^4}$ AND q/q_o IN LOAD BEARING TESTS ON SILICA FLOUR (Fig. 34)	50
36	S/B AS A FUNCTION OF $q/B\gamma$ FOR VARIOUS CONTAINER SIZES (Fig. 34)	61
37	SLOPE AND INTERCEPT PARAMETERS AS A FUNCTION OF DENSITY	62
38	S/B AS A FUNCTION OF $\frac{q\ \text{Atm.}}{B\gamma\ \text{Vac.}}$ FOR γ = 70.6 PCF	64
39	α AS A FUNCTION OF VACUUM LEVEL	65
40	S/B AS A FUNCTION OF $\frac{q\ \text{Atm.}}{B\gamma\ \text{Vac.}}$ FOR VAC $\simeq 2 \times 10^{-6}$ TORR	66
41	DRAWDOWN CURVE FOR DIRECT SHEAR SAMPLE TO MEASURE IRREVERSIBLE INTERPARTICLE FORCES	69
42	DRAWDOWN CURVE FOR PENETRATION SAMPLES TO MEASURE IRREVERSIBLE INTERPARTICLE FORCES	70
43	PENETRATION AS A FUNCTION OF LOAD BEFORE AND AFTER STORAGE IN VACUUM	71
44	ENERGY CURVES FOR IDEALIZED COLLOID MODEL (36).	74
A-1	140 LITER/SEC. ION PUMP SYSTEM	A-3
A-2	400 LITER/SEC. ION PUMP SYSTEM	A-4
A-3	ULTRA-HIGH VACUUM DIFFUSION PUMP SYSTEM	A-5
A-4	VERY-HIGH VACUUM DIFFUSION PUMP SYSTEM	A-6

LIST OF TABLES

Table		
1	VALUES OF m AND α DETERMINED FROM FIGURE 40	63

STUDIES OF LUNAR SOIL MECHANICS

I. INTRODUCTION

With the present emphasis on exploration of the other celestial bodies in our solar system and in particular the use of the moon as a space station, it is necessary to learn more about the properties of the materials which are expected to be encountered on these bodies. The success of the lunar mission is particularly dependent upon the successful design of the vehicles and structures which will be placed on the moon as well as the correct interpretation of data gathered by in-situ measurements on the lunar soil. It is, therefore, essential to have a basic knowledge of the mechanics of the material composing the lunar surface.

Because of the extreme differences between the lunar and terrestrial environments, the most important of which is the virtual absence of an atmosphere on the moon, it would not be expected that the lunar soil would have the same properties as a similar material on earth. The purpose of the research described in this report was to provide data on basic engineering lunar soil properties. The investigation consisted of determining the effect on the porosity attained by simulated lunar soil when deposited in a vacuum and the effect on shear strength of soil as determined by direct shear and load-bearing tests in a vacuum.

Because of the lack of information on the nature of the material which composes the lunar surface an important part of the effort on this program was directed towards a review, analysis and evaluation of the most recent literature dealing with lunar surface studies. These analyses have formed the basis for the selection of materials to represent the lunar soil used in the program and the most important actual and/or probable lunar environmental conditions which would influence their engineering properties.

Although the research program has been largely an experimental investigation of specific properties of selected soils under prescribed environmental conditions, an important underlying concept throughout the conduct of the program has been to allow sufficient latitude so that at least some of the results would indicate true lunar soil behavior according to almost any reasonable estimate of the lunar surface.

II. THE NATURE OF THE LUNAR SURFACE

Observations of the lunar surface even through relatively low powered telescopes reveal the existence of two distinctly different types of regions, the maria or lunar "seas", which have rather smooth surfaces, and the mountainous regions or highlands.

The maria are widely believed to have been formed by lava flows resulting from the outpouring of huge quantities of molten rock onto the surface. It is believed by some (1) that the development of large heat sources in the moon's interior produced large quantities of molten magma which poured out onto the surface under forces developed from a slowing down of the rotation of the moon about the earth. The latter was also responsible for a change in the shape of the moon from that of an oblate ellipsoid to a shape approaching a sphere. This explanation of the origin of the maria would also explain the existence of the belt formed by the larger maria in the subequatorial regions.

Urey(2), however, presents a convincing argument against this view. He points out that the temperature of the lava could not have been much above its melting point and consequently would not have been capable of flowing great distances without solidifying. Rather, he believes the maria to be due to the collision between large planetesimals and the moon. According to this theory, it is possible that these planetesimals could also have produced a large dust cloud which might have spread a layer of fine material over the lunar surface. This idea, however, is largely discounted by evidence that the material making up the maria was at one time fluid.

Another explanation of the origin of the maria combines this theory of "ballistic" origin with that of the outpouring of molten rock (1). This explanation attributes the formation of the maria to the impact of meteorites at a time when the moon was largely molten having a rather thin crust. The impact on this crust caused fracture to occur, releasing the molten material onto the surface. This would allow the outpouring of the lava at numerous points eliminating the necessity of flow over large distances.

The origin of the craters covering the highlands is a subject on which there is much more agreement among investigators. It had originally been proposed that they were the result of volcanic acivity (3) but comparison of

the lunar craters with terrestrial volcanoes does not lend support to this theory (4). It is now generally accepted that they are mostly the result of meteoritic impact (1), (5), (6), with a small number of craters which show distinct evidence of being of volcanic origin (7).

The question may then be raised as to whether the floors of the craters and maria are rock or if soil of some kind overlies the base material. Earlier hypotheses of the lunar surface held that due to the absence of a lunar atmosphere and hence erosional processes, the lunar surface would consist of bare unweathered magmatic rock (1). However, direct observation has given strong indications of the presence of material which has been deposited at some time after the formation of the craters. This may be seen in Fig. 1 in which just a portion of the uppermost points of the crater rim seen above the crater Aristillus are visible, the remainder of the crater apparently being filled in with overlying material (6). Lesser amounts of deposition are evidenced by the fact that the central peaks which have been observed on the floors of some craters are not visible in others. This, however, is not conclusive because the existence or non-existence of a central peak can be accounted for by the nature of the impact which formed the crater (5). It has also been observed that in some cases the floor of the crater has an elevation above that of the surrounding plane outside the crater lip (1). It is difficult to see how this could have occurred in a crater formed by the impact of meteorites. It would be possible, however, in volcanic craters. All of these factors point to the existence of a surface material formed by deposition. The important question is then the nature of this material.

On the basis of measurements of the thermal and reflecting characteristics of the moon's surface, which will be discussed later, it has been established that the lunar surface consists of a highly porous material. In fact, the porosity is indicated to be of a magnitude greater than that achieved by terrestrial granular materials. On this basis it has been concluded by many (mostly Soviet scientists) that the lunar surface consists of a "grain porous conglomerate" or slag like material (1) (8). This is also seemingly substantiated by the observance of almost vertical slopes on the moon, which could not be attained by cohesionless granular materials. However, as will be shown later in this report, it is entirely possible and in fact probable that a fine-grained material

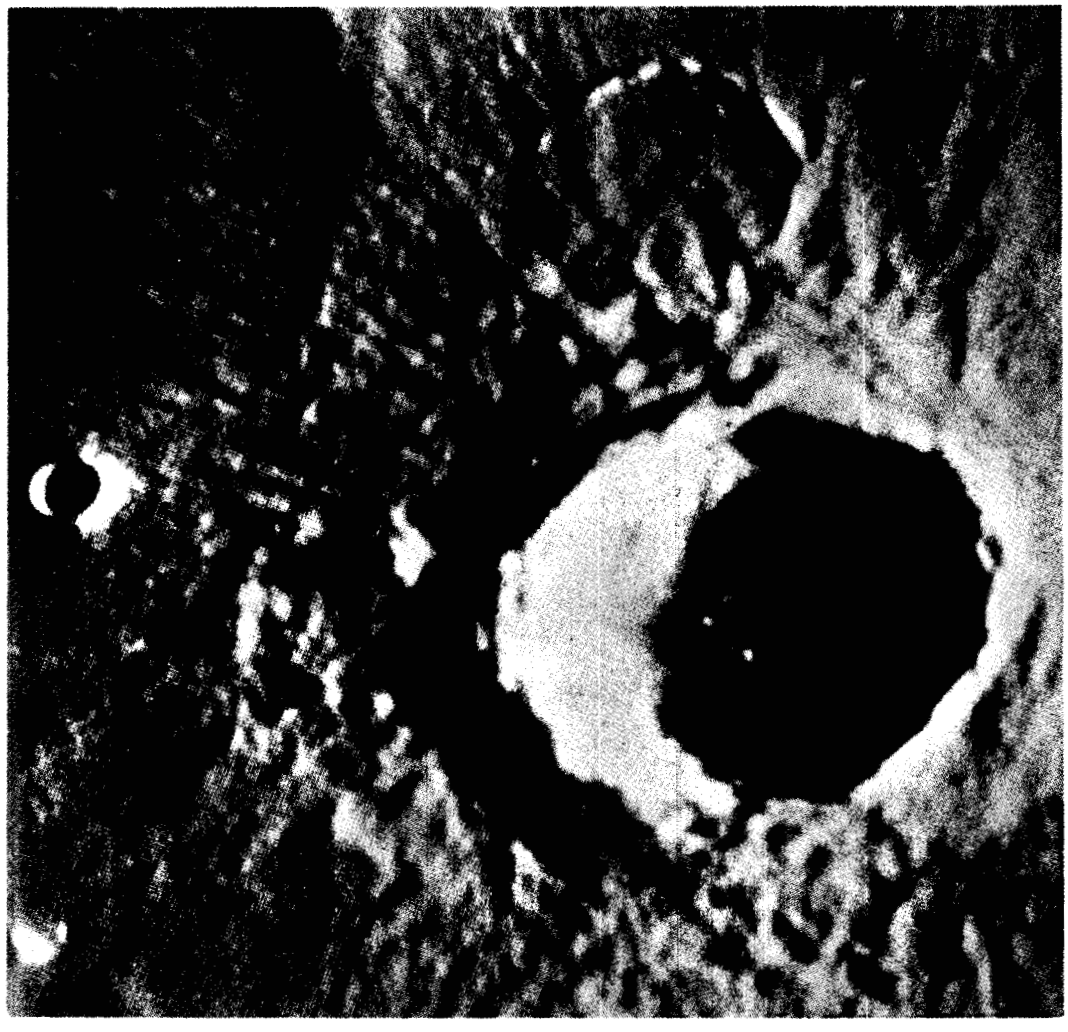

Fig. 1 PHOTOGRAPH OF CRATER ARISTILLUS (6)

on the lunar surface would exhibit a substantial apparent cohesion, thereby allowing a granular material to support vertical slopes and attain rather high porosities. This has also been demonstrated by Hapke (11) and Salisbury, et. al. (10)

This theory of a slag character of the lunar surface formed by impacting meteors does not appear reasonable on the basis of other considerations. The fact that the depressions on the moon's surface appear to be covered by deposits of material but the high points of the crater rims, mountains, etc. do not, suggest that the material has migrated to the lower points necessitating the transport of material by some mechanism. This migration of a slag-like material would be possible only in the event of erosion of the material in which case it would be reduced into a granular form in the process.

By comparing the diffusion of light reflected from the moon's surface with radio observations it has been concluded that the lunar surface is rough on the scale of light waves (400-800μμ) but smooth on the scale of radio waves (10 cm) (11). This smoothness (on the order of magnitude of inches) could be explained by the existence of a dust layer overlying the surface (12). Further evidence of this dust layer was also provided by Fielder (13) who estimated the moon's albedo to be not more than 10%. This would indicate that the surface is either dark or composed of some material, such as a layer of stones, in which some of the incident light gets trapped in small hollows. In addition, it was found that only by using a finely ground or ash-like rock could a reasonable match be made between the polarization-phase curve of lunar light and that reflected from laboratory specimens.

Hapke (9) also studied the photometric properties of the lunar surface including the albedo, the backscattering characteristics, and the polarization of the reflected sunlight. He concluded that the lunar surface cannot consist of "... pumaceous and scoriaceous rocks foams and slags" but must be covered with a layer of rock dust having a very high porosity. Measurements of the thermal properties have substantiated these conclusions (14)(15).

Based on the foregoing discussion it may then be reasoned that the lunar surface is covered by a granular material, the grain size of which can be inferred from the possible soil producing mechanisms which could have

been operative on the moon. Obviously the major erosional processes which exist on the earth could not have been operative on the moon due to the absence of an atmosphere. Because of the large difference in temperature between the lunar night and day, Weil (12) attributes the major portion of soil to thermal exfoliation in which case the particle sizes may range from quite large to very fine dust like material, the major portion being from 1 to 100 μ in diameter. Ryan (16), however, presents experimental evidence in which various rock types were cycled over wide temperature ranges and showed no indications of thermal fracture. This in itself does not discount this theory entirely but places serious limitations on the amount and size of grains of the soil which could have been formed by this process.

Gold (5) attributes a considerable amount of lunar erosion to solar radiation, and he is supported in this theory by Grannis (17). Additional mechanisms include fast impinging gas molecules and continuous impacting of micrometeorites. Each of these processes as well as deposition from the micrometeorites themselves could be effective in creating a fine dust like cover on the lunar surface.

Another highly probable soil producing mechanism is the vaporization and subsequent condensation of meteorites upon impact. Salisbury (18) states that the impact of meteorites would result in a layer of rubble many feet thick, with particle sizes ranging from microns to a few feet. According to this theory, upon impact on the lunar surface a portion of the meteorite and some of the surrounding material would be broken up and thrown outward from the surface, the smaller sized particles being thrown outward greater distances than the larger ones. Depending on the velocity of impact a portion of the material would be vaporized. The larger sized particles would then settle back onto the surface followed by the smaller sized ones which had been thrown farther, which in turn are followed by a very fine grained material resulting from the condensation of the vaporized material. A portion of the ejecta may be thrown outward at velocities such that they escape the gravitational field of the moon, but the major portion would settle back on the surface. This ejecta could possibly be the origin of a portion of the solid material in space as well as some meteorites (19). Because of the rotation of the moon and because the material is ejected at some angle to the zenith,

the falling material would be deposited over a continuously different area. This could account for a soil mantle overlying the maria as well as portions of the highlands. Transport mechanisms such as micrometeoroid bombardment (5) (20) would cause migration of this material downward along the slopes of the crater rims and lunar mountains, leaving bare these uppermost regions and increasing the depth of the soil layer at the lower points. As the result of numerous impacts it would then appear that almost the entire lunar surface could be covered with a soil mantle overlying the parent rock.

The results of the investigation by Hapke (9) indicate that the average particle size of this uppermost material is of the order 10μ. Thus it may well be expected that the lunar surface consists of a granular material with particle sizes of the order of 10μ at the surface and increasing in size with depth. The depth to which the very fine grained material exists may be of the magnitude of meters(9) with some deposits having larger grain sized soil underlying the fine material and extending to depths up to 100 ft or more in the intercrater areas (18).

The shape of the soil grains would be expected to be quite angular in view of the absence of weathering such as exists on earth. This angularity of the grains and the existence of interparticle forces which could exist on the "clean" surfaces of the particles would result in very high porosities of the fine grained surface soil.

Because of the differences between the lunar and terrestrial environments the behavior of the lunar soil would not be expected to be the same as that of a similar soil on the earth. The most significant difference is the almost total absence of an atmosphere. Earlier estimates of the atmospheric density arrived at a density of 10^{-12} times that of the earth's (37). More recent investigations, however, have shown it to be somewhat lower than this (21) and the best current estimates place it at 2×10^{-13} times that of the earth's (1). This corresponds to a pressure of 1.5×10^{-10} torr. Other factors influencing lunar soil properties are the extremes of temperature on the lunar surface, ranging from about +260° F during the lunar day to -230° F at night, and a gravitational field which is only one-sixth that of the earth's. In addition to these known conditions, there are the possible effects of constant

bombardment of the moon's surface by solar and cosmic radiation and the constant influx of micrometeorites and cosmic dust.

As will be seen later in this report, some of these factors may have advantageous effects on the bearing capacity and shear strength of the soil. The very low environmental pressure will undoubtedly result in "clean" particle surfaces causing interparticle forces to exist which may very well increase the apparent cohesion of the soil. In addition the"clean" particle surfaces will result in a higher angle of internal friction. The reduced gravitational field will tend to decrease the bearing capacity, but on the other hand, all loads that are placed on the soil will produce a pressure only one-sixth of that which they would produce on the earth. High temperatures and radiation effects could possibly cause cold welding of the particles which will have the effect of further increasing the shear strength. It would then appear that the overall effect of the "harsh" lunar environment would be one of increasing the shear strength of the lunar soil and its bearing capacity rather than reducing it.

III. PREVIOUS STUDIES OF LUNAR SOIL MECHANICS

Within the broad field of soil mechanics, relatively little research has been done specifically on lunar soils. In those few studies which have been conducted, the principal environmental factor that has been considered has been the environmental pressure and in only one study has the vacuum achieved been in the 10^{-10} range. In all other studies reported, vacuum levels have been of the order of 10^{-8} torr or below.

One of the earliest reported studies was conducted by R. L. Geer (22). This study consisted of measuring the penetration of spherical balls dropped into samples of various materials at vacuums of 10^{-5} torr. Although actual void ratios or porosities were not reported in this study, vibration techniques were employed in an attempt to maintain a constant density of the soil samples throughout the investigation. The effects of outgassing of the soil were also recognized and studied. It was found that the penetration of the balls decreased with an increase in the "hold" time under vacuum. In some cases a greater penetration was indicated under vacuum than under atmospheric conditions. The results were inconclusive regarding the behavior of lunar soils, primarily because of the low vacuum levels under which the experiments were performed.

Dynamic penetration studies were also reported by Roddy et. al. (23). Investigations were performed under atmospheric and vacuum conditions in the 10^{-5} torr range, on samples of crushed olivine at high and low relative densities. The results indicated an increase in the penetration resistance under vacuum in samples having a high void ratio but a decrease in penetration resistance under vacuum in samples having low void ratios. In these studies, as was the case in those reported by Geer (22), the vacuum levels were such as to remove the pore air but were probably not sufficient to remove a significant amount of adsorbed gas layers from the particle surfaces. Thus, the experiments merely evaluated the effects of pore air pressures. Therefore, Roddy et. al. explained the changes in penetration resistance under vacuum in the following manner. The void ratio in the regions of shear failure in a sample having a high void ratio would decrease upon penetration and thus force out any pore fluid or gas. This would result in low effective stresses in the soil under atmospheric conditions and hence , high effective stresses in vacuum. Under the latter condition the penetration resistance would be greater.

In a sample having a low void ratio, the porosity would tend to increase under the disturbance of impact and air would be drawn into the pores (negative pore pressure) under atmospheric conditions, resulting in an increase in effective stresses and increased resistance to penetration. Penetration resistance of the material under vacuum for these void ratios would, therefore, be lower than in atmosphere.

A similar phenomenon (increased penetration under vacuum conditions) was reported by Weide (24). However, this increase in penetration occured only at pressures down to the 10^{-3} or 10^{-4} torr range, below which the penetration decreased with an increase in vacuum.

Static penetration tests under vacuum were performed by Halajian (25). In those studies also, the density was presumably held constant by means of controlled vibration techniques. Accurate pressure measurements were not reported but vacuum levels in the 10^{-8} torr range were presumably achieved. The number of tests was very limited in Halajian's studies but indicated an increase in load bearing capacity due to vacuum. The pore air effects were presumed to be insignificant under static loading and therefore, the increase in bearing capacity was attributed to an increase in friction or interparticle bonds due to outgassing of the soil.

Both static and dynamic penetration studies were conducted by Rowe and Selig (26) at the Armour Research Foundation. A number of experiments were conducted on soil samples having various densities. The results indicated an increase in both the static and dynamic bearing capacity under low and high vacuum levels at all densities. The bearing capacity in both cases (static and dynamic) showed a small increase as vacuum levels were increased from atmospheric up to 10^{-6} torr. At higher vacuum levels there appeared to be a much greater increase in shear strength. This indicated an increase in interparticle friction and/or cohesion at these vacuum levels. The results of this study are analyzed further in Section V of this report.

All work done up to this point involved bearing capacity measurements on soil under vacuum conditions from which the shear strength of the soil was inferred. Such experiments, gave little insight as to the factors to which the observed increase in shear strength should be attributed.

Direct shear tests performed on glass spheres under vacuum levels up to 10^{-5} torr were reported by Sjaastad (27). The experiments were preliminary in nature but an increase in the angle of internal friction under vacuum was again reported. This is as might be expected on the basis of friction studies for other materials conducted in a space environment (28). However, it tells little regarding the interparticle interaction which might occur in real soils.

Investigations of the cohesive behavior of soils under vacuum levels up to 10^{-9} and 10^{-10} torr were presented by Stein and Rostoker (29). Tensile stress experiments showed a definite increase in the apparent cohesion of soil under vacuum which was attributed to cold welding between the particles. These results were substantiated further by Martin (38) who studied the water vapor adsorption characteristics of kaolinite which had been stored under vacuum levels to 10^{-5} torr for various periods of time. Although these vacuum levles are not very high, permanent particle coalescence of the clay particles was observed to develop in a period of time greater than 9 days but less than 60 days.

These studies all indicate that the increase in shear strength of soil under lunar environmental conditions could be expected to be due to increases in both the apparent cohesion and the internal friction of the soil.

IV. DESCRIPTION OF REPRESENTATIVE LUNAR SOIL

As was pointed out in Section II, there is considerable controversy regarding the type of material which constitutes the lunar surface. Even less is known regarding the mineralogical composition of this material although it is generally agreed that it consists principally of silicates similar to that found in terrestrial rocks (30). Added to these unknowns is the variation in soil composition which undoubtedly exists from one location to another on the lunar surface. Thus, the task of selecting a soil representative of the surface material is not an easy one.

If the lunar surface material resulted mainly from meteoritic impact as indicated in Section II of this report, it would be reasonable to expect that at least part of the soil would consist of material similar in composition to that of the meteorites. The major silicates found in stony meteorites are olivine and pyroxene (31). This is in accord with the results obtained by Hapke (32) who attributes the darkening of the lunar surface to the action of solar wind on ferro-silicates. Urey (33) also concludes from his studies that the surface is quite probably rich in "silicates of basaltic composition".

On the other hand, the relatively low density of the moon suggests that the lunar material probably contains very little of the heavy elements (34). Measurements of the moon's radio emission (8) indicate that the lunar soil contains little meteoric iron.

On the basis of the aforementioned results and a digest of a great many more deductions and opinions by a number of investigators, the two materials selected to be representative of the lunar soils were silica flour and finely ground olivine. The silica flour is a commonly found non-metallic mineral of relatively low specific gravity while the olivine is representative of a material of meteoritic origin.

The silica flour is a commercially available material derived from finely ground sand which is commonly referred to as Ottawa sand because it is obtained from sandstone deposits in Ottawa, Illinois. It is composed of quartz crystals which are almost pure silicon dioxide, having a specific gravity of 2.64. The grain size distribution curves for the material used in the tests are shown in Fig. 2.

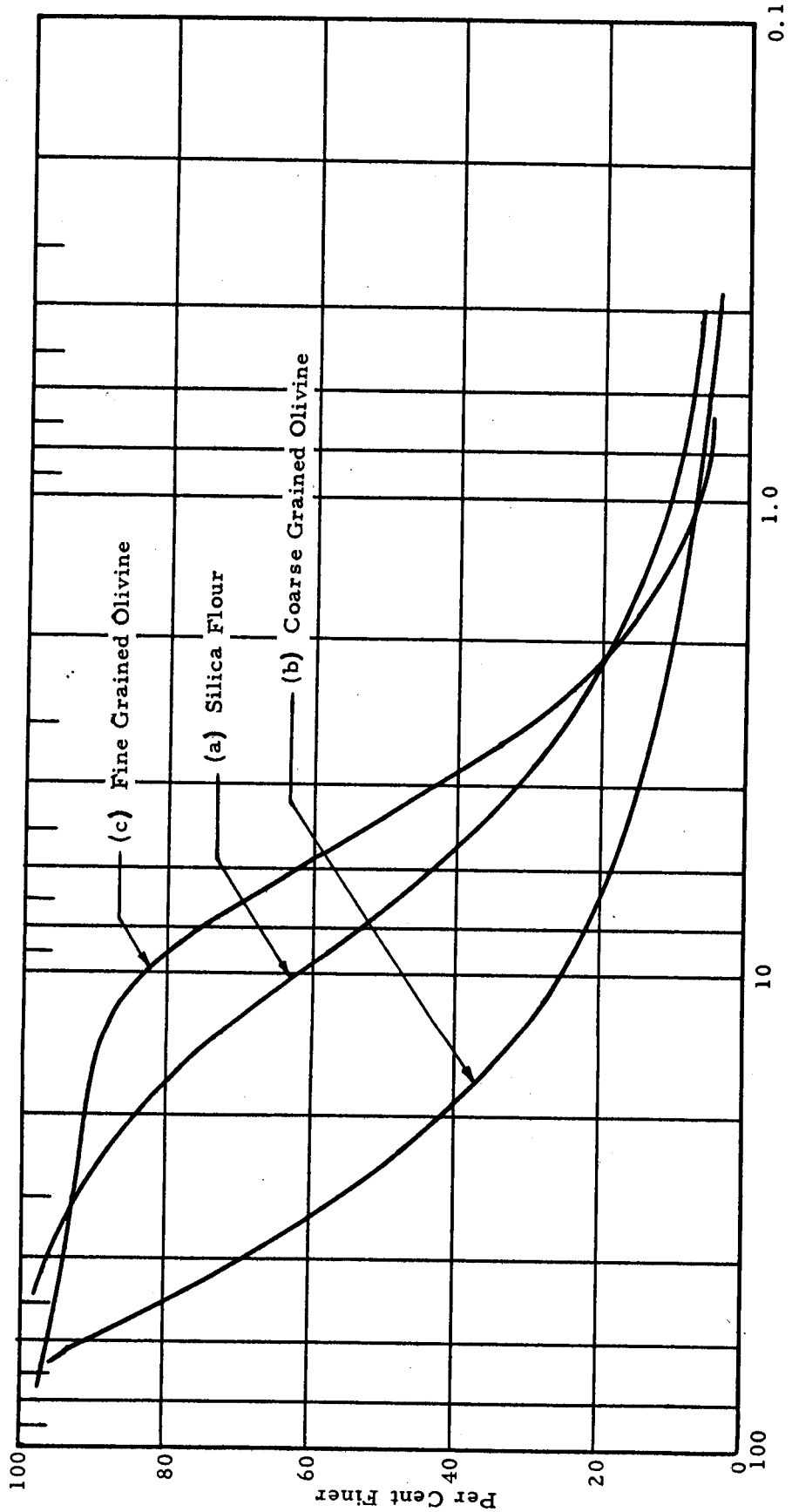

Fig. 2 GRAIN SIZE ACCUMULATION CURVES FOR REPRESENTATIVE LUNAR SOILS

The olivine was mined in Jackson County, North Carolina and was obtained in rock form. The rock material was ground in a ball mill and the portion of the material thus produced which passed a #200 mesh sieve was separated out and used for experimentation. The material retained on the #200 mesh sieve was further ground in an eight inch rubber lined fluid energy mill. Two samples having different particle size spectra were used in the experiments. The grain size distributions are shown in Fig. 2, curves b and c.

The olivine is a ferromagnesium silicate having a specific gravity of 3.27. This relatively low value indicates that its composition is predominantly magnesium silicate, the ratio of magnesium to iron being roughly from 12:1 to 16:1.

In selecting these two materials it was felt that there is a reasonable degree of certainty that their major constituents would at least be found in the lunar surface material and that there is a high probability that the major constituents of at least one of the materials would also be the major constituents of some sections of the lunar surface. Within the confines of what is known categorically of the lunar surface it was deemed unwise to try to base the study outlined in this report on a more precise definition of the true lunar soil.

V. VACUUM IN SOIL PORES IN RELATION TO CHAMBER VACUUM

In experimental work dealing with material under vacuum conditions, the environmental pressure is usually taken to be that which is recorded by a vacuum gage mounted in the wall of the chamber. In all experiments in the present study conducted under very-high or ultra-high vacuum levels, it was observed that the pressure in the vacuum chamber increased whenever the soil was disturbed in any way. It was suspected, therefore, that the vacuum level in the soil pores was not that recorded near the inner surface of the chamber wall.

If this were so , the true environmental pressure could not be determined unless it was measured at various points in the soil itself. To do this for every test conducted in the vacuum chamber would have required elaborate pressure measuring devices in the soil sample which would have interfered with the performance of the experiment. It was decided, therefore, to make a separate study of the pressure measured at some point below the surface of the soil in relation to the chamber pressure and drawdown time. The apparatus used for this experiment is shown schematically in Fig. 3. Although it is obvious that the arrangement shown did not measure the actual pore air pressure, it did, however, give a closer approximation to this pressure.

A complete description of the vacuum facilities used in this and subsequent studies is given in the appendix. For this particular study, pump down of the chamber was achieved by a six-inch oil diffusion pump for a period of 5 hours, after which pumping was discontinued over night. Pumping was resumed the next day for 6-1/2 hours after which it was again discontinued. This procedure was repeated for four consecutive runs. The chamber remained sealed overnight but due to the absence of pumping, the pressure in the chamber and in the soil rose above the operating range of the ion gages. It was assumed that the pressure to which it rose was between 1.0 and 10^{-3} torr.

The chamber pressure and the pore air pressure is shown as a function of time in Fig. 4. For pressures above 10^{-5} torr, the pore pressures are very nearly the same as the chamber pressures; however, for pressures in

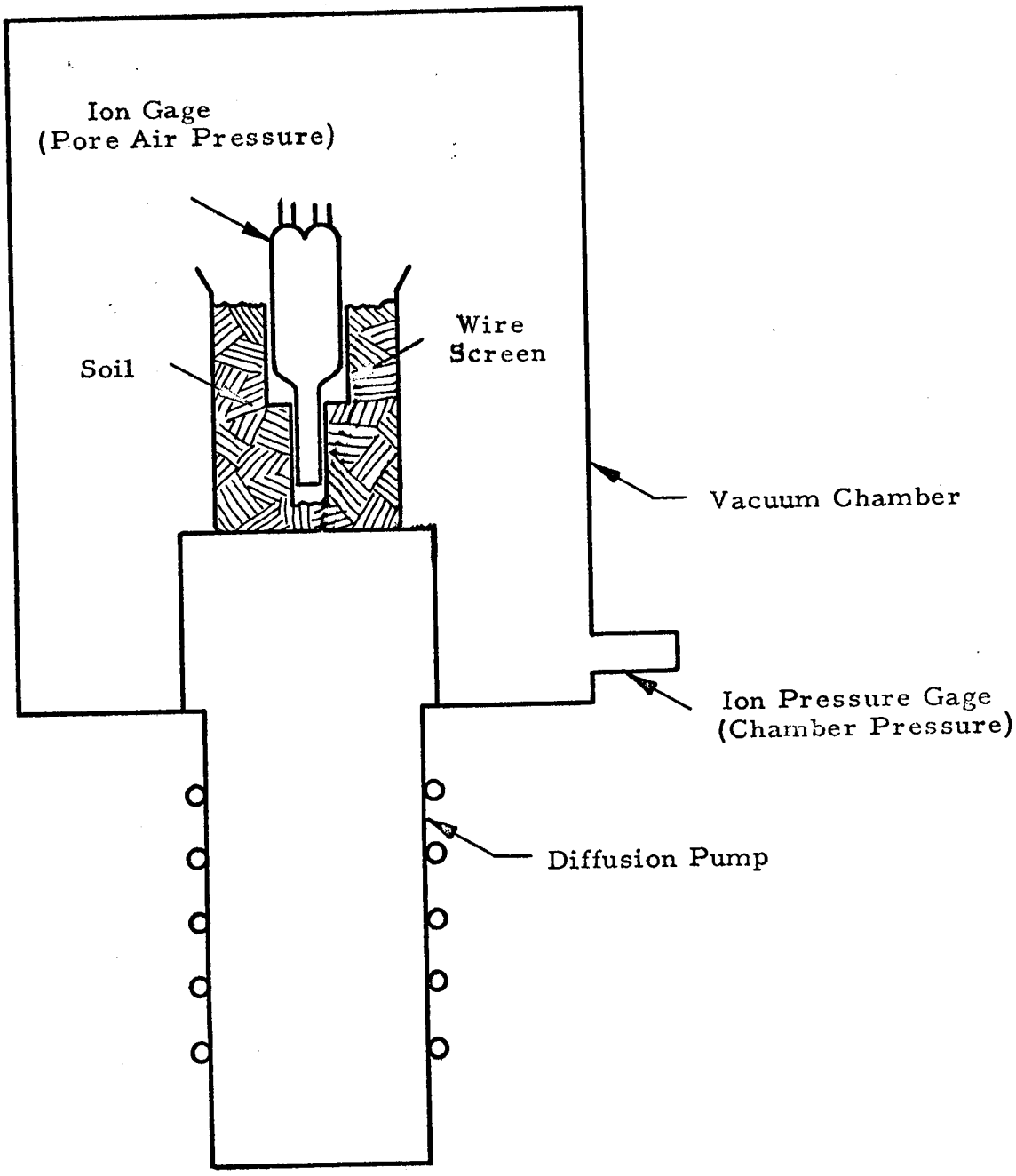

Fig. 3 TEST ARRANGEMENT FOR PORE AIR PRESSURE MEASUREMENTS

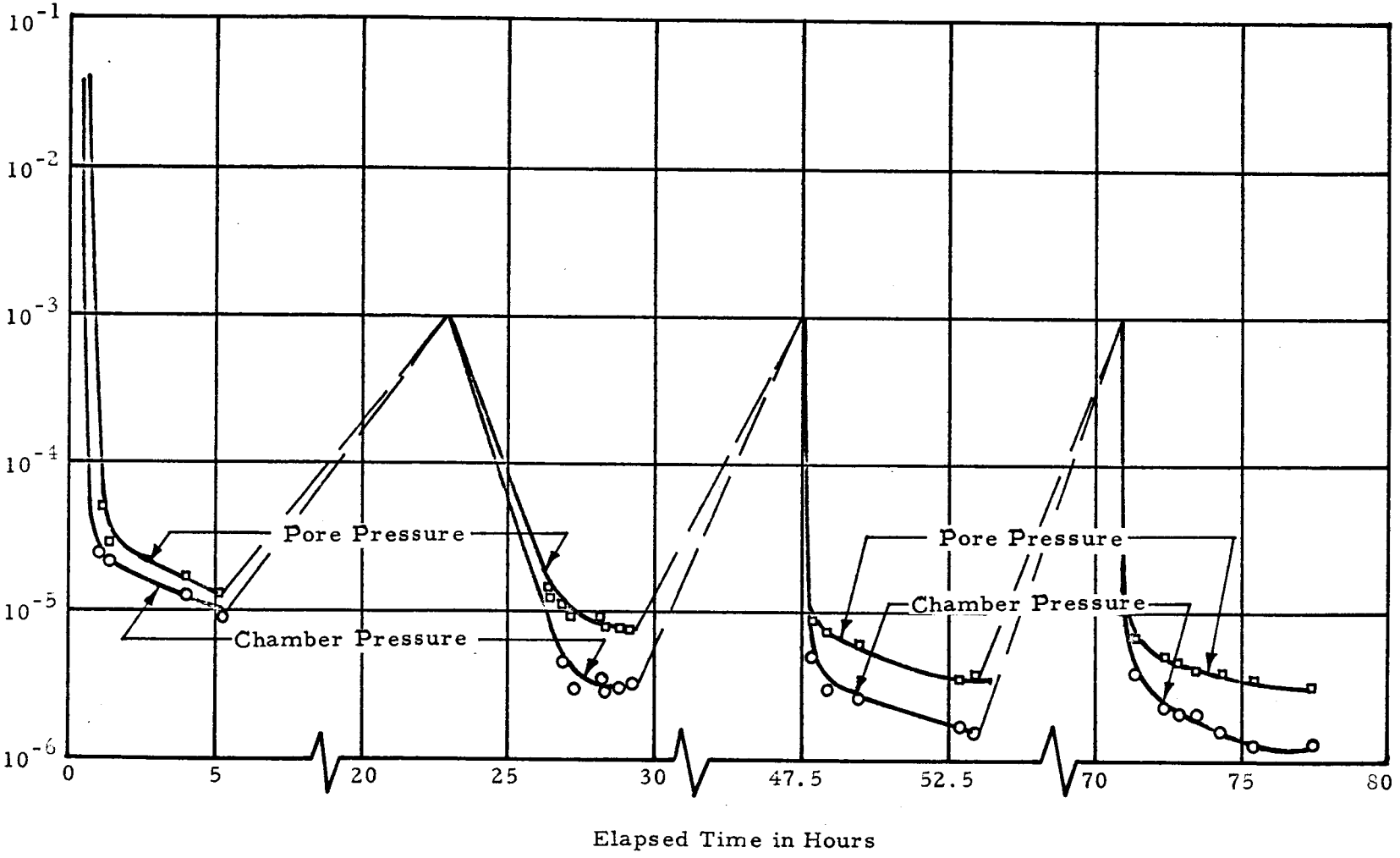

Fig. 4 CHAMBER PRESSURE AND PORE AIR PRESSURE AS A FUNCTION OF DRAWDOWN TIME

the 10^{-6} range and lower, the difference between the two is much greater. For a constant chamber pressure maintained over a period of time, there was an accompanying decrease in soil pore pressure due to the continued outgassing. It can be seen that the attainable pressure levels decreased for each successive pumpdown period. This indicates the effect of continued outgassing of the soil overnight even as the pressure was steadily increasing.

Thus, the vacuum level attained in the soil pores is a function of the vacuum in the chamber and the time of drawdown. This is shown in Fig. 5 on a logarithmic plot. The initial pressure as well as the amount of initial outgassing of the soil were probably different for each successive run. This outgassing of the soil may account for the wide range of scatter of the data in the first two runs.

From Fig. 5, the pressure in the soil pores can be expressed by the equation

$$P_s = k \left(\frac{P_c}{T}\right)^m$$

where

P_s = the pressure in the pores

P_c = the chamber pressure

T = the time of drawdown, and

k and m are constants.

The constants k and m would be functions of the distance from the particular point in the soil to an exposed soil surface, the initial pressure in the chamber and in the soil, the amount of outgassing of the soil prior to pumpdown, the soil permeability, the geometry of the specimen, the particular vacuum system and possibly other factors. It is obvious then, that to determine a unique relationship for any particular soil sample would be extremely difficult. The data is sufficient, however, to give an order of magnitude of the ratio of the environmental pressure of the soil to the chamber pressure. Thus, to provide as nearly complete outgassing of the soil as possible it is necessary to extend the drawdown time to the longest time feasible at the lowest pressure attainable. If possible it would be desirable to expose the

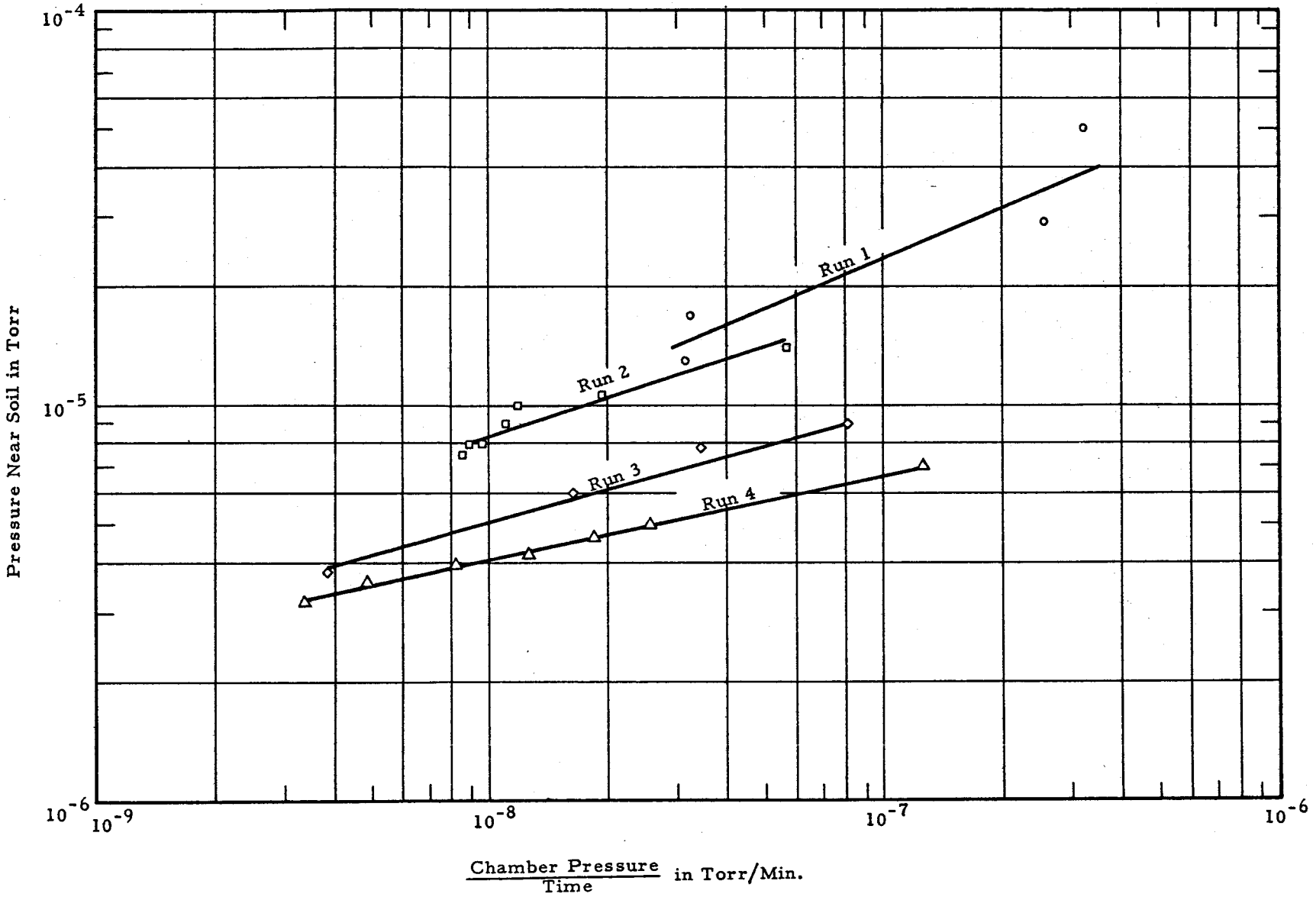

Fig. 5 PRESSURE NEAR SOIL AS A FUNCTION OF CHAMBER PRESSURE AND TIME

soil sample to vacuum levels lower than that at which the experiment is to be performed and then allow the chamber pressure to rise to that desired. This, however is not practical because of the difficulty in reaching ultra high vacuum levels.

VI. CHARACTERISTICS OF SOIL DEPOSITED UNDER VACUUM

Since the lunar soil is very likely the result of the deposition of a particulate material a probable source of this material is the disintegration of larger masses under the action of impacting meteors and meteorites. Upon impact a portion or all of this material was probably thrown outward and then settled back on the surface. The nature of these deposits, particularly with respect to porosity, might be approximated by depositing material in an ultra high vacuum. A parameter which is very difficult to duplicate in the laboratory is the terminal velocity of particles reaching the moon's surface. This is a function of the velocity of throwout and, for most of such lunar deposits, will be greater than can be obtained under earth gravity in a vacuum chamber. The greatest porosities, however, would be attained by material whose throwout velocities were low.

Since shear strength and load-settlement characteristics of a soil are so sensitive to porosity, an investigation was carried out to observe the effect on porosity of depositing soil under vacuum. The apparatus used in this study is shown in Figs. 6 and 7. Experiments were performed using the silica flour samples and the two samples of olivine (Fig. 2). The materials were first placed on a #10 sieve. Arching of the soil across the sieve openings prevented the soil from falling through as long as the sieve was held stationary. When the pressure had been reduced to that at which the experiment was to be performed, the shaft holding the sieve was vibrated by hand through the steel bellows shown attached to the top of the vacuum chamber (Figs. 6 and 7) and the soil fell freely into small containers below. The chamber was then vented to the atmosphere (very slowly so as not to disturb the soil), the containers removed, leveled off, weighed and the porosity computed.

Experiments were performed at absolute pressures ranging from atmospheric (760 torr) to 4.4×10^{-9} torr. Pressures down to 10^{-3} torr could be obtained in a matter of minutes using only a mechanical pump but to obtain pressures below this an oil diffusion pump was used. To obtain pressures below 10^{-8} torr it was necessary to extend the drawdown times to 35 hours or longer. The chamber pressure as a function of time is shown in Fig. 8, in which the increase during the deposition at high vacuum levels is evident. At pressures above 10^{-2} torr no such pressure increase was observed. Due

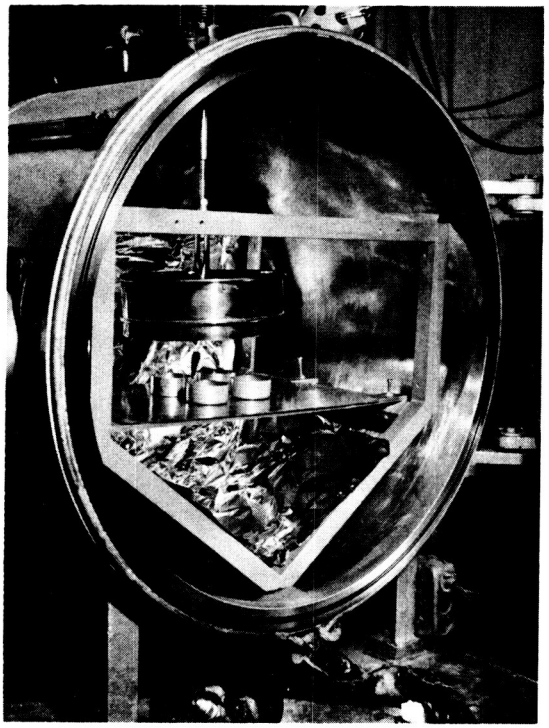

Fig. 6 SOIL IN APPARATUS PRIOR TO DEPOSITION UNDER HARD VACUUM

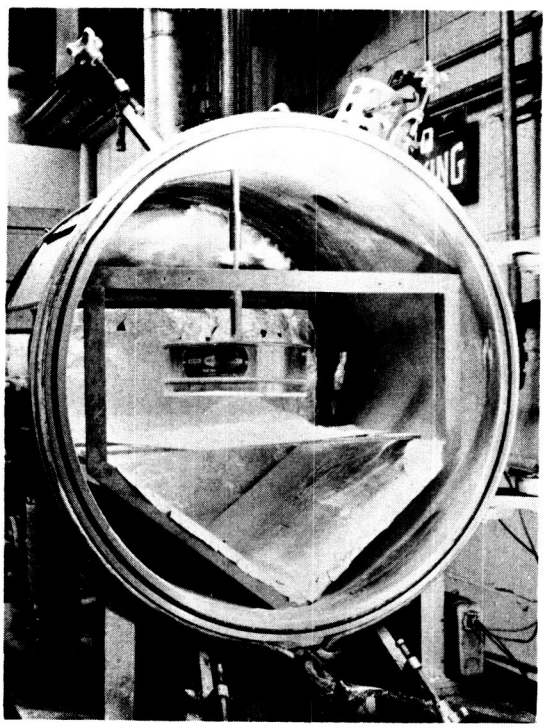

Fig. 7 SOIL AFTER DEPOSITION UNDER HARD VACUUM

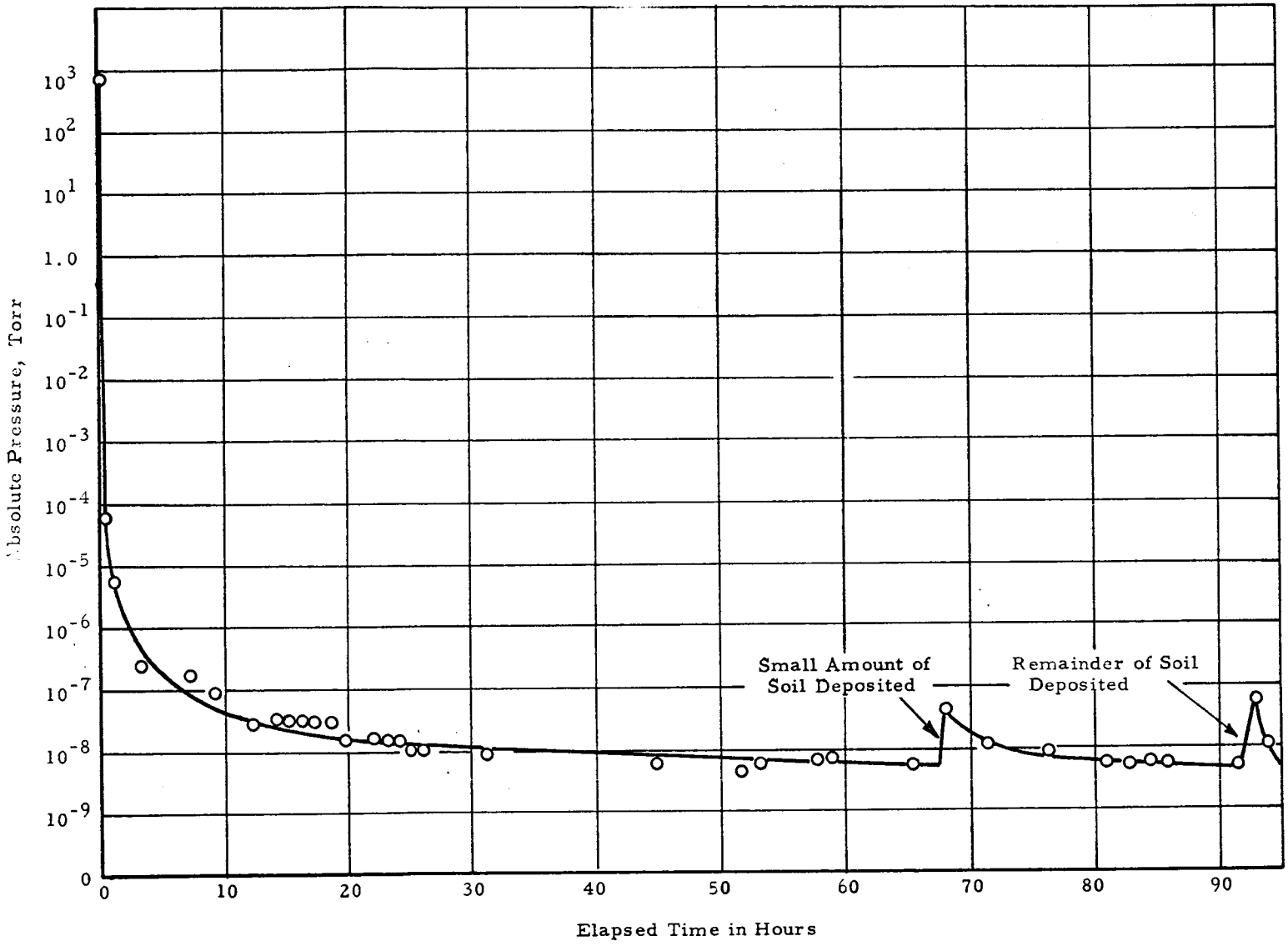

Fig. 8 VACUUM ACHIEVED IN CHAMBER AS A FUNCTION OF DRAWDOWN TIME BEFORE, DURING AND AFTER DEPOSITION OF SILICA FLOUR

to uncertainties regarding the true environmental pressure at the time of impact of the soil particles as they were deposited, the pressure which is reported for the individual experiments is the pressure just prior to deposition. At pressures below 10^{-2} torr, therefore, the true environmental pressure is somewhat greater than that shown.

A. Porosity Attained by Silica Flour

The porosity attained by the silica flour as a function of absolute pressure is shown in Fig. 9. It can be seen that there is a decrease in porosity with a decrease in pressure for low vacuum levels but for high and ultra-high vacuums this trend is reversed. The decrease in porosity at the low vacuum is due mainly to the removal of frictional air resistance resulting in an increased impact velocity. Another, although probably less important consideration, is that all stresses induced in the deposited material by impacting particles were effective stresses and no resistance to movement of the particles in the already deposited mass was offered by pore air. This permitted the existing grain structure to be more easily broken down by succeeding deposition.

Attractive and repulsive surface forces exist on soil particles which may be developed under ultra-high vacuum levels. This will be discussed more fully in Section X of this report. The increase in forces then caused the particles to flocculate during deposition and allowed a honeycomb or flocculent grain structure to be built up. This was evidenced during the experiments by the fact that the surface of the bulk material when deposited in atmosphere was relatively smooth, whereas the surface of the material deposited under vacuum was not. This is clearly seen in Figs. 10 and 11. Surface forces also served to hold the soil together in the latter case under the impacting forces of additional deposition. Thus, the porosity attained by the soil increased under these very low pressures, and in some instances (pressures below 10^{-7} torr) the porosity was greater than that attained under atmospheric conditions. It can be seen from Fig. 9 that there is a rather sudden increase in porosity between pressures of 10^{-2} and 10^{-4} torr. At pressures below this level, the increase in porosity is more gradual with decreasing pressure, indicating that the pressure at which a sufficient amount of adsorbed gas is removed to allow the surface forces to be of the same order of magnitude as

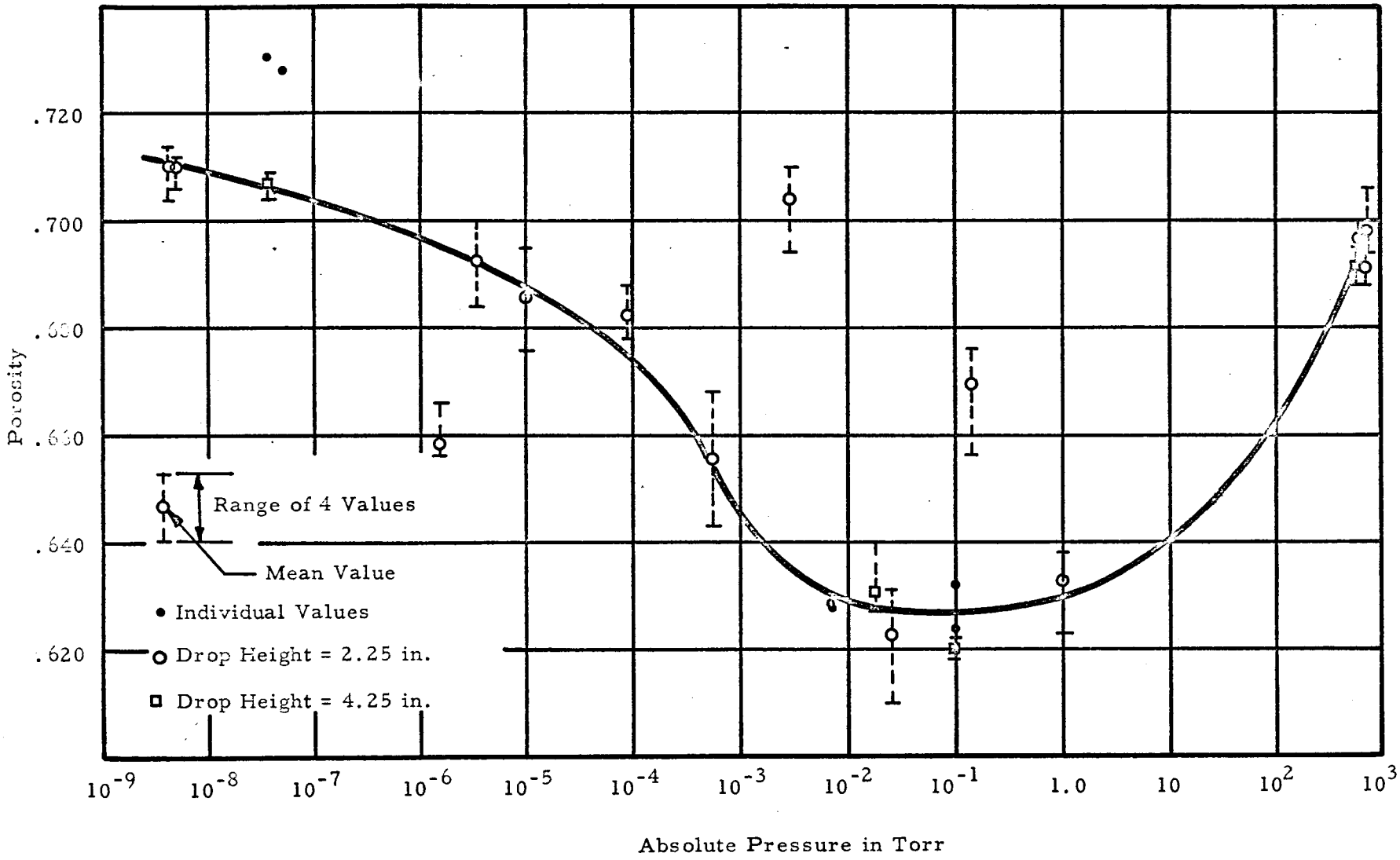

Fig. 9 POROSITY OF SILICA FLOUR DEPOSITED UNDER VACUUM AS A FUNCTION OF PRESSURE

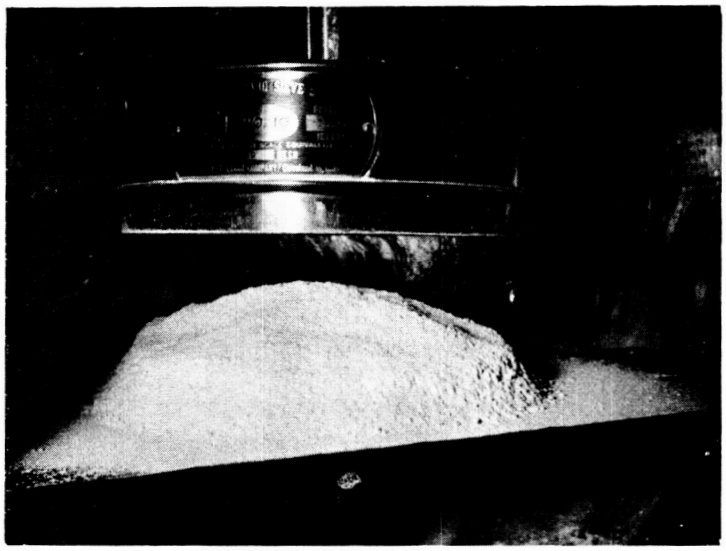

Fig. 10 SILICA FLOUR DEPOSITED IN ATMOSPHERE

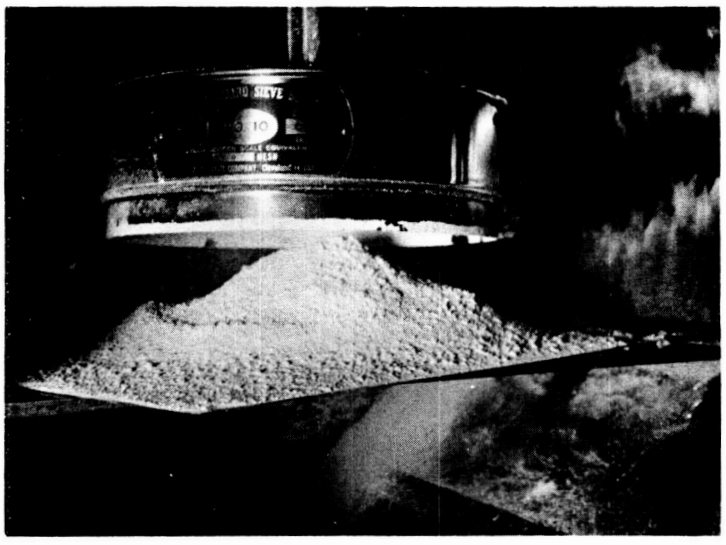

Fig. 11 SILICA FLOUR DEPOSITED IN ULTRA-HIGH VACUUM

the gravitational forces is around 10^{-3} torr for this particular material (silica flour).

B. Porosity Attained by Coarse Grained Olivine

In Fig. 12 is shown the porosity attained by the coarser grained sample of olivine flour (identified by grain size distribution curve b in Fig. 2) as a function of pressure. It is seen that a decrease in pressure resulted in a decrease in porosity at low vacuum levels and an increase in the porosity at very high vacuums. However, the pressure at which the porosity began to increase above that attained at lower vacuum levels was around 10^{-6} torr in contrast to 10^{-3} torr for the silica flour. Also the amount by which the porosity increased was much smaller for this material. It is believed that this difference in behavior of the two materials may be attributed to the following factors:

1. Both the grain size and absolute specific gravity of the olivine was greater than that of the silica flour. Therefore, the surface forces necessary to overcome the gravitational forces on the particles and thereby allow a flocculent or honeycomb grain structure to be attained were considerably greater. This would account for the very-high vacuum levels (pressures below 10^{-6} torr) necessary to cause any increase in porosity. Also the energy imparted to the deposited soil by impacting particles was greater for this sample due to the greater mass of the soil grains and this energy would have been sufficient to break down any loosely held grain clusters which might have formed.

2. The difference in the mineralogical composition and, hence, the physico-chemical properties of the materials may have caused the interparticle forces between the olivine grains to be smaller than between silica particles. If this were true, the interparticle forces which could have been developed would not have been sufficient to achieve and maintain a porous grain structure under impact by other particles.

Some flocculation of the particles was also observed in the olivine deposited under hard vacuum. This is shown in Figs. 13 and 14. Microphotographs were taken of the olivine and of the clusters formed in the material under vacuum. Due to the limitations on the magification imposed by

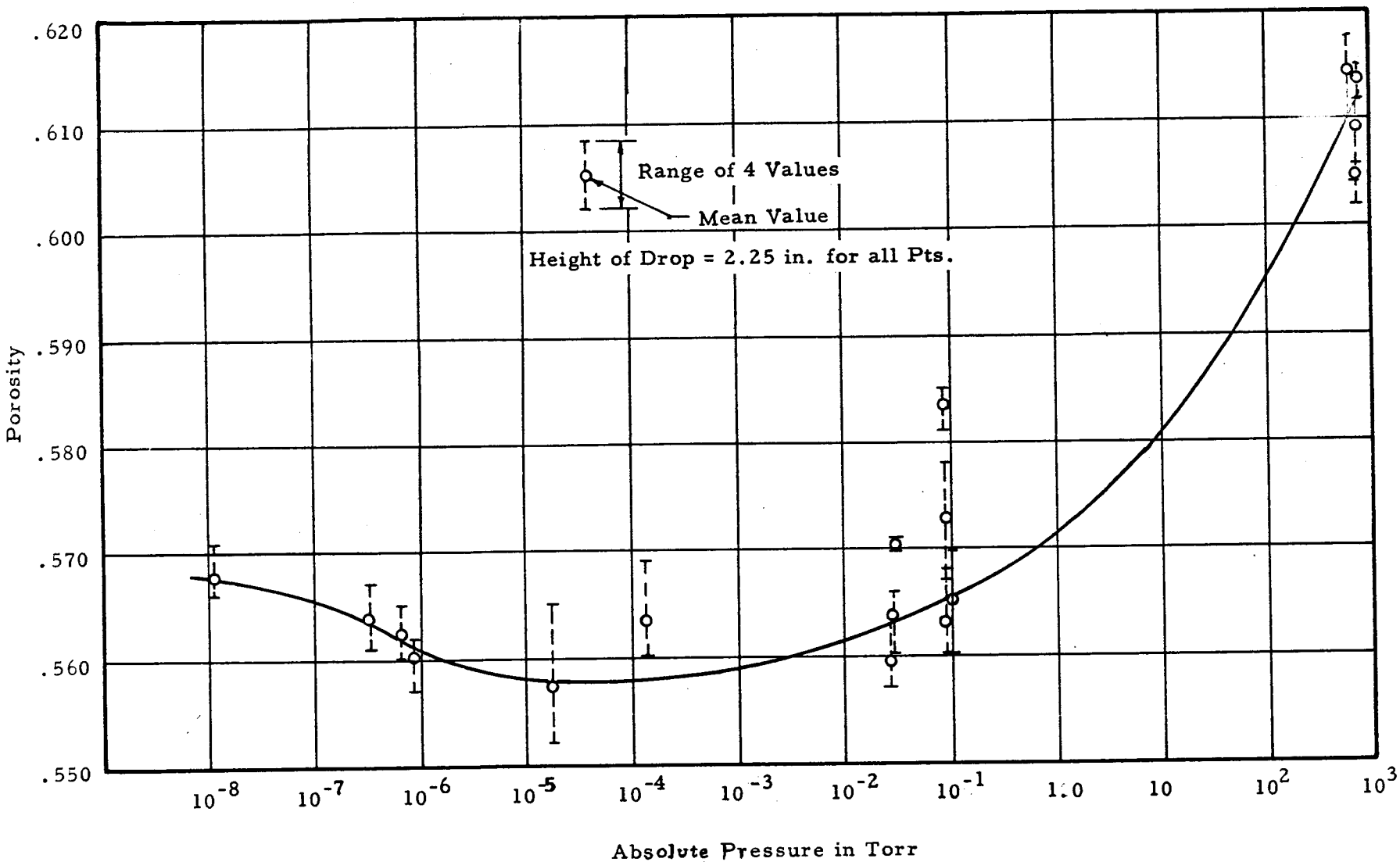

Fig. 12 POROSITY OF COARSE OLIVINE FLOUR DEPOSITED UNDER VACUUM AS A FUNCTION OF PRESSURE

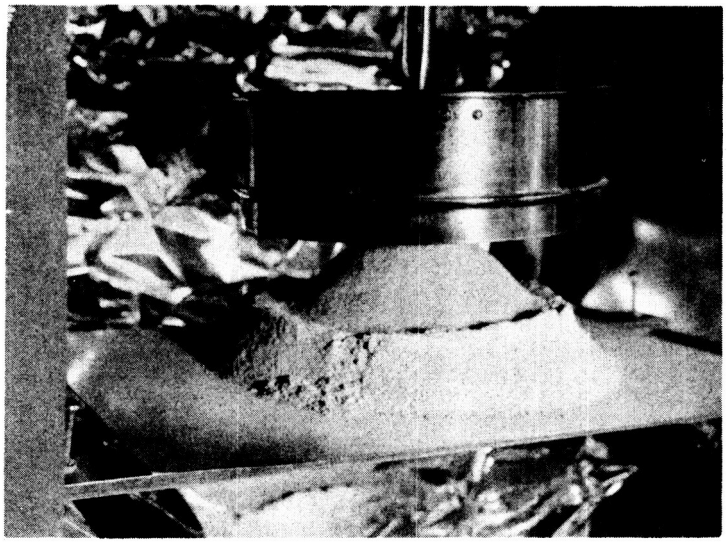

Fig. 13 COARSE GRAINED OLIVINE DEPOSITED IN ATMOSPHERE

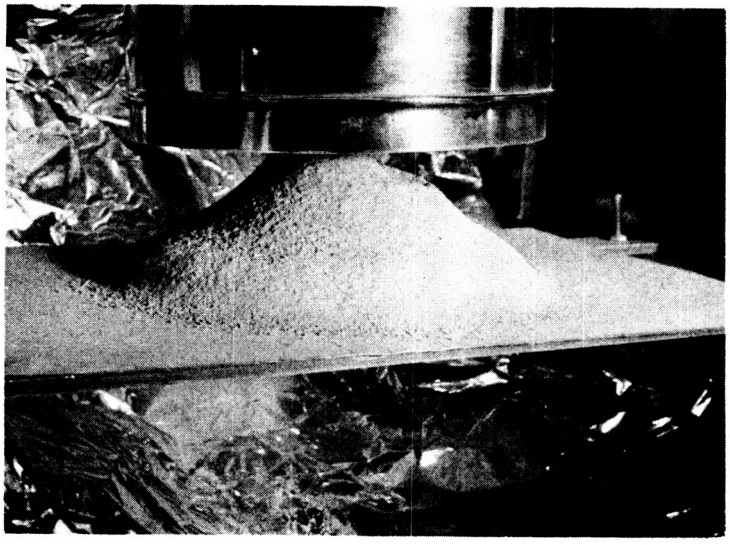

Fig. 14 COARSE GRAINED OLIVINE DEPOSITED IN ULTRA-HIGH VACUUM

the equipment readily available, this was not possible for the silica flour which had a much smaller grain size. Individual grains of the olivine are shown in Fig. 15. A cluster of these particles formed during deposition under hard vacuum is shown in Fig. 16. The irregularity of the cluster is evident. In a large mass of soil the cluster could then be considered to be a large porous individual particle which would result in a highly porous mass. These clusters could be observed only on the surface of the soil and if the energy imparted by impacting soil grains were sufficient to break them down or cause the structure formed by them to be destroyed then a denser state of the mass would be produced.

C. Porosity Attained by Fine Grained Olivine

Further experiments were also conducted on the fine grained olivine (curve c, Fig. 2). The results of these experiments are shown in Fig. 17 in the form of the porosity plotted as a function of pressure. Although not as much data was obtained for this sample as for the previous ones it can be seen that the material behaves quite similar to the silica flour. It should be noted that the grain size for the fine grained olivine is considerably smaller than for the silica flour. Therefore, even though the specific gravity of the olivine is greater, the mass of the individual particles is relatively small. Thus, the gravitational forces and the energy of impacting particles are also smaller than for the coarser grained material and the magnitude of the interparticles forces which must be developed to maintain a porous grain structure is also smaller. Because of this a flocculent grain structure is more easily attained.

Thus, it is apparent that the principal factor influencing the porosity attained by any of these materials under various vacuum levels is the grain size.

D. Effect of Grain Size on Porosity

In order to study the effect of grain size on the porosity of SiO_2 (silica flour and Ottawa sand) a limited number of experiments were performed under atmospheric conditions.

Eight samples having different mean particle sizes were obtained by sieving a sample of uniformly graded Ottawa sand through a set of U.S. standard sieves. Two samples of commercially available silica flour were also

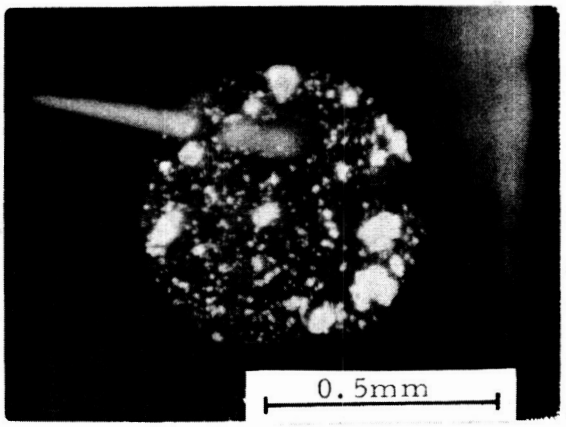

Fig. 15 INDIVIDUAL OLIVINE GRAINS

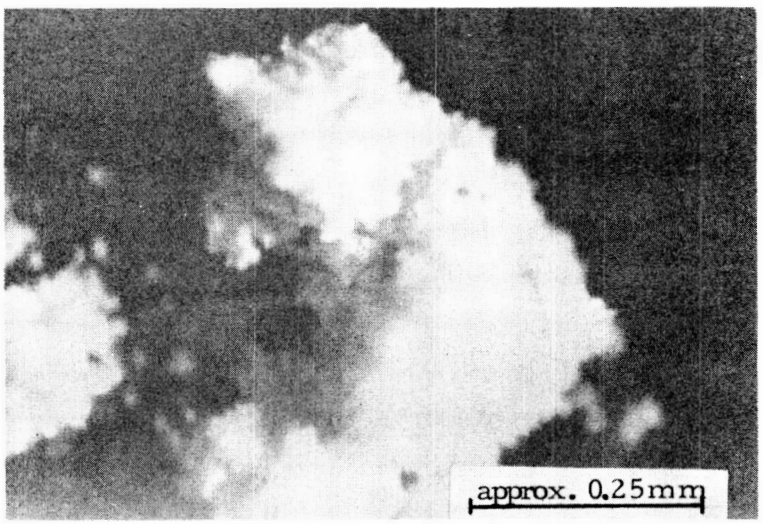

Fig. 16 CLUSTER OF OLIVINE GRAINS FORMED DURING DEPOSITION IN VACUUM

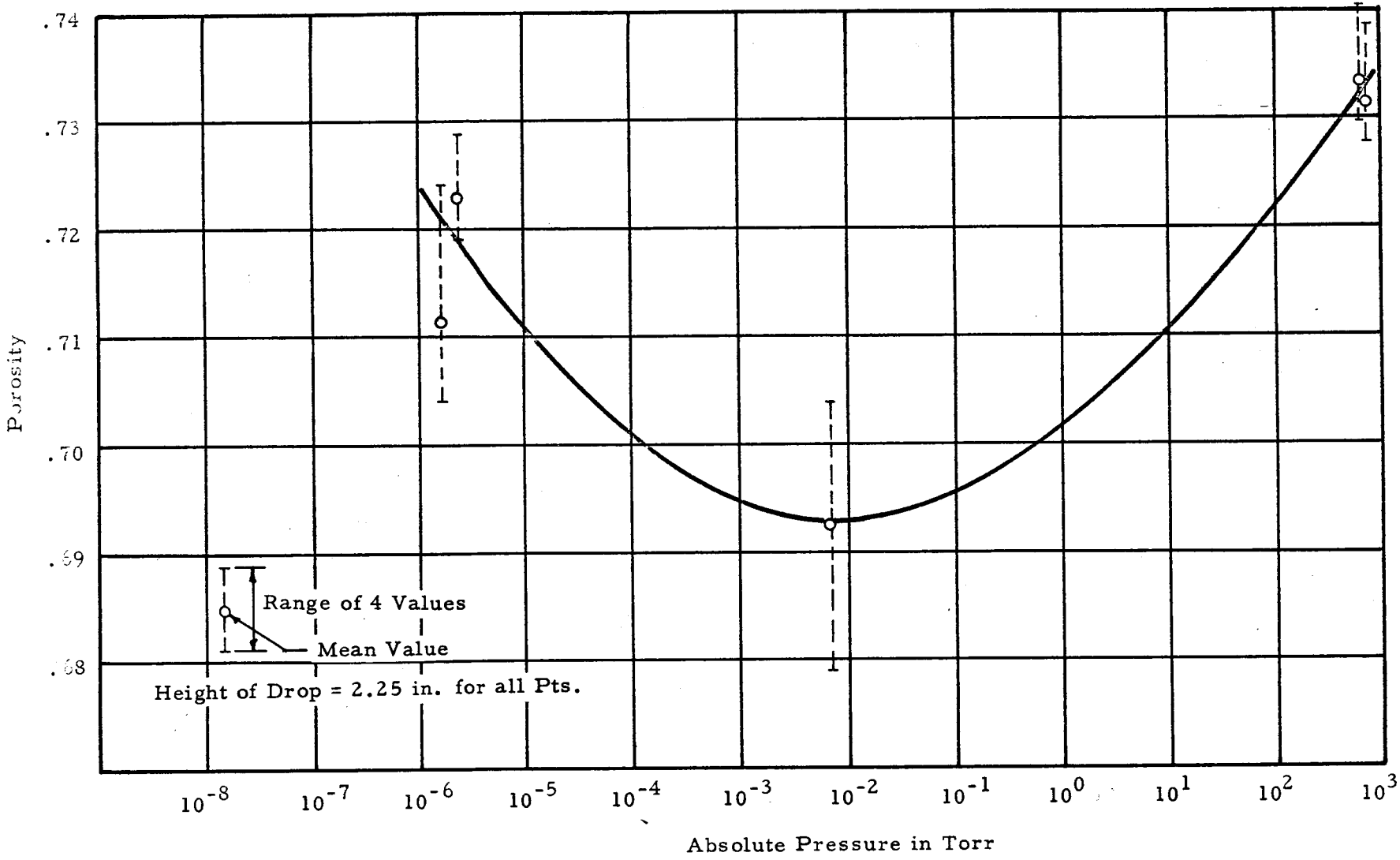

Fig. 17 POROSITY OF FINE OLIVINE FLOUR DEPOSITED UNDER VACUUM AS A FUNCTION OF PRESSURE

obtained. The sieve sizes used were nos. 25, 35, 40, 35, 50, 60, 70, and 100. Except for the material retained on the #25 sieve that portion of the sample retained on each sieve was used in the experiments. An additional sample made up of the material passing a #40 sieve and retained on a #50 sieve was also used. Since a further grain size analysis of the individual samples thus obtained was not feasible, the mean particle size was assumed to be the average of the maximum and minimum diameters. This would be reasonably accurate for a uniformly graded sand. It was further assumed that the mean grain size corresponded to D_{50} (the median of the grain size distribution). These samples were then deposited by dropping the material through a height of 2.25 in. into small containers. Two of the samples had a maximum size of 40 microns and were deposited through a sieve as before. Due to the large particle size, the remaining samples could not be held on a #10 sieve. These samples were, therefore, deposited through a funnel having the lower opening closed off except for a thin slot which allowed the soil to pass through. This insured that the soil particles had an initial velocity close to zero. Insofar as possible, the drop height was held constant so that the impact velocities of the soil would be nearly the same in all tests.

The porosity of the soil as a function of the mean particle diameter is shown in Fig. 18. It should be noted that the samples having mean diameters of 179 μ and 359 μ attained porosities that fall below the curve. This may be accounted for by the fact that for both samples, the particle size spectrum was larger than that for the other samples. This large range of particle sizes permitted smaller particles to fill more of the voids between the larger particles, thereby giving a lower porosity. It may be seen from Fig. 18 that an increase in mean particle size resulted in a decrease in the porosity attained by the soil. Samples having very small particle sizes attained quite high porosities partly due to the presence of hygroscopic moisture on the surfaces of the particles which provided a surface tension bond between the particles. It is obvious, therefore, that the size spectrum of the soil and the particle size have a significant effect on porosity.

E. Angle of Repose of Material Deposited Under Vacuum

The angle of repose (i.e., the angle which the slope of the soil makes with the horizontal) of the soil was measured in a representative number of

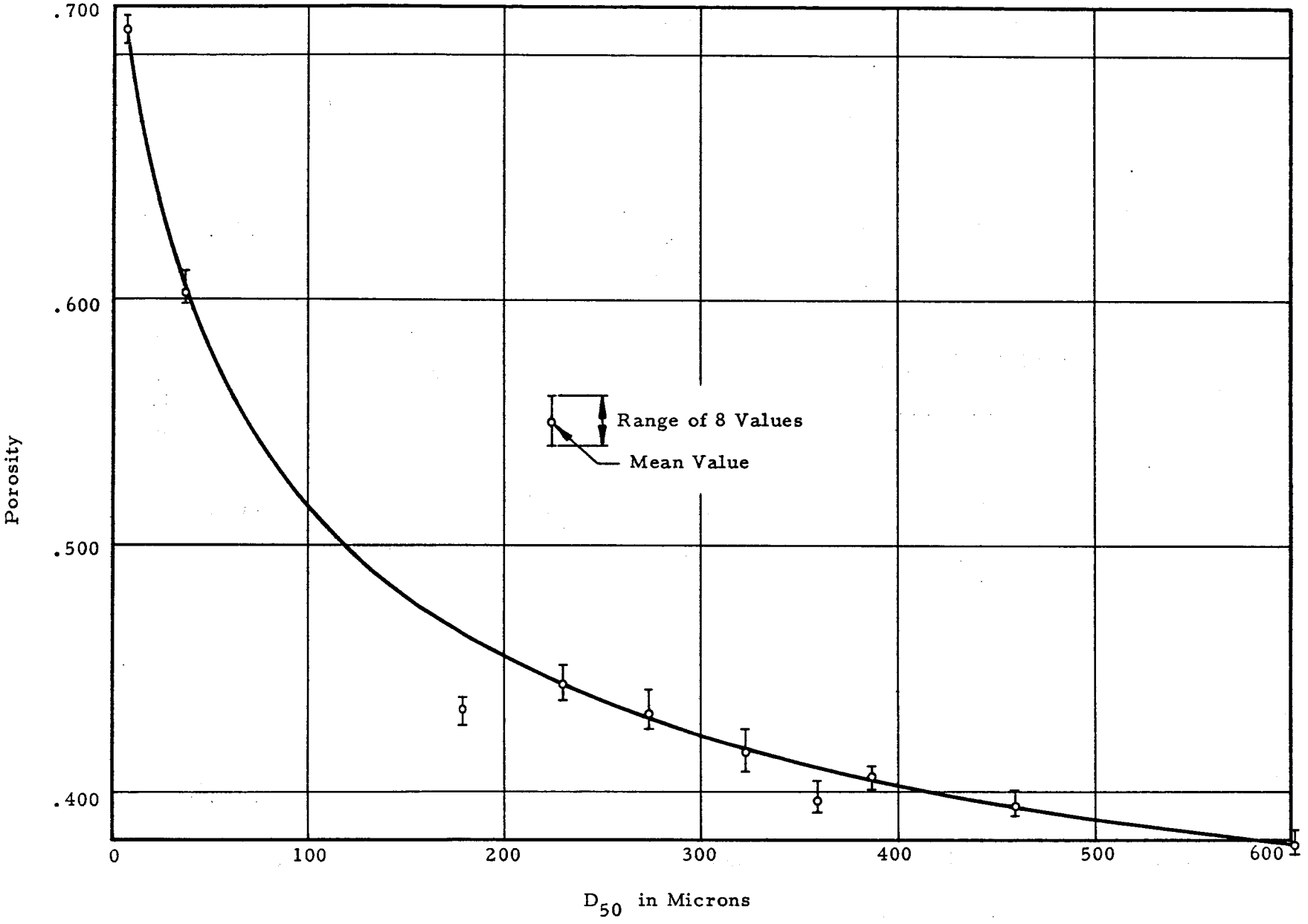

Fig. 18 POROSITY AS A FUNCTION OF GRAIN SIZE FOR SILICA DEPOSITED IN ATMOSPHERE

experiments when the soil was deposited under vacuum conditions. The angle of repose of the various materials is shown as a function of pressure in Figs. 19, 20, and 21. It may be seen that for all materials the angle of repose appeared to decrease with a decrease in pressure. This would indicate that the angle of internal friction of the material decreased under vacuum since for a dry cohesionless material the angle of repose is approximately equal to the angle of internal friction. However, the material used in this investigation was not totally cohesionless. It should be pointed out that the angle of repose has no real significance for a material which exhibits an apparent cohesion such as the soils used in these investigations. This decrease in angle of repose with a decrease in pressure may be explained by the increased mobility of the soil grains which will be discussed below and cannot be used as a measure of the shear strength of the soil.

F. General Behavior of Soil Under Vacuum

It was observed during the experiments that under high and ultra-high vacuum conditions the material scattered much more widely over the inside of the chamber than under atmospheric conditions. This was attributed to the lack of frictional resistance of the air which allowed the particles to travel over greater distances upon collision with others. Also the removal of adsorbed gas layers on the particles may have caused the impact between particles to be more elastic under these conditions than in the atmosphere or even at low vacuum levels.

Adhesion between the soil and the stainless steel interior of the vacuum chamber occured under hard vacuums. In some cases considerable deposits of soil were built up on the walls of the chamber and the bronze sieve. This can be seen in Fig. 7. This effect was more pronounced for the fine grained samples than for the coarser grained olivine.

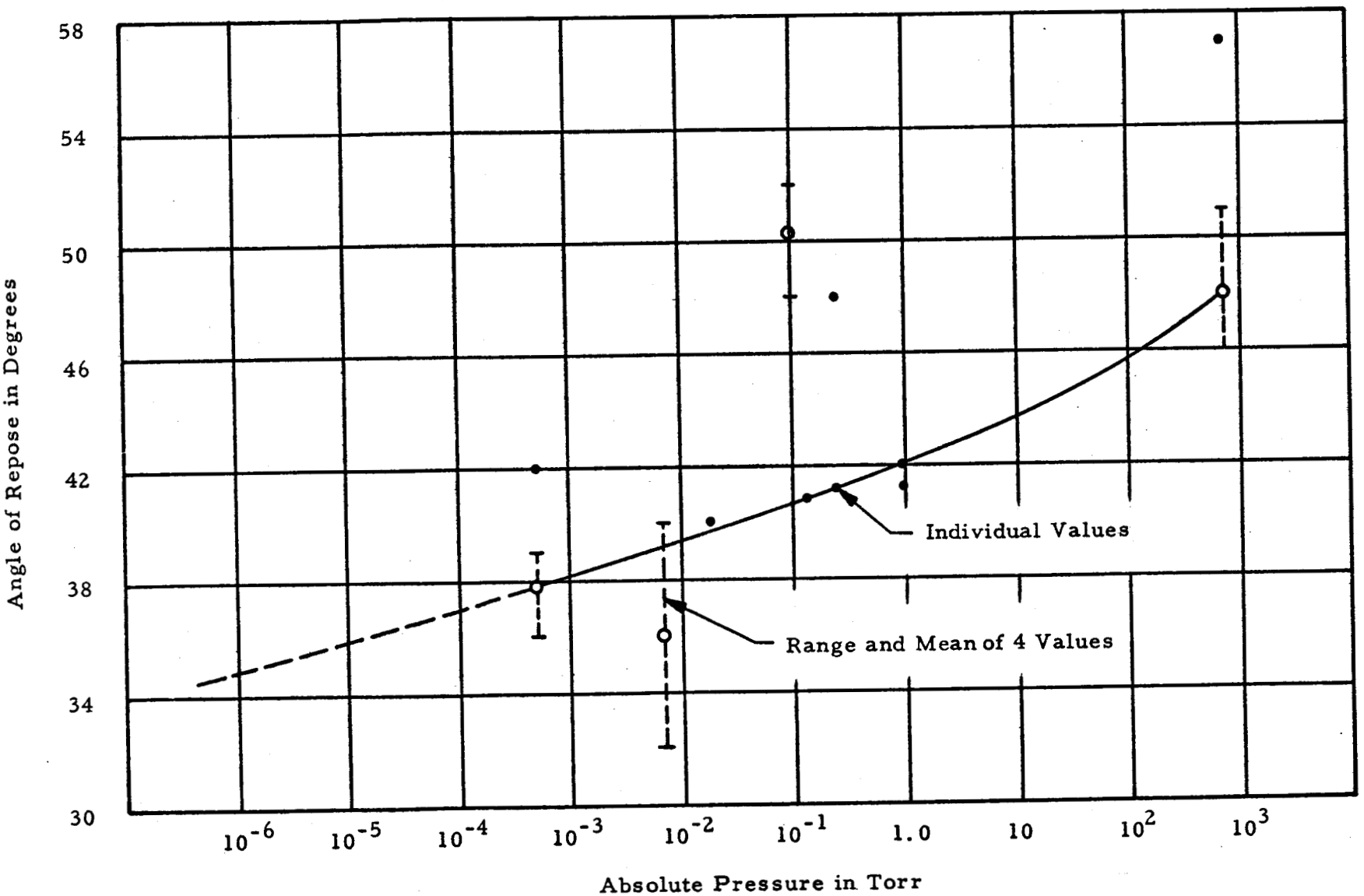

Fig. 19 ANGLE OF REPOSE OF SILICA FLOUR AS A FUNCTION OF PRESSURE

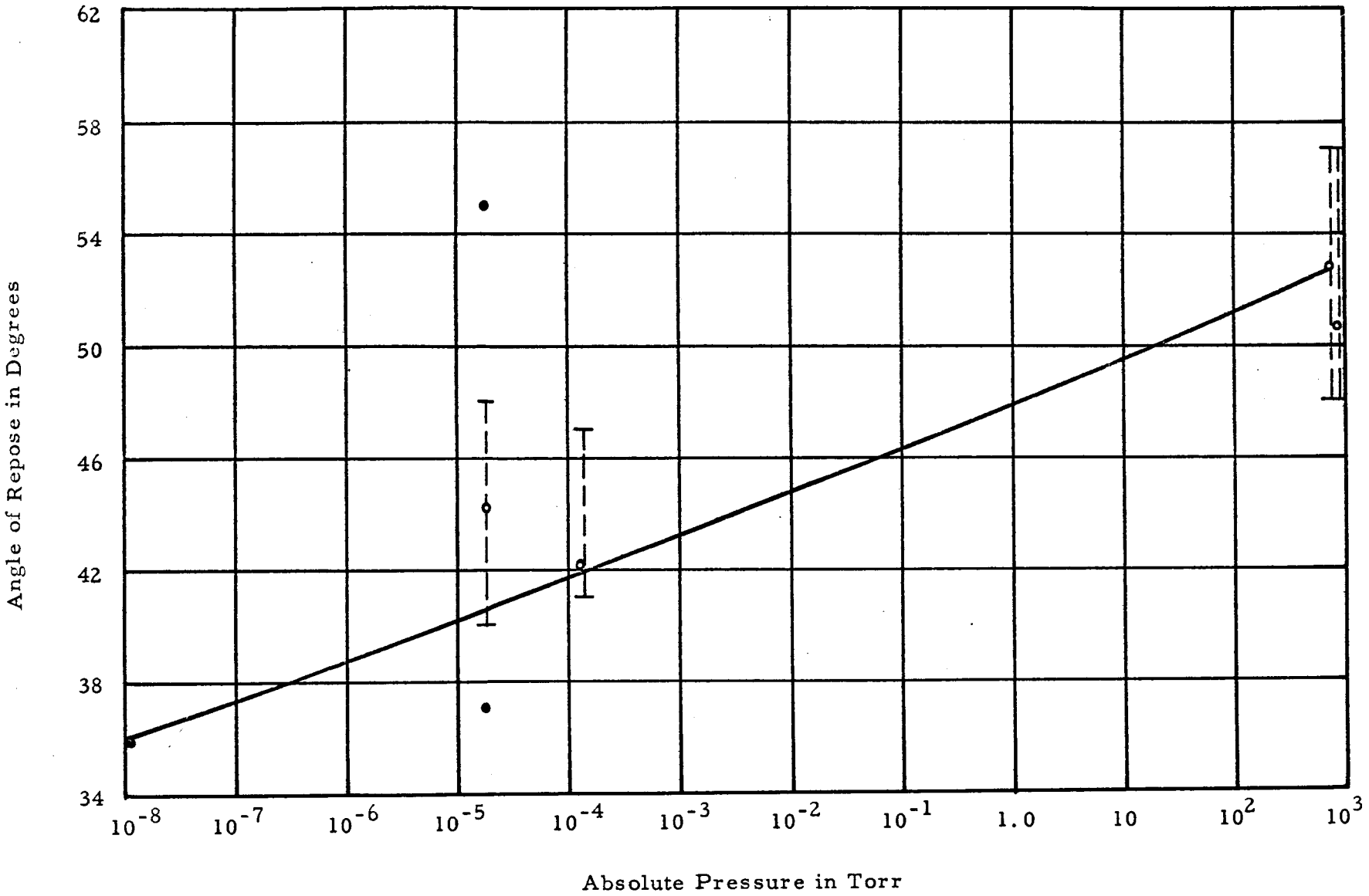

Fig. 20 ANGLE OF REPOSE OF COARSE GRAINED OLIVINE AS A FUNCTION OF PRESSURE

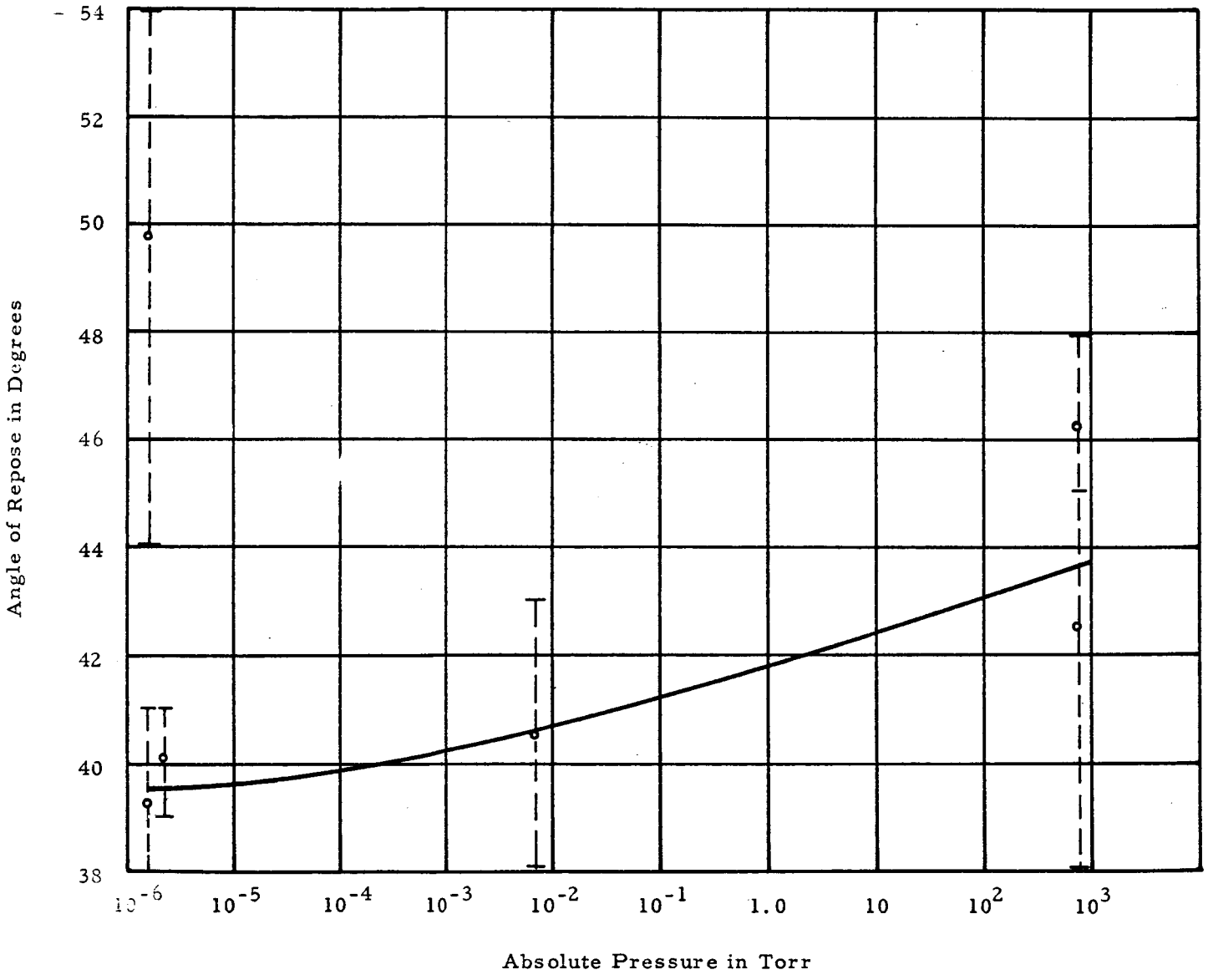

Fig. 21 ANGLE OF REPOSE OF FINE GRAINED OLIVINE AS A FUNCTION OF PRESSURE

VII. DETERMINATION OF SHEAR STRENGTH PARAMETERS UNDER VACUUM

The most direct means of studying the shear strength of soil is by means of either triaxial compression or direct shear tests. Because of limitations on attainable vacuum levels imposed by the outgassing of rubber membranes necessary in triaxial testing, it was decided to use direct shear tests in this investigation. This method consists of prescribing a failure plane in the soil on which the shear stress and normal stress are known. The curve defined by plotting the shear stress at failure as a function of the normal stress is referred to as the Mohr's rupture diagram. This curve is generally a straight line except near the origin for granular materials close to or at the critical density and at stress levels at which deformation of the particles occurs. From this diagram the shear strength parameters ϕ (the angle of internal friction) and C (the apparent cohesion) may be determined, the slope of this line being equal to tan ϕ and C being the intercept at the axis of zero normal stress.

There has been some criticism of the direct shear method for the determination of the shear strength parameters of earth soils. One disadvantage of the method is the reduction of the area of the failure surface due to relative movement of the two parts of the apparatus. A displacement of 10 per cent of the diameter of the ring will cause a reduction in area of approximately 10 per cent. However, friction developed between the soil and metal of the apparatus also produces a resistance to displacement. Thus, the error which is introduced is due to the difference between the coefficient of friction of the soil on the metal of the shear box and the internal friction of the soil itself. This difference is usually small and as is pointed out below, the normal stress at the outer edge and the resulting shear stress at this point are small. Therefore, the error introduced would be expected to be small.

It is obvious that the shear stress is not uniform over the area of the failure surface. If one considers an infinitesimal element at the point A shown in Fig. 22 (a) the state of stress would be as shown in Fig. 22 (b). In the ideal situation in which there is no friction between the walls of the shear box and the soil, the shear stress τ_{xz} at this point must be equal to zero and hence τ_{zx} must also equal zero. At point B, B' or O the shear stress $\tau_{xz} = \tau_{zx}$ will have some magnitude but must be equal to zero again at point A'.

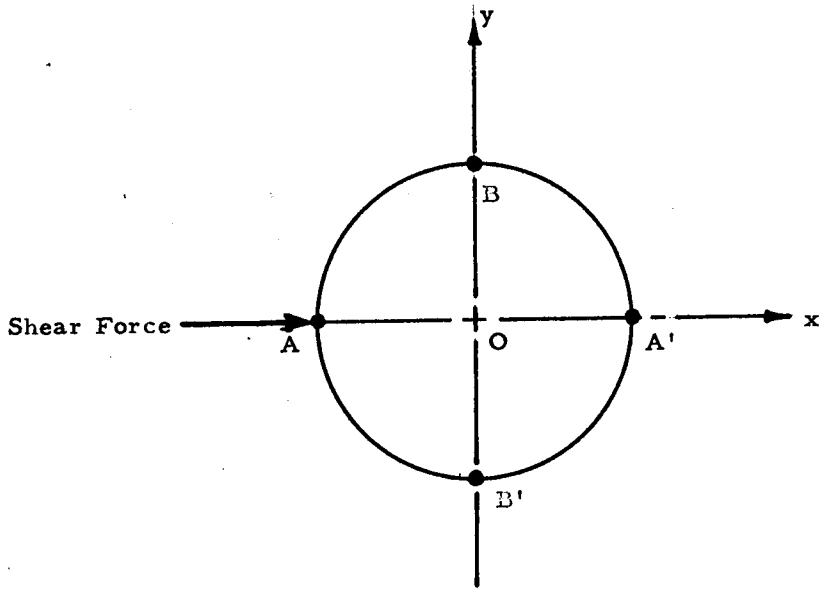

a) Shear Surface in Direct Shear Specimen

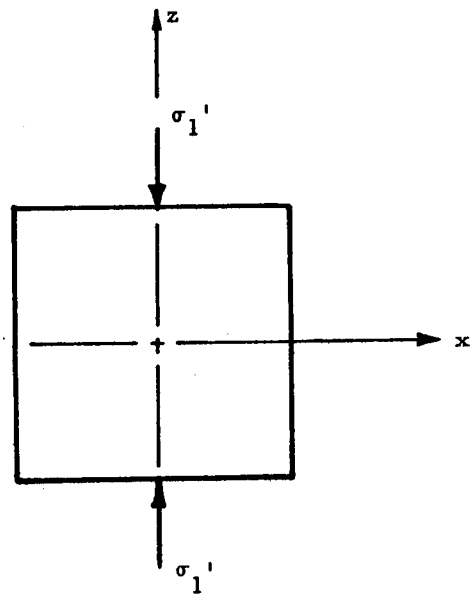

b) State of Stress at Point A

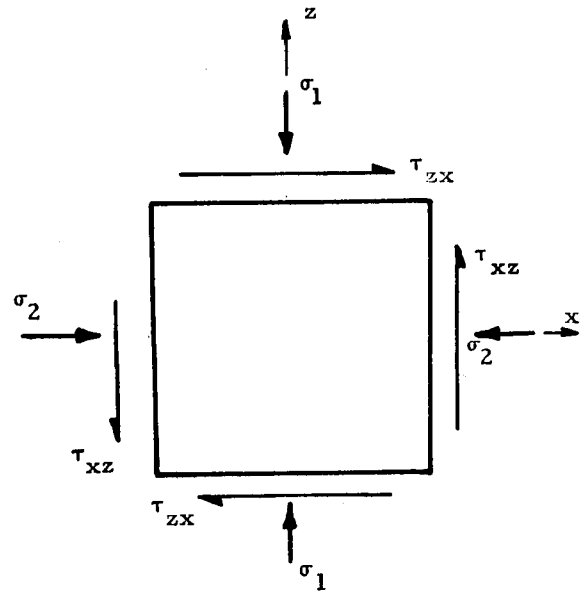

c) General State of Stress at a Point

Fig. 22 STATE OF STRESS IN DIRECT SHEAR TEST

Therefore, due to symmetry about line yy it would be expected that the shear stress on the failure surface increases from zero at points A and A' to a maximum along line yy. Also due to friction along the walls of the shear box the normal stress is not uniformly distributed over the failure area. Thus, when the average shear stress is plotted as a function of the average normal stress to determine the Mohr's rupture diagram this does not always represent the state of maximum stress within the material. However, for a material which exhibits plastic properties and in which failure occurs in the plastic region, the maximum shear stress at failure would be quite close to the average.

It should be noted that failure of the soil in the direct shear test does not occur on a plane but rather along some finite height of the sample as shown in Fig. 23(a). A modification of the conventional test has been suggested by Roscoe (35) and is as shown in Fig. 23(b). In this method failure occurs along the entire height and eliminates the undesirable reduction in area with shearing strain. It also gives a more realistic representation of shear within the soil, and could be easily adopted to testing of soils under vacuum.

Another disadvantage of the use of this method, particularly in studies of this type involving the testing of materials under vacuum, is that of friction developed within the apparatus itself. This limitation was recognized in the design of the equipment used in these studies and, as is described below, the shear box was supported on ball bearings. A test was performed in a vacuum of 1.1×10^{-8} torr with no soil in the apparatus and a normal load of 1.7 lbs applied to the shear box. The shear force required to displace the upper ring relative to the bottom under these conditions was not measureable.

For these first shear studies under ultra-high vacuums the more conventional and simpler method of direct shear was considered to be the more desirable at the expense of permitting the relatively small inaccuracies described above. The apparatus used in these experiments is shown in Figs. 24 and 25 and schematically in Fig. 26. To minimize outgassing , the entire equipment except for the force transducer was made of stainless steel. The apparatus was very similar to the conventional direct shear apparatus and consisted of a two piece cylindrical mold into which the soil sample was placed. The upper part of the mold was then displaced relative to the lower part which then prescribed the shear failure plane. The normal force was applied through

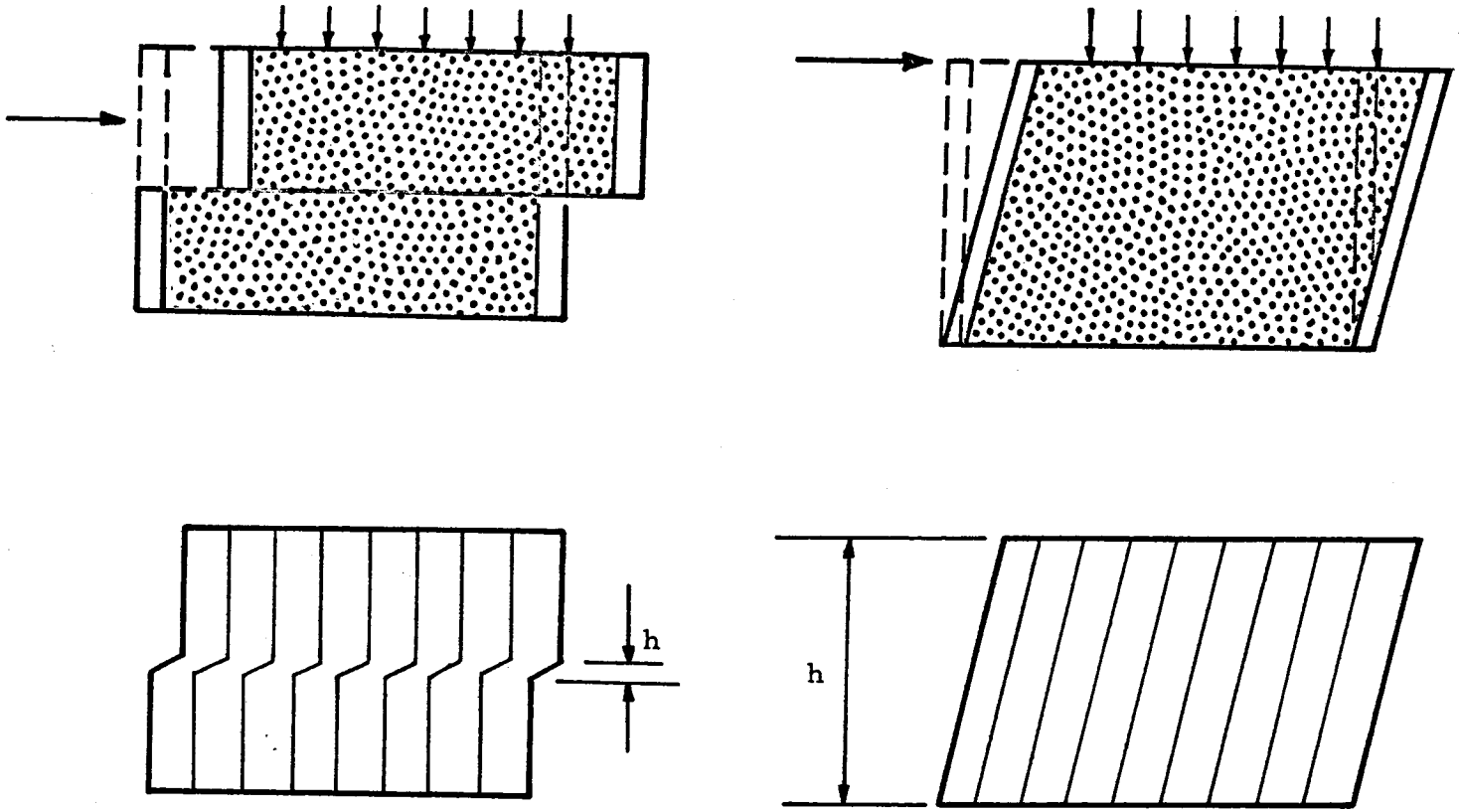

(a) Failure of Soil in Conventional Direct Shear Test

(b) Failure of Soil in Modified Direct Shear Test

Fig. 23 FAILURE OF SOIL IN THE DIRECT SHEAR TEST

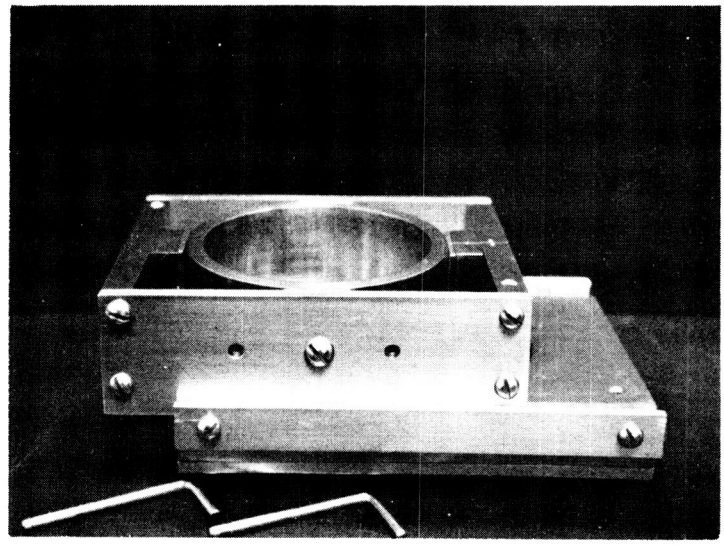

Fig. 24 DIRECT SHEAR BOX FOR USE IN VACUUM

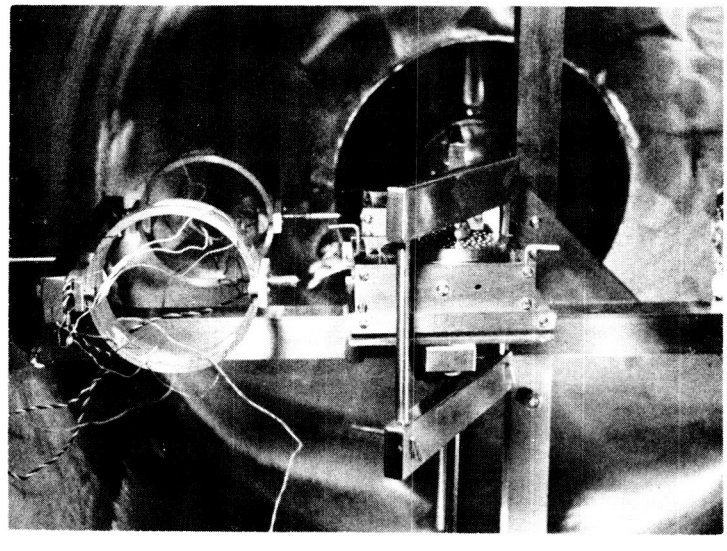

Fig. 25 DIRECT SHEAR APPARATUS IN VACUUM CHAMBER

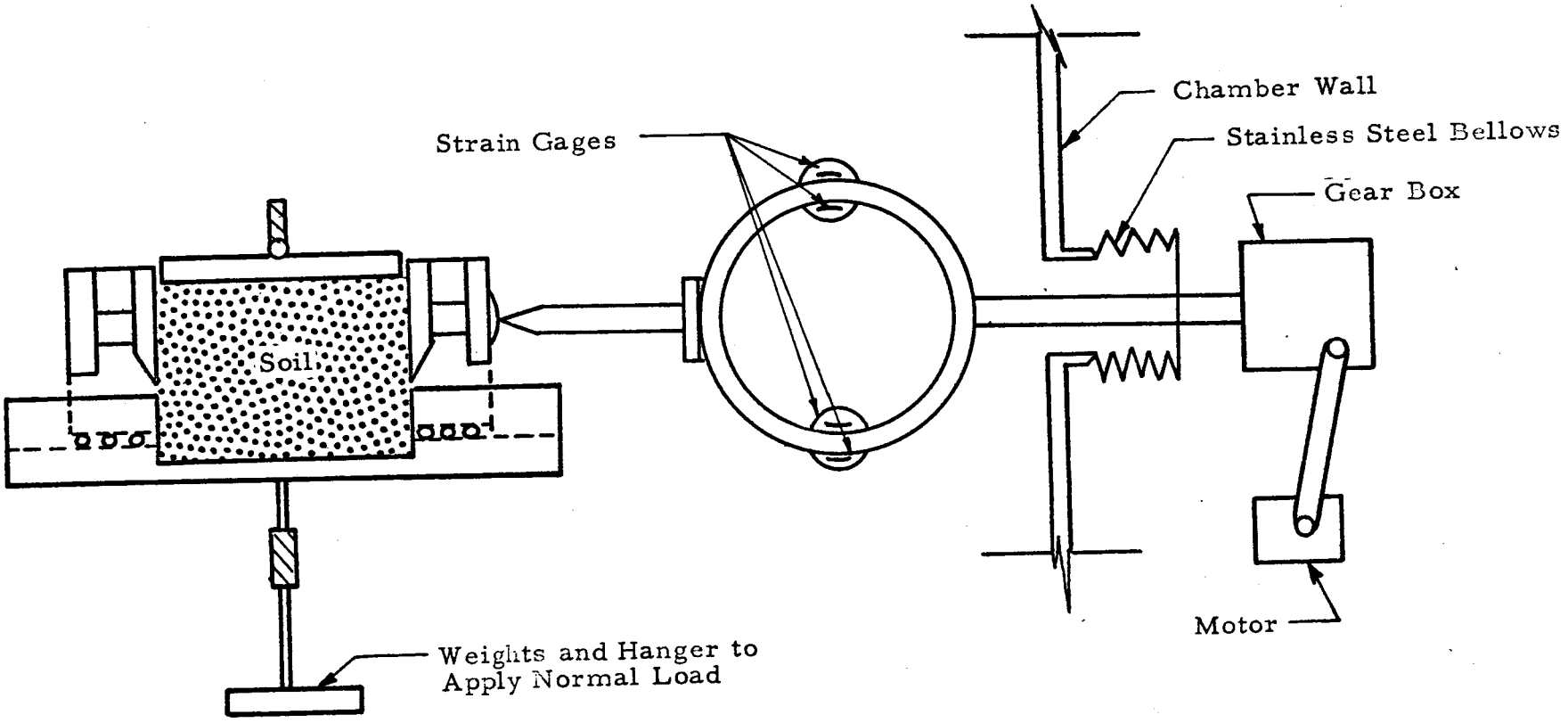

Fig. 26 SCHEMATIC DIAGRAM OF DIRECT SHEAR APPARATUS

a movable perforated cover by means of a hanger and weights. To reduce friction in the apparatus the upper part was supported on stainless steel balls with a clearance between the two parts no greater than .005 in.

The shear force was measured by means of a thin aluminum ring with four, 1/8 in. foil strain gages covered with high-vacuum epoxy and mounted as shown in Fig. 26. These then formed the four active elements of a wheatstone bridge which was calibrated for the load on the ring.

After the apparatus had been developed and had been used successfully under vacuum conditions, an identical second shear box was constructed and mounted in the chamber together with the first. This permitted two tests to be performed simultaneously under identical vacuum levels.

The average shear stress required to produce movement of the upper ring of the shear box was plotted as a function of the displacement and the peak value of stress plotted as a function of the normal stress to determine the Mohr's rupture diagram.

Experiments were conducted using the silica flour (Fig. 2, curve a) and the finer grain sized olivine (Fig. 2, curve c). Pressure levels ranged from 760 to 8×10^{-10} torr. The vacuum levels were attained using an oil diffusion pump system with drawdown times as long as 101 hours for pressures in the 10^{-10} torr range. Due to the epoxy coating on the strain gages used for the shear force measurements inside the vacuum chamber only moderate bake-out temperatures (250° F) could be tolerated. The vacuum levels which could be achieved depended greatly on the length of the bakeout period which was extended to 72 hours to achieve pressures in the 10^{-10} torr range. As was discussed previously, it was observed that during shear deformation of the soil specimen there was an increase in the pressure in the chamber. It should be noted, therefore, that the pressure level which is reported for the various experiments is the pressure prior to shearing the soil and that the true environmental pressure on the surface of failure is undoubtedly somewhat greater.

The porosity of the soil samples used in the tests was controlled by placing the soil in the apparatus at the highest porosity achievable and then consolidating it under the maximum normal load used in any test. This re-

sulted in fairly uniform porosities of the various samples. Excluding the one highest and one lowest values obtained which were .586 and .549, the porosities on silica flour ranged from .560 to .576 (< 3%) with an average of .570 for all tests. The porosities in the olivine samples ranged from .622 to .644(<4%) with an average of .633 excluding the one highest and one lowest value which were .647 and .609.

A. Results of Direct Shear Tests on Silica Flour

In Fig. 27 are plotted typical curves showing the shear stress as a function of the displacement for a representative number of direct shear tests on silica flour. It can be seen that all curves have the same general shape. However, in the region between the point at which the slope of the curve begins to change (analagous to the proportional limit) and the peak value of stress, the displacement produced by any particular value of shear stress was greater under atmospheric conditions than under vacuum. It may also be seen that under high vacuum levels the displacement corresponding to any value of shear stress was greater than under ultra high vacuum levels but less than in atmospheric tests. Thus, a decrease in the environmental pressure caused an increase in the resistance to shear displacement, i.e., stiffness of the soil.

Mohr's rupture diagram for silica flour at various pressure levels is shown in Fig. 28. From this the values of apparent cohesion (C) and internal friction (tan ϕ) of the soil at various pressure levels were determined and plotted as a function of pressure in Fig. 29. It is evident from Fig. 29 that at pressure levels of 10^{-6} torr and above, the pressure had a negligible effect on the internal friction, but below this the friction showed an increase with a decrease in pressure. The apparent cohesion showed some increase even at relatively low pressure. However, a pronounced increase of cohesion as a function of vacuum took place at approximately 10^{-7} torr and at 10^{-9} torr was as much as twice the atmospheric value. Thus, the silica flour exhibited a considerable increase in shear strength as the vacuum level increased, the major portion of which was due to an increase in apparent cohesion.

B. Results of Direct Shear Tests on Olivine

Typical curves showing the shear stress as a function of the displacement in the olivine (Fig 2, curve c) are contained in Fig. 30. It can be seen

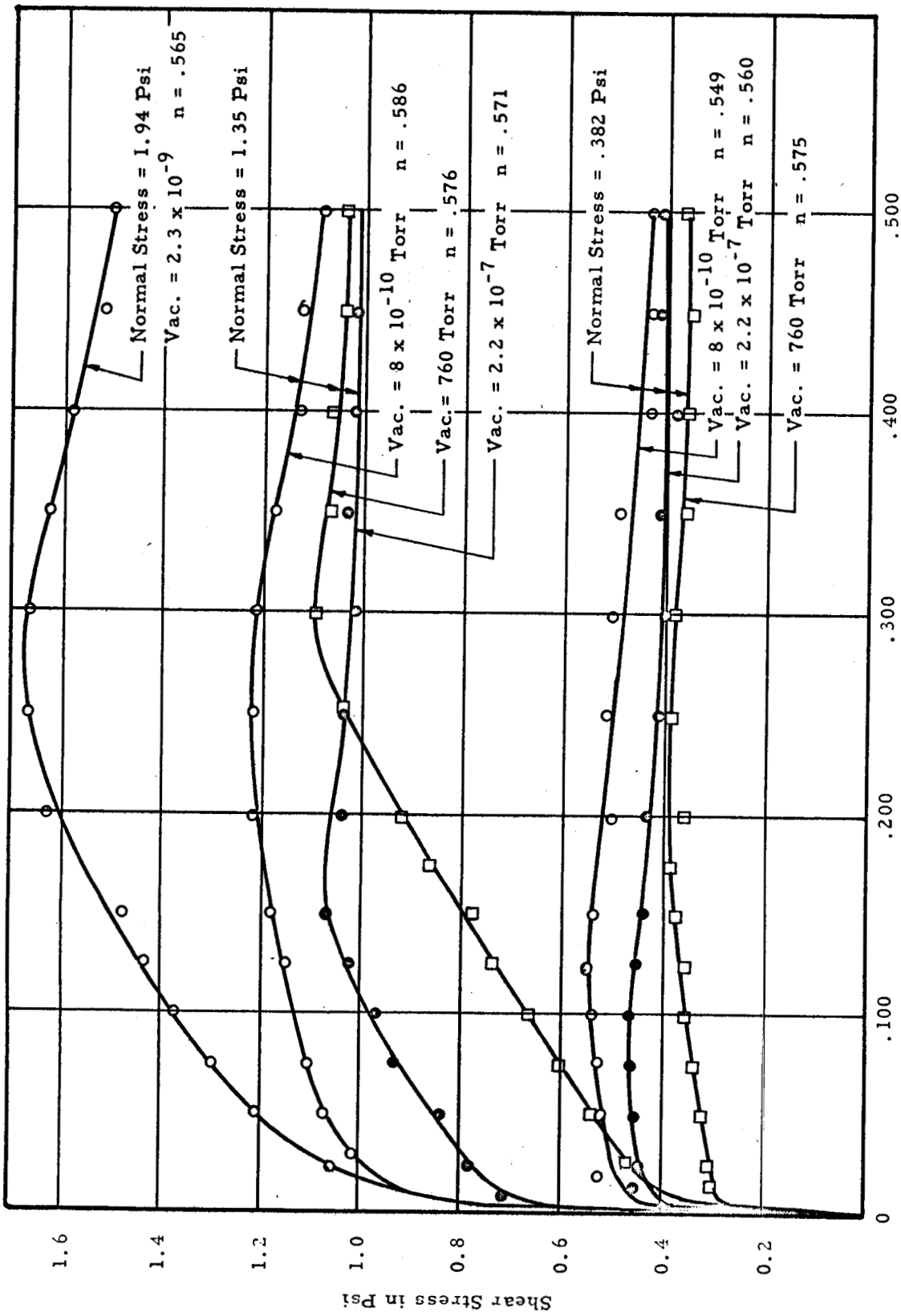

Fig. 27 SHEAR STRESS AS A FUNCTION OF DISPLACEMENT IN SILICA FLOUR FROM DIRECT SHEAR TESTS

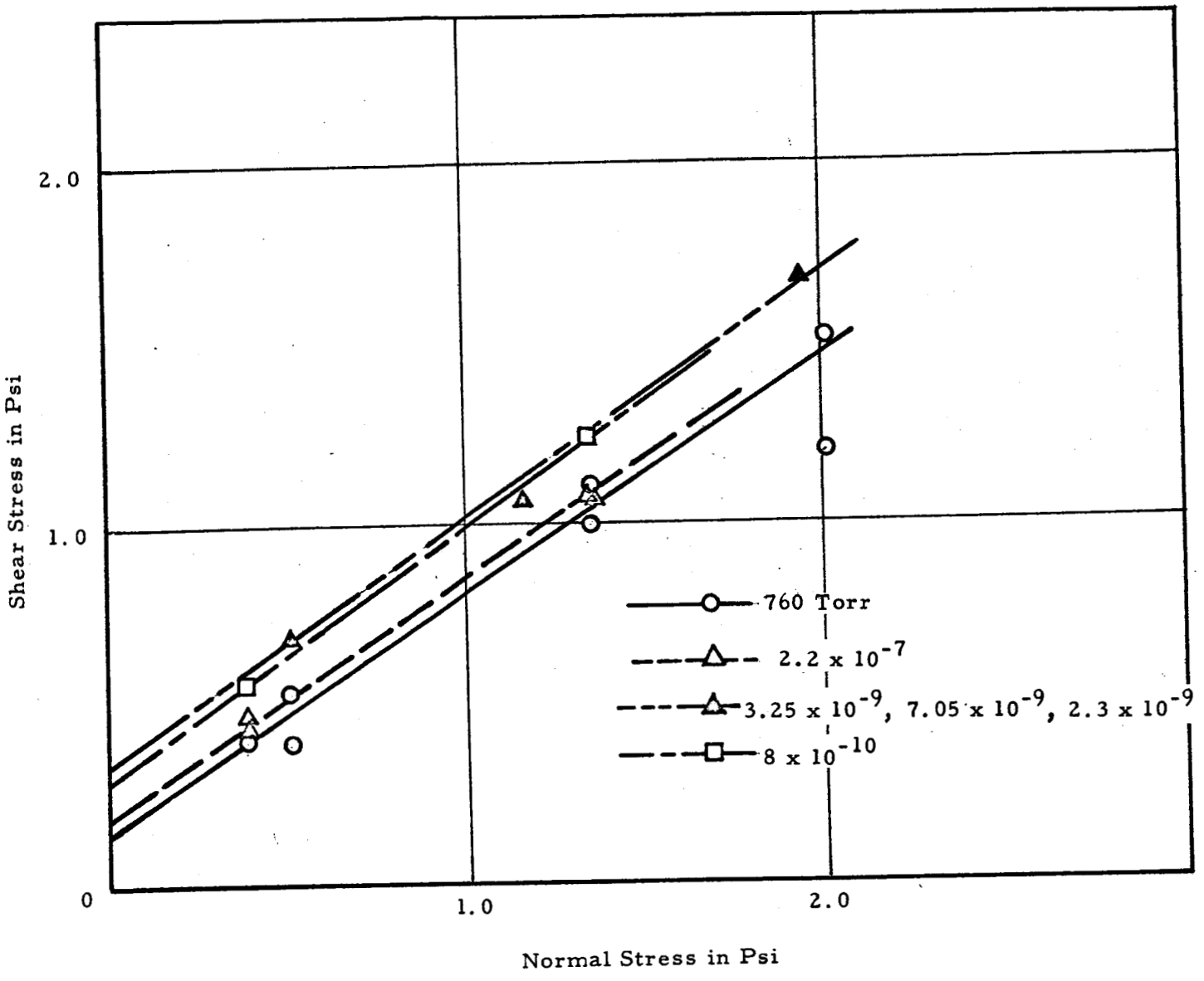

Fig. 28 MOHR'S RUPTURE DIAGRAMS FOR SILICA FLOUR AT VARIOUS VACUUM LEVELS

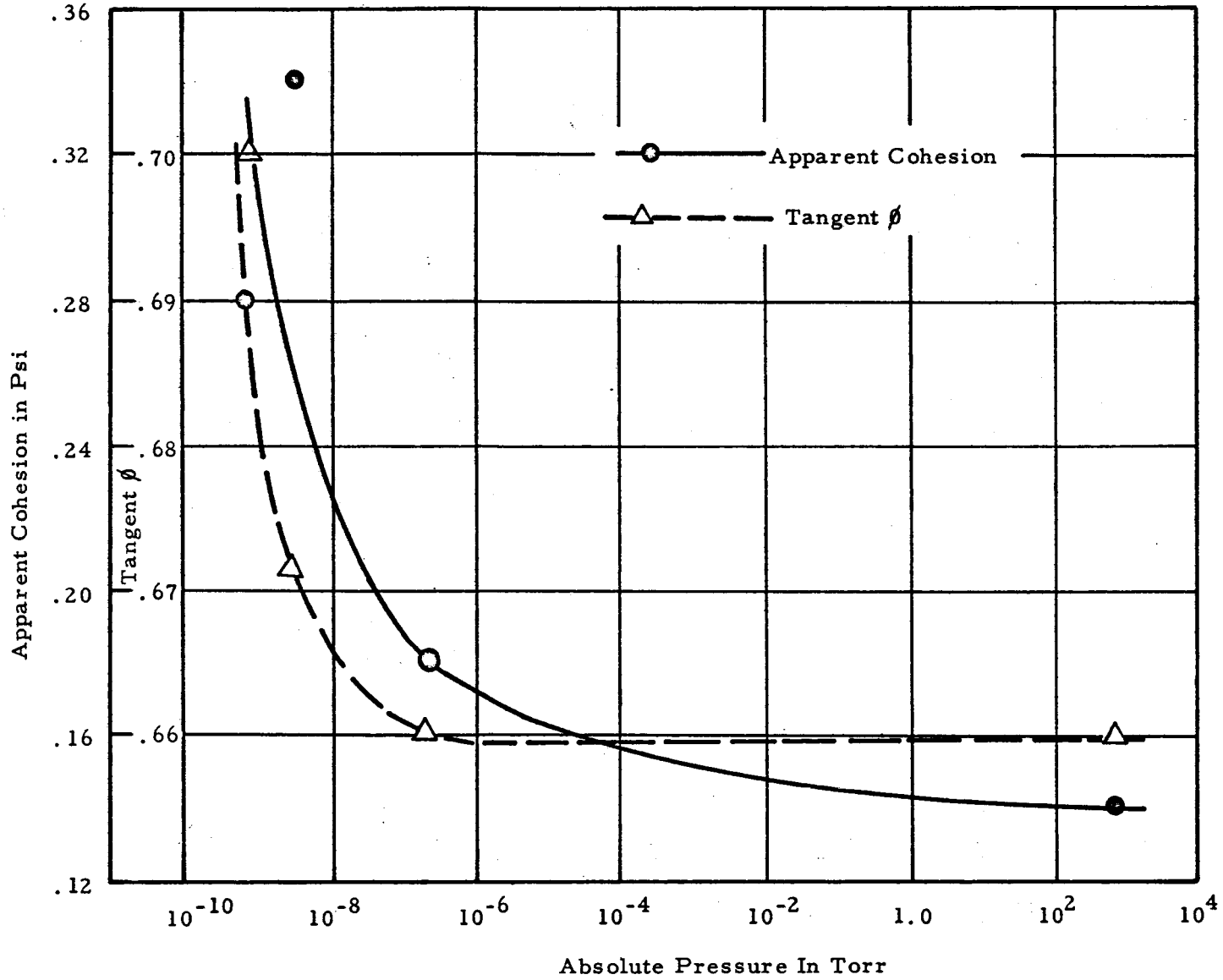

Fig. 29 APPARENT COHESION AND INTERNAL FRICTION OF SILICA FLOUR AS A FUNCTION OF VACUUM

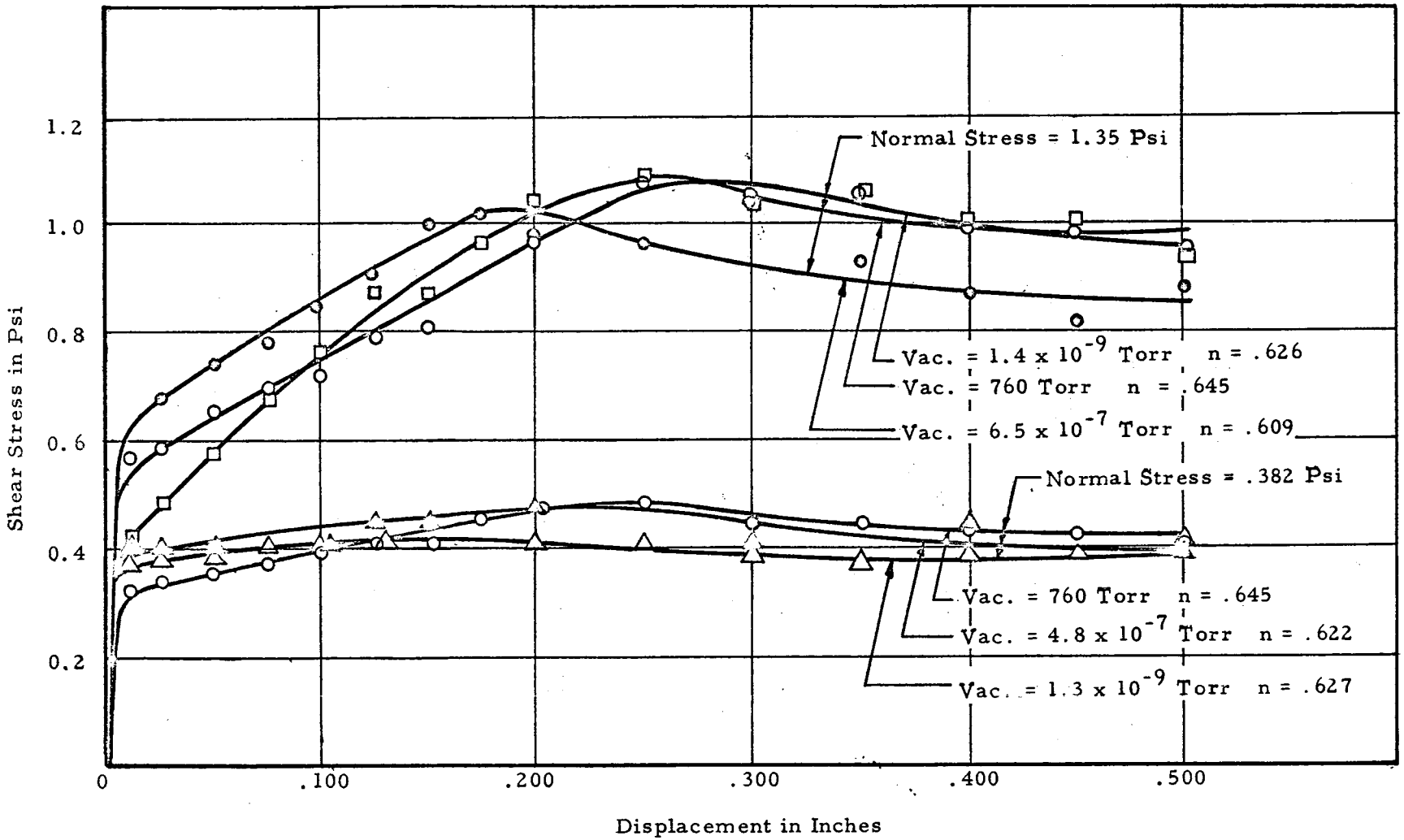

Fig. 30 SHEAR STRESS AS A FUNCTION OF DISPLACEMENT IN OLIVINE IN IN DIRECT SHEAR TESTS

from this figure that all curves have essentially the same characteristic shape and the displacements corresponding to particular values of shear stress do not differ greatly under various vacuum levels. Thus, the stiffness of the olivine was not affected appreciably by the vacuum as was the case with the silica flour. Mohr's rupture diagrams for the olivine under atmospheric and vacuum conditions are shown in Fig. 31, and the values of apparent cohesion (C) and internal friction (tan ϕ) are plotted as functions of the pressure in Fig. 32. Again it should be noted that the pressures plotted are those prior to starting the shear test. On the basis of these limited data it is difficult to draw any general conclusions; however, it appears that pressure levels above 10^{-6} torr have little effect on the shear strength of the olivine, but at pressures below this the apparent cohesion decreases while the internal friction increases.

C. General Observations in Direct Shear Tests

Temperature effects were not included in the present investigation and all the direct shear tests were performed at room temperature. However, due to failure of an ion gage during the bakeout period in one experiment on silica flour it was necessary to perform that test at a temperature of approximately 200°F. The results of this test showed a considerably greater shear resistance. Since the force transducer was not calibrated for elevated temperatures it was not possible to say definitely if this apparent increase was due to a change in the sensitivity of the transducer or to an increase in shear resistance of the soil. However, the transducer consisted of four active elements and should have been temperature compensating. It is believed, therefore, that changes in temperature of this magnitude would have minor effects on the sensitivity of the gage and the major portion of the increase should be attributed to increases in the shear strength of the soil with temperature.

It was demonstrated previously (Section V) that the vacuum in the soil pores is generally less than that in the chamber. Since the soil was considerably more confined in the direct shear apparatus than in the other apparatus the pressures in the soil pores might well be expected to be as much as two orders of magnitude greater than that in the chamber. It is interesting to note that this makes the vacuum levels at which the apparent cohesion and internal friction began to increase, as determined from the direct shear tests, more consistent with those levels at which the porosity of the soil also began to

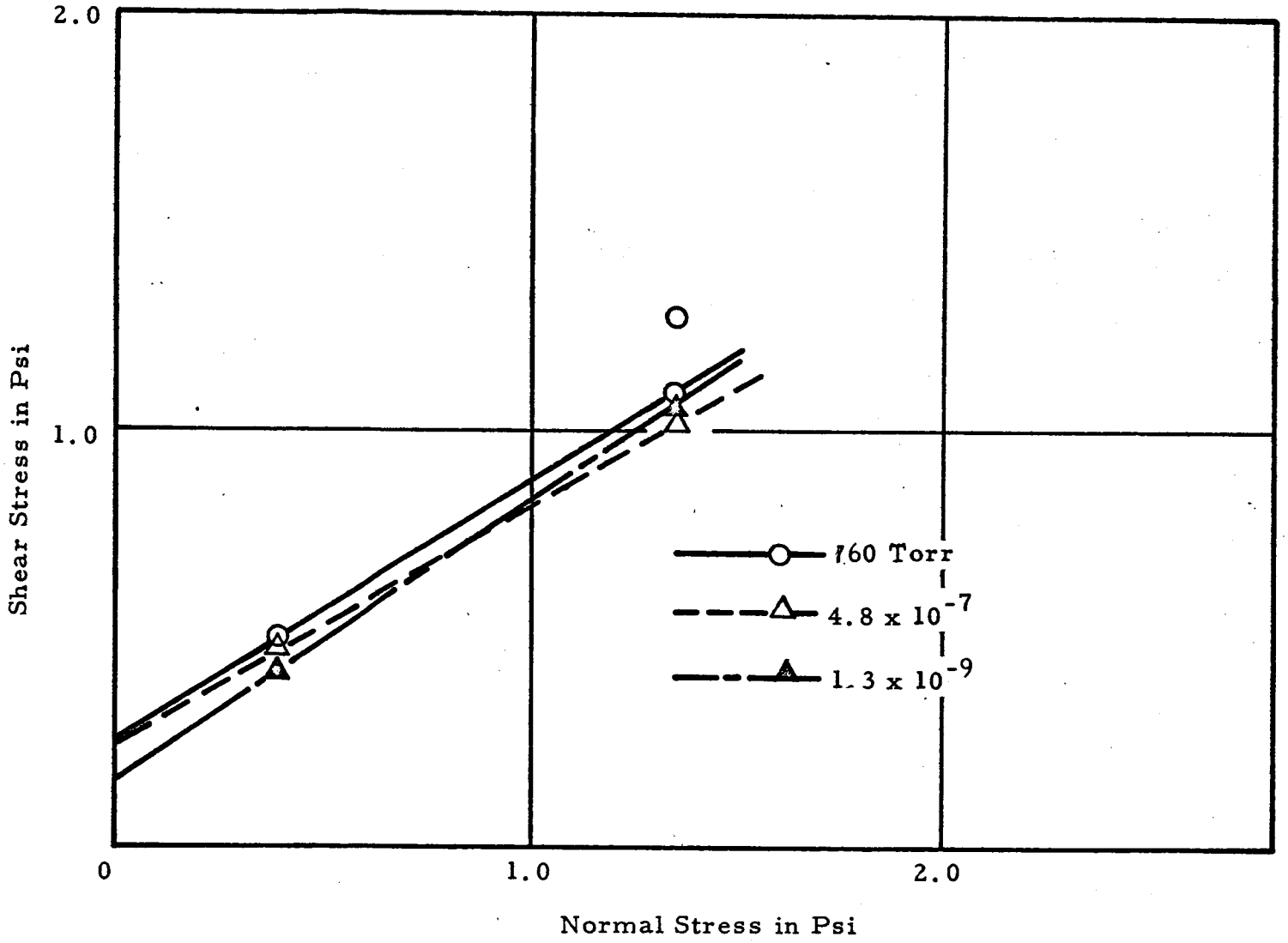

Fig. 31 MOHR'S RUPTURE DIAGRAM FOR FINE GRAINED OLIVINE AT VARIOUS VACUUM LEVELS

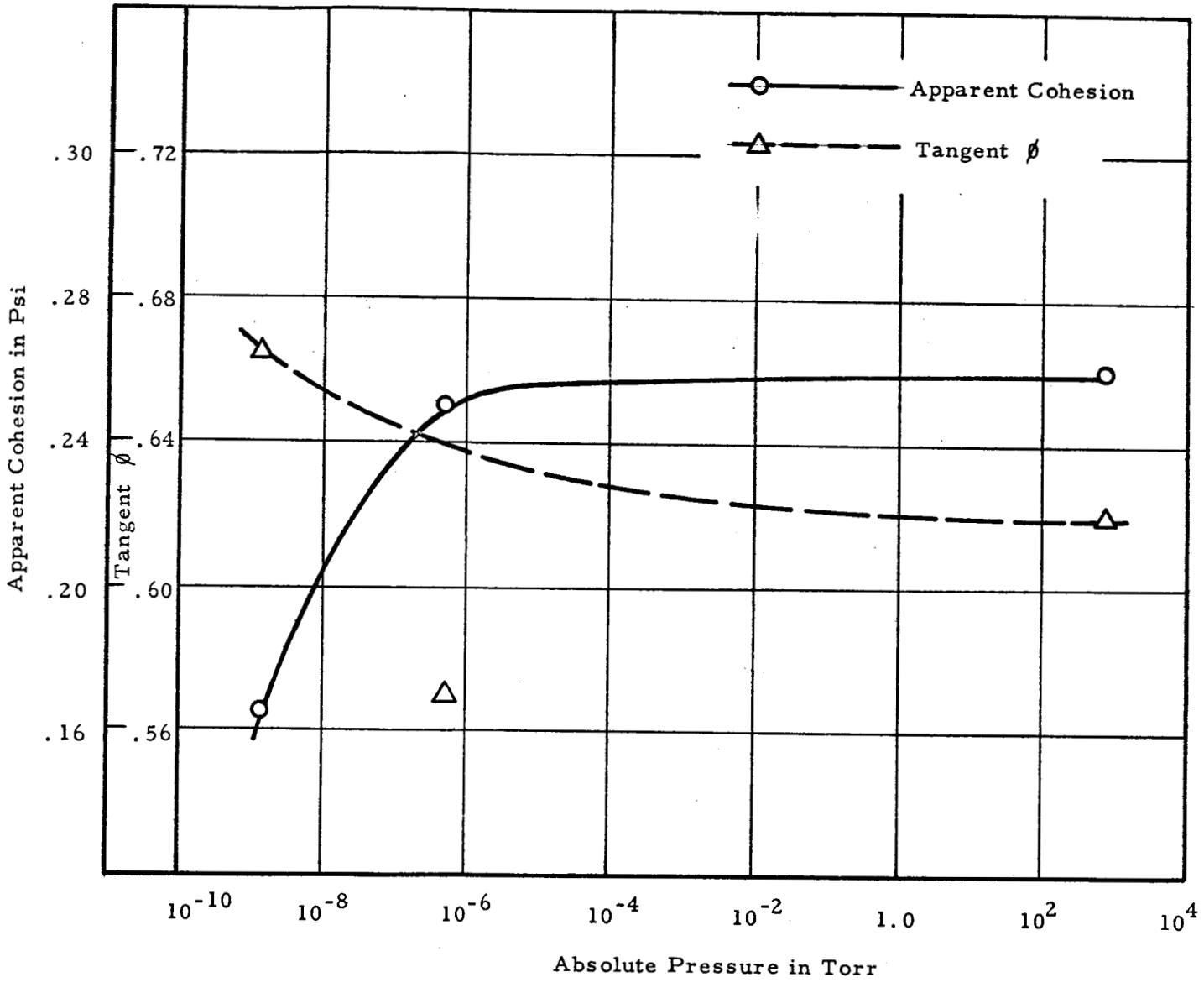

Fig. 32 APPARENT COHESION AND INTERNAL FRICTION OF FINE GRAINED OLIVINE AS A FUNCTION OF VACUUM

increase.

It can be seen from Fig. 29 that the apparent cohesion of the silica flour appears to increase without bound for increases in vacuum. However, the upper bound of the cohesion which the soil could attain would be that of a porous rock formed by cold welding of the individual soil grains. The lower bound (Fig. 32) would be that of a mobile dust as suggested by Gold (5). This could even have a negative value i.e., it would require the application of force to prevent movement of the grains relative to one another. This would result in a very unstable condition which is highly improbable since, under the combined effect of overburden pressure and ultra-high vacuum levels attractive inter-particle forces, seem more likely. This will be discussed in some detail in Section X.

VIII. BEARING CAPACITY OF SMALL FOOTINGS

An analysis of the data obtained in a previous internally sponsored program was carried out to investigate the possibility of establishing relationships which would permit prediction of load-settlement for sizes of loaded areas and unit loads outside those of the tests. Hopefully this could be extended to full size vehicles and landing craft.

This program consisted of the following:

1) Plate loading (2 inch square plates) and penetration measurements on simulated lunar dust performed at various vacuum levels.

2) Evaluation of bearing and penetration resistance as a function of dry density and environmental pressure.

3) Determination of apparent friction angle of the simulated lunar dust as a function of dry density at atmospheric pressure.

4) Development of techniques for measurement of physical properties of soil under high vacuum levels.

The bearing penetration tests performed under varying environmental pressures suggest that for the material used, both penetration resistance and load carrying capacity increase as the absolute pressure decreases. In Figure 33 the dimensionless parameters S/B and $q/B\gamma$ are used to determine the basic equation for penetration prediction in experiments conducted under atmospheric conditions. The proposed equation relates the settlement to the parameters y and m in the following manner.

$$\frac{S}{B} = y\left[\frac{q}{B\gamma}\right]^{m} \qquad \text{(a)}$$

where

S = settlement
B = width of footing
y = intercept on the S/B axis
q = load per unit area
γ = unit weight of soil
m = slope of the log-log plot

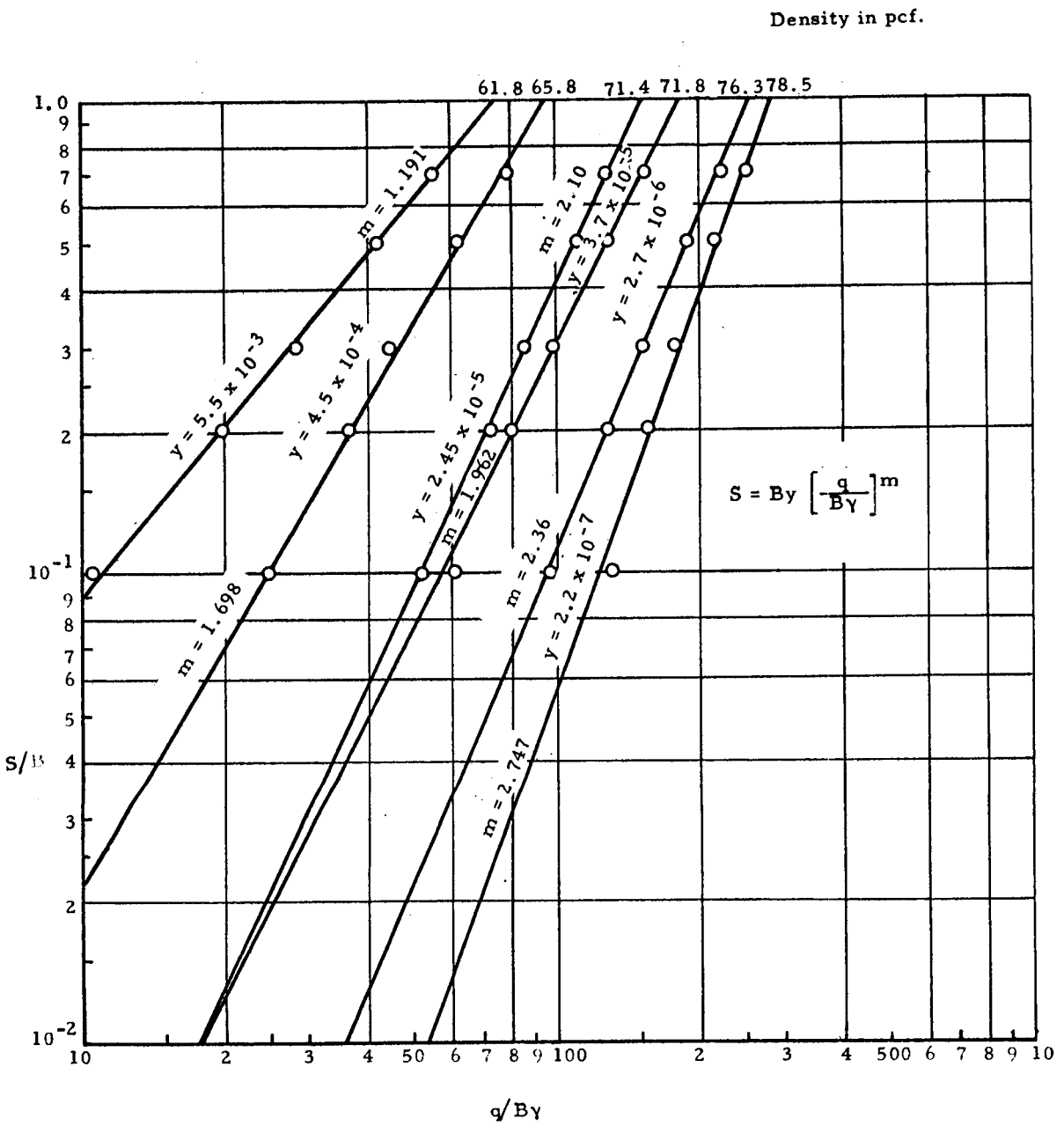

Fig. 33 S/B AS A FUNCTION OF q/By IN ATMOSPHERE

From previous studies conducted with dry silt (39), it was found that m remained constant, and for the particular silt tested, m was equal to unity. Hence, with m=constant, the equation can be written as,

$$S = By\left[\frac{q}{B\gamma}\right]^{\text{constant}} \qquad (b)$$

In Figure 33, however, m is a variable - perhaps due at least in part to the limitations of the Z/B ratio where Z is the depth of soil below the loaded area. It will be seen later (Figure 38) that with a larger Z/B ratio and a constant density, m could remain constant. There is also the possibility of pore air pressure affecting the m value for material within the particle size range 2-40 μ.

Because of the uncertainty regarding the possible influence that the size of the container which was used in these previous studies had on the results of the experiments, and in order to select a container and footing size which would permit further experiments to be performed in the limited space available in the vacuum chamber and still have a negligible effect of container size, a number of experiments were performed in the present program under atmospheric conditions using various container and footing sizes. The results of these experiments also provided some insight into what influence the size of the container had in the previous investigation.

Experiments were performed using three containers having widths of 6", 12" and 18" and depths of 6" and 16" to 18". Three square footings having widths of 1", 1-1/2" and 2" were used. The experiments were performed on silica flour and although it was attempted to maintain a constant density throughout the investigation, the densities varied from 61.5 to 69.4 #/ft^3 with an average density of 66.3 #/ft^3.

The average bearing pressure under the footings is shown as a function of the penetration in Figure 34. A comparison of curves a, b, and c with the other curves shows the effect of the container. Experiments a, b, and c were all performed using a 6" container. It can be seen that even a substantial change in the ratio Z/B (Curves a and b) does not affect the results greatly and, therefore, the major influence was probably due to friction along the walls of the container and arching developed in the soil below the footing as a

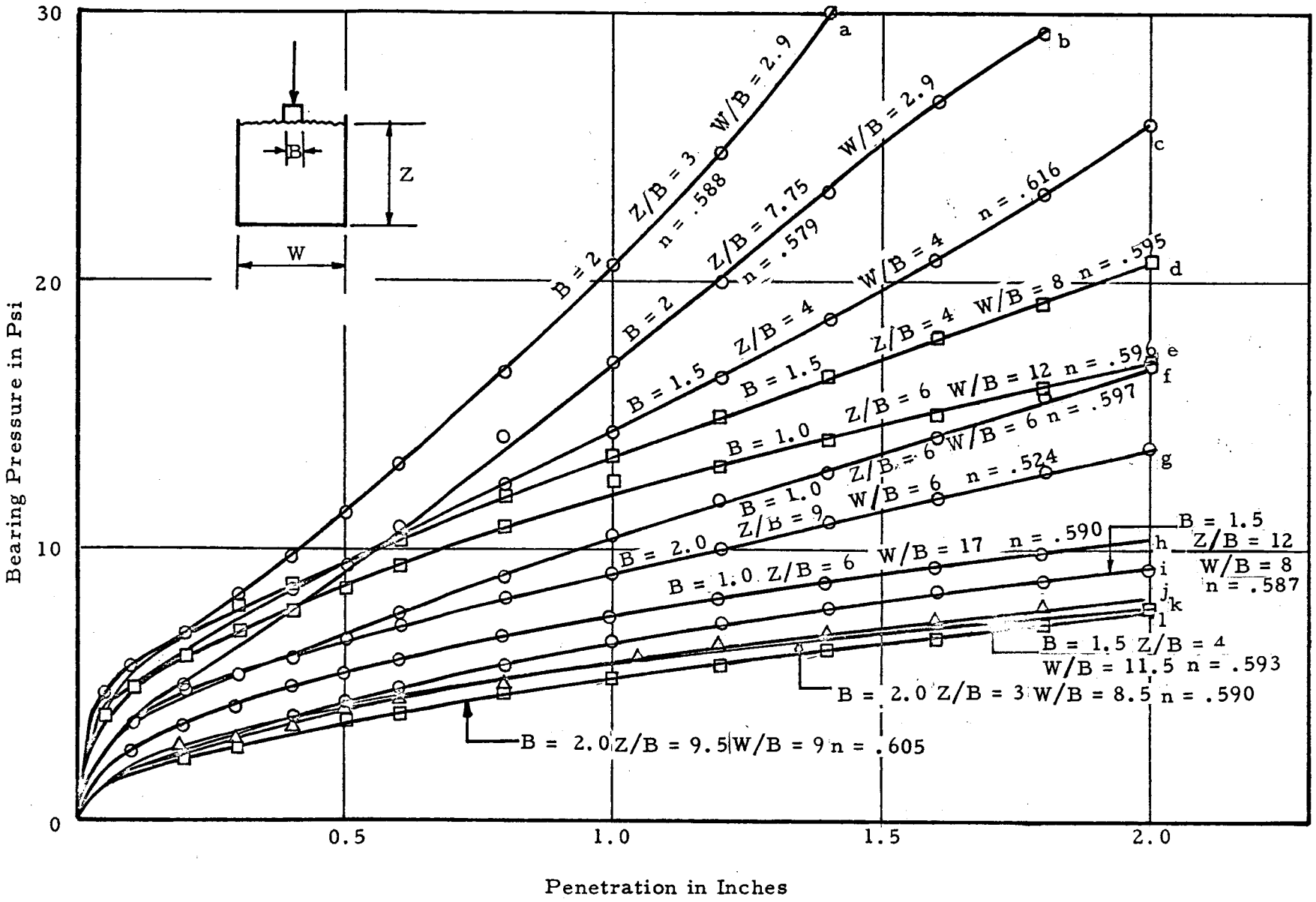

Fig. 34 AVERAGE BEARING PRESSURE UNDER FOOTING AS A FUNCTION OF PENETRATION FOR VARIOUS RATIOS OF Z/B AND W/B

result of this friction. This is demonstrated further in comparison of curves k and e in which the ratio W/B was large and in which an increase in the ratio Z/B from 3 to 9.5 produced an almost negligible effect on the bearing capacity. The curves do not show any definite ratio of Z/B or W/B for which the container size has no effect. There appears rather to be an interaction between the two ratios with the ratio W/B being the more important of the two. This can be seen in Figure 35 in which a combination of the two ratios and the porosity in the form $(Z/B)(W/B)^3 n$, in which Z, W and B are as shown in Figure 34 and n is the porosity, is plotted against the ratio of the bearing pressure at 1.0 in penetration to the lowest bearing pressure at 1.0in. penetration obtained from all the tests (curve 1, Figure 34). This curve obviously does not establish any relationship from which the container size effects can be determined but it does give an indication of the relative importance of the two ratios Z/B and W/B as they affect the bearing capacity. It should be noted, however, that the bearing capacity of the 1.0in. footing appeared to be affected by the smaller sized containers even though the quantity $\frac{ZW^3n}{B^4}$ was quite large. Thus, it would seem that the absolute size of the container should be considered as well as the ratio of footing size to container size.

The data presented in Figure 34 were plotted in dimensionless form and are shown in Figure 36. It can be seen that the slope of the curves does not change appreciably with changes in Z/B and W/B factors. However, the curves representing tests conducted in which these factors were small are not straight lines in the upper portion, the deviation from a straight line being greater for the small sample size. Although the data is too limited to be conclusive, it appears that containers having a W/B ratio greater than 8 and a Z/B ratio greater than 3 for a 2in. footing have a relatively small effect on the bearing capacity. It may also be said that the major portion of the variation in y and m in Figure 33 is due to changes in the dry density (γ) of the soil.

The variation between y and γ, and m and γ (Fig. 33) have been recorded in Figure 37. The procedure for calculating S from the settlement equation is as follows:

A. For the particular dry density the value of y is read in Figure 37 (y vs. γ curve). With the value of y obtained, the same Figure will yield the value of m (y vs. m curve).

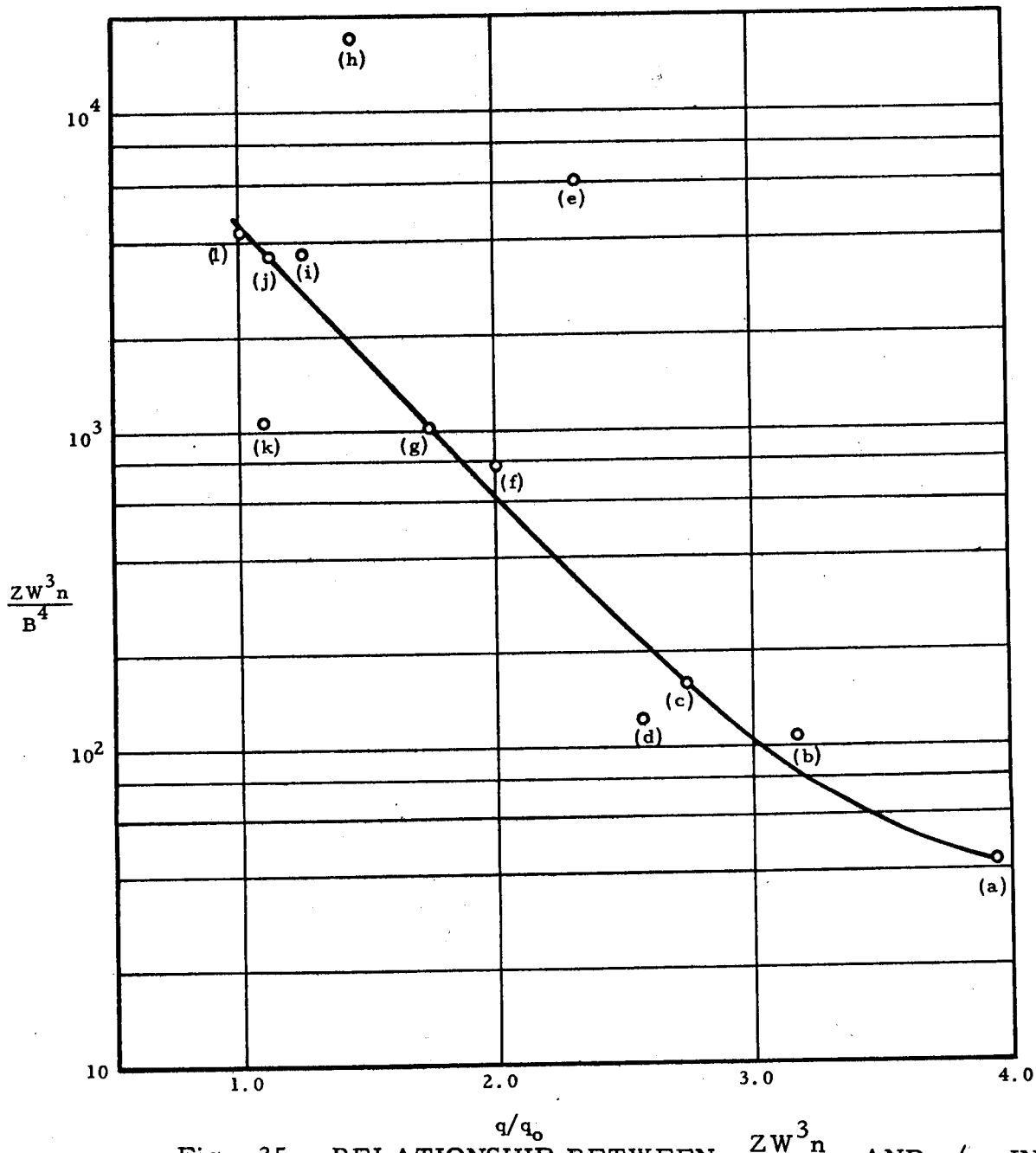

Fig. 35 RELATIONSHIP BETWEEN $\frac{ZW^3n}{B^4}$ AND q/q_o IN LOAD BEARING TESTS ON SILICA FLOUR (Fig. 34)

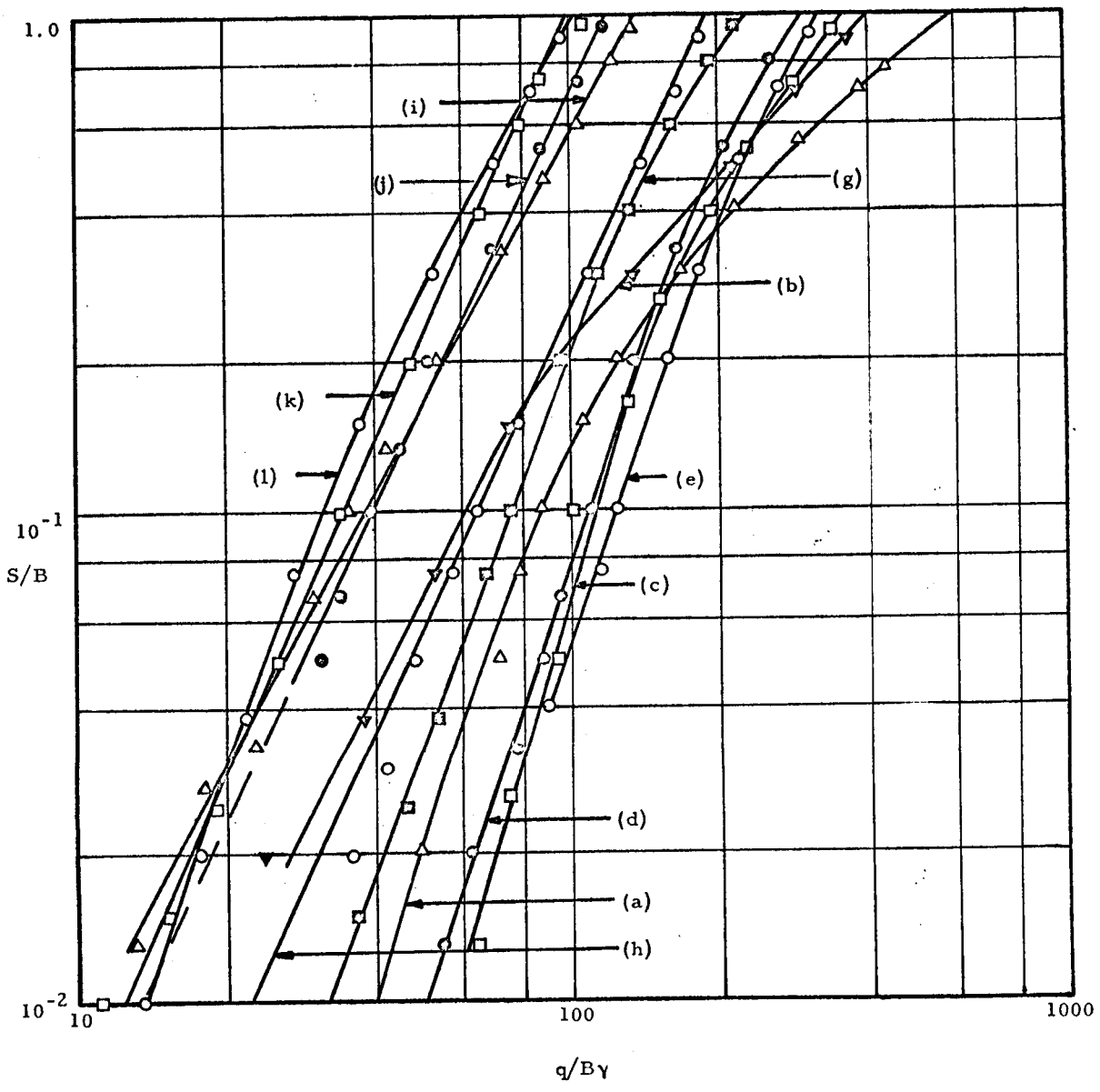

Fig. 36 S/B AS A FUNCTION OF q/Bγ FOR VARIOUS CONTAINER SIZES (Fig. 34)

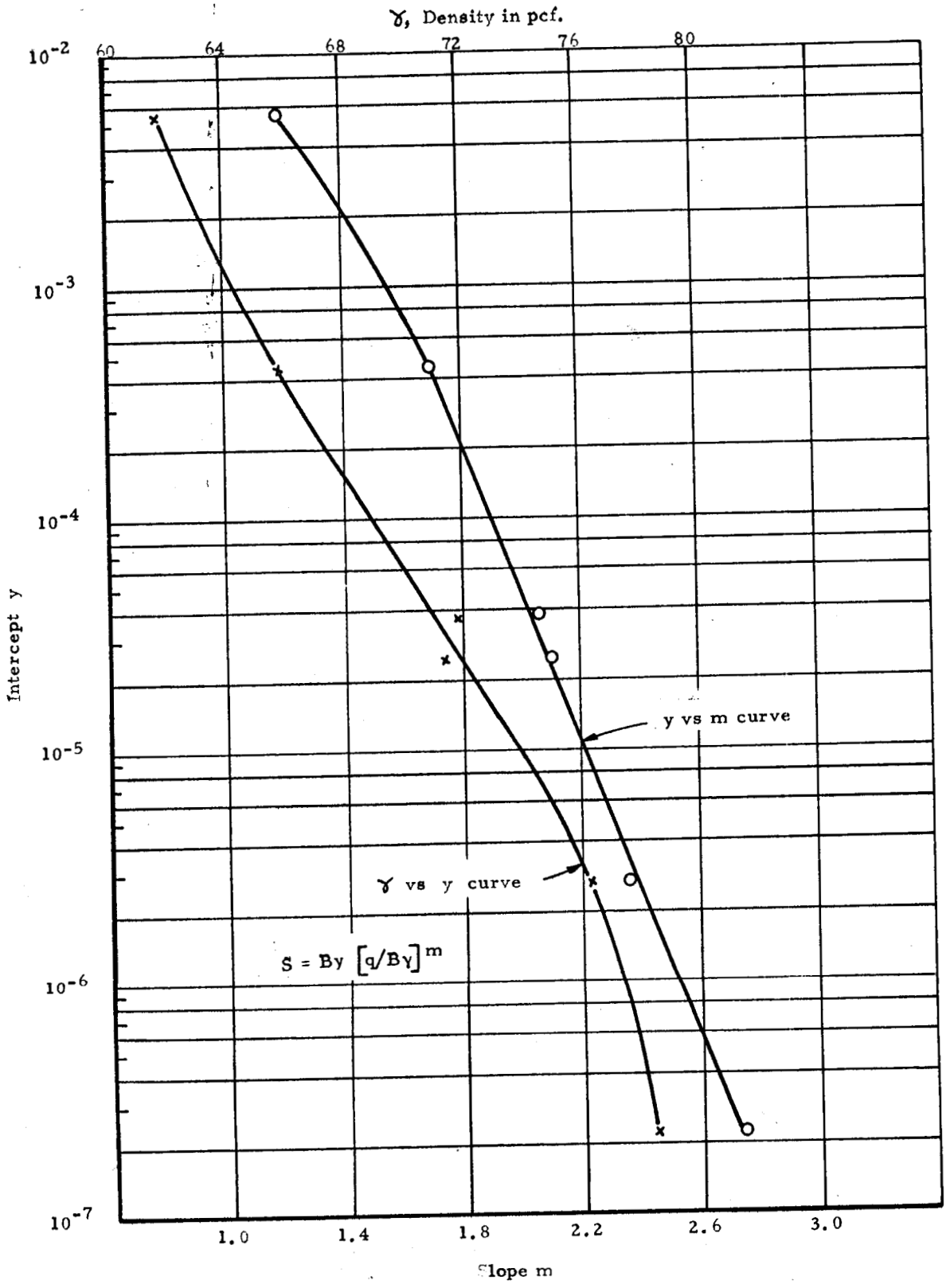

Fig. 37 SLOPE AND INTERCEPT PARAMETERS AS A FUNCTION OF DENSITY

B. The values of y and m are substituted into Equation (b) and S calculated therefrom.

In extending this method to account for vacuum effects, use is made of Figure 38 which shows the relationship between S/B and q(Atm)/B γ Vac. in tests having a constant density where Atm. = 760 mm Hg. and Vac. = absolute environmental pressure in mm Hg. The intercept is designated α and the slope remains as m. As can be seen from this, m remains constant. For γ = 70.6 pcf., the settlement equation may then be written as follows:

$$S = B\alpha\left[\frac{q\ \text{Atm.}}{B\gamma\ \text{Vac.}}\right]^{1.65}$$

where

γ = 70.6 pcf. = 0.042 pci.

Since γ is constant, the relationship between absolute pressure and α can be obtained as shown in Figure 39, and S can be computed at least for the range of absolute pressure considered.

To determine the variation of m and α with density, experiments were performed at various densities and at approximately the same vacuum level. Due to limitations on time, only two experiments were performed, both of which used silica flour. The vacuum chamber which was used allowed only a relatively small container (12in. x 12in. x 14in. deep). Thus, it may be expected that container size effects are present but not in amounts to seriously affect the results. The results of these two experiments are shown in non-dimensional form in Figure 40 (curves a and b) along with the results of one experiment performed in the internally sponsored study (curve c). The values of m and α obtained therefrom are tabulated in Table 1.

Table 1

VALUES OF m AND α DETERMINED FROM FIGURE 40

Density (lbs/ft^3)	Vacuum Torr.	m	α
54.5	2×10^{-6}	1.77	2.1×10^{-18}
63.5	4×10^{-6}	1.64	5.6×10^{-18}
70.6	1.6×10^{-6}	1.65	8.0×10^{-19}

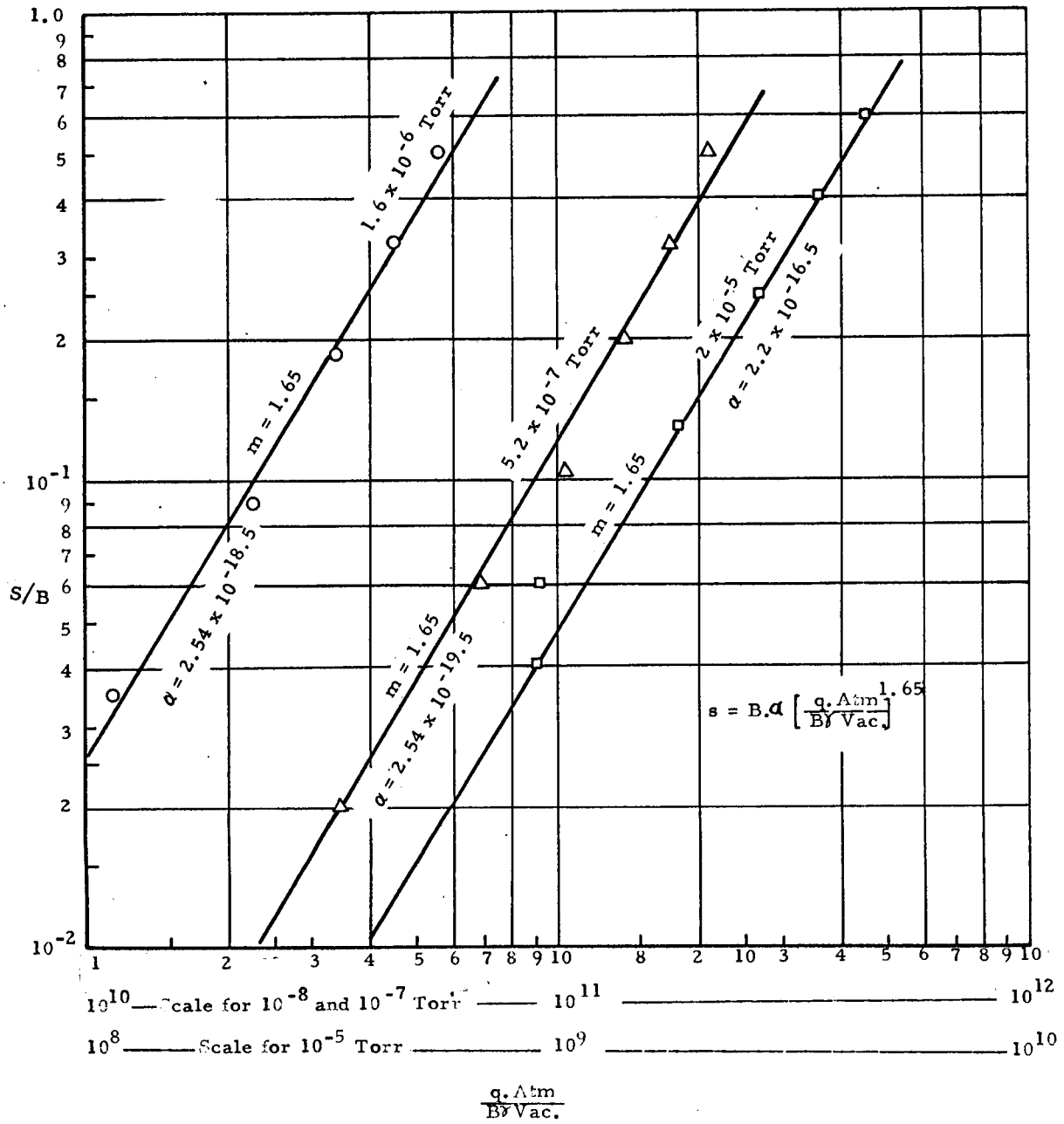

Fig. 38 S/B AS A FUNCTION OF $\frac{q\ Atm.}{B\sqrt{\ } Vac.}$ FOR $\sqrt{} = 70.6$ PCF

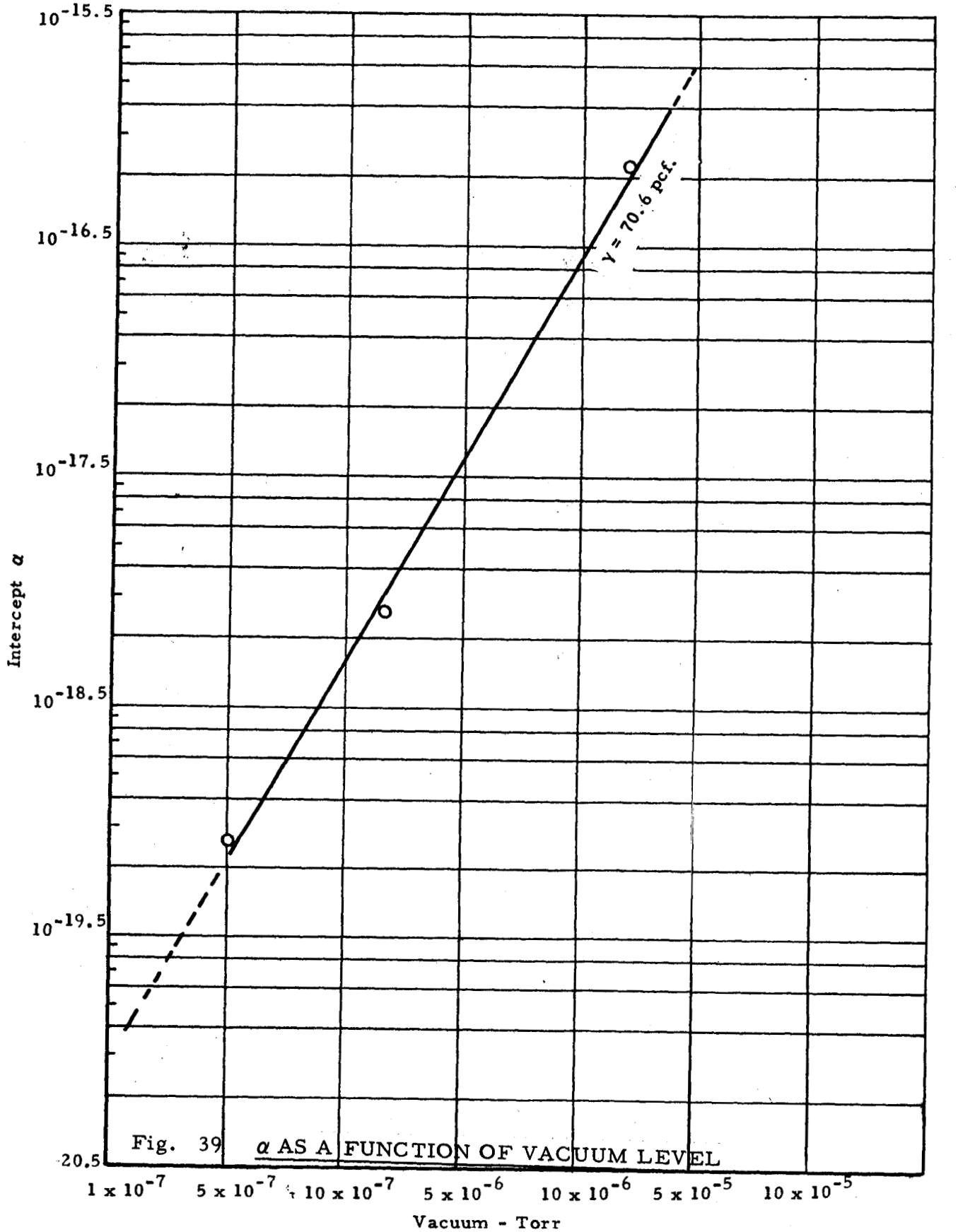

Fig. 39 α AS A FUNCTION OF VACUUM LEVEL

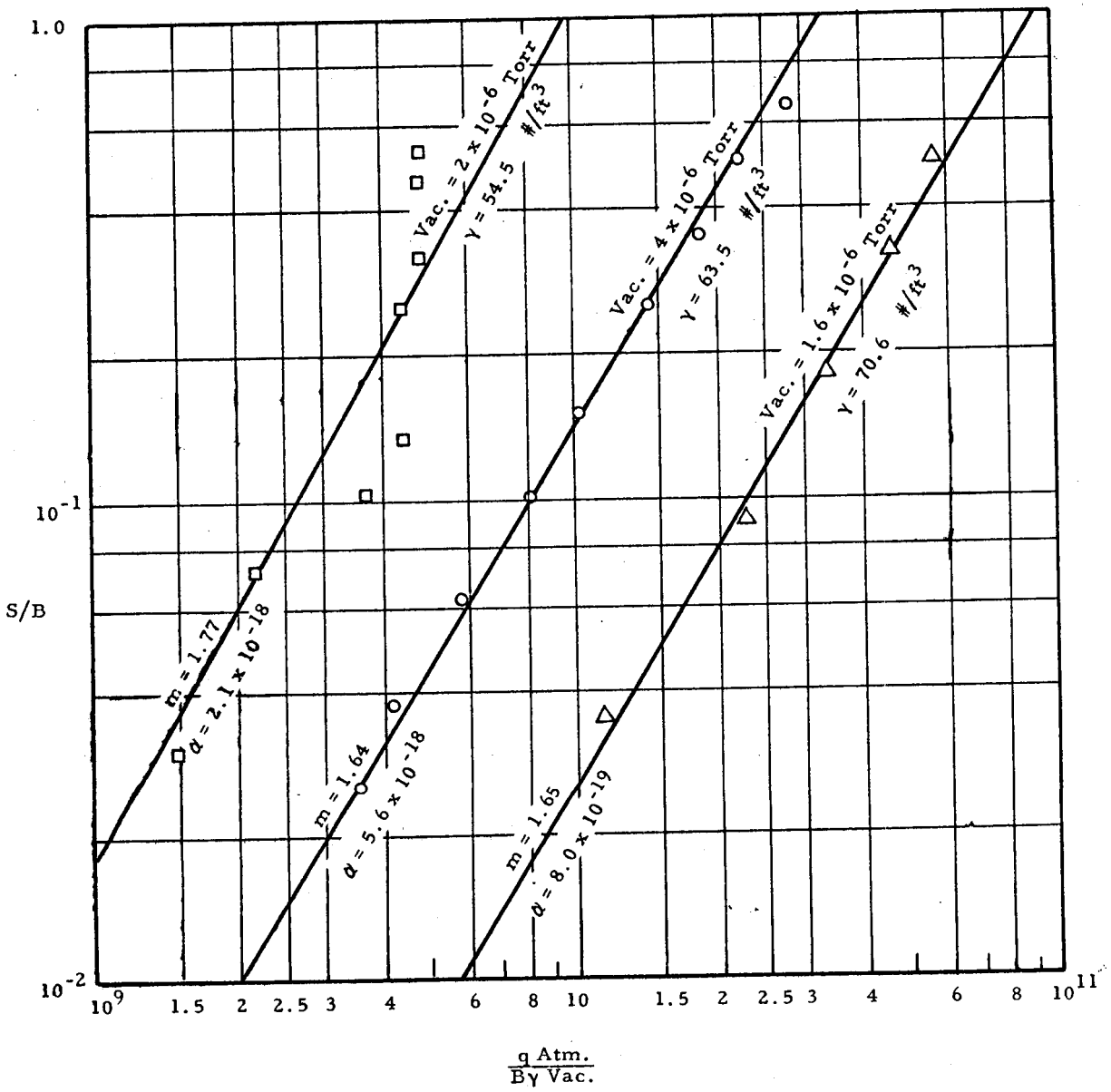

Fig. 40 S/B AS A FUNCTION OF $\frac{q\ \text{Atm.}}{B\gamma\ \text{Vac.}}$ FOR VAC. ≈ 2 x 10^{-6} TORR

From Table 1 it can be seen that the relationships between γ, m and α do not appear to be similar to those shown in Figure 37. Rather there appears to be a maximum value of α and a minimum value of m between densities of 63.5 and 70.6.#ft.^{3}.

This may be due in part to the fact that the experiment at 70.6 #/ft.^{3} was performed in a container of a different size than the other two. To draw any definite conclusions, however, more data is needed. Experiments should be performed for a greater number of densities and at a number of vacuum levels.

It is hoped that with the elimination of container size restrictions and limitations, a general theory may be arrived at, which would allow one to predict settlement for any load, size of loaded area and environmental pressure and temperature within prescribed bounds.

IX. IRREVERSIBLE EFFECTS OF VACUUM

It has been seen that the cohesion between soil particles and adhesion between soil and other materials may increase substantially in a vacuum environment, indicating the development of interparticle forces. If the development of these forces is due to the closer proximity of the soil grains upon removal of adsorbed gas layers it is possible that upon re-exposure to the atmosphere, pressures will not be sufficient to cause greater separation between the particles, i.e., the interparticle forces developed under vacuum will be great enough to hold the particles in close proximity and thereby prevent or at least retard the formation of the original adsorbed gas layers. If this were true, or in the extreme case if cold welding between the particles were to occur, then the effects of the vacuum would be, at least in part, irreversible.

In order to explore this further, a number of experiments were performed in atmosphere using soil that had been stored under high vacuum for a period of time. In one experiment silica flour was placed in a conventional direct shear apparatus that had been fabricated of stainless steel and the unit was then placed in a 400 l./sec.ion pumped system for 238 hrs. The drawdown curve (pump pressure v. time) is shown in Fig. 41. The sample was then removed and subjected to shear. The porosity of the soil was .595 and the applied normal stress was 0.51 psi. The shear stress at failure was 1.87 psi which is substantially greater than that corresponding to the same normal stress in the previous tests under atmospheric or vacuum conditions (Fig. 28). This large shear stress could be attributed to friction in the shear apparatus and, therefore, does not definitely indicate the development of irreversible interparticle forces.

Two other samples, one of olivine and one of silica flour were stored in a 140 l./sec.ion pumped system at high vacuum levels for two periods of 162 and 172 hrs. respectively. The drawdown curve for this experiment is shown in Fig. 42. After the samples were removed from the vacuum chamber, penetration tests were performed in which the penetration caused by incremental loads on a penetrometer having an area of .292 $in.^2$ was measured. The penetration as a function of the applied load is shown in Fig. 43. It can be seen from this figure that for the silica flour the penetration was greater

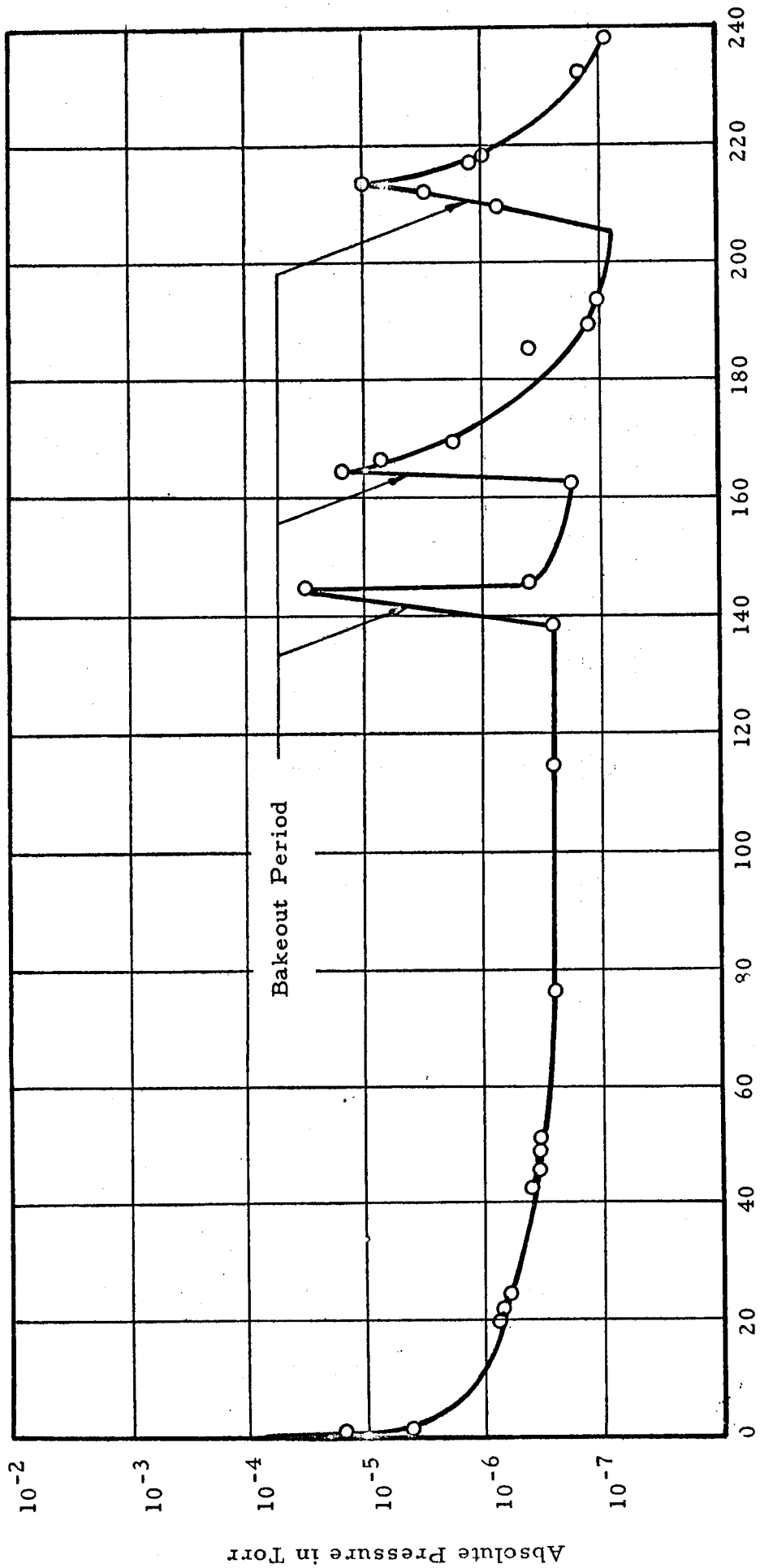

Fig. 41 DRAWDOWN CURVE FOR DIRECT SHEAR SAMPLE TO MEASURE IRREVERSIBLE INTERPARTICLE FORCES

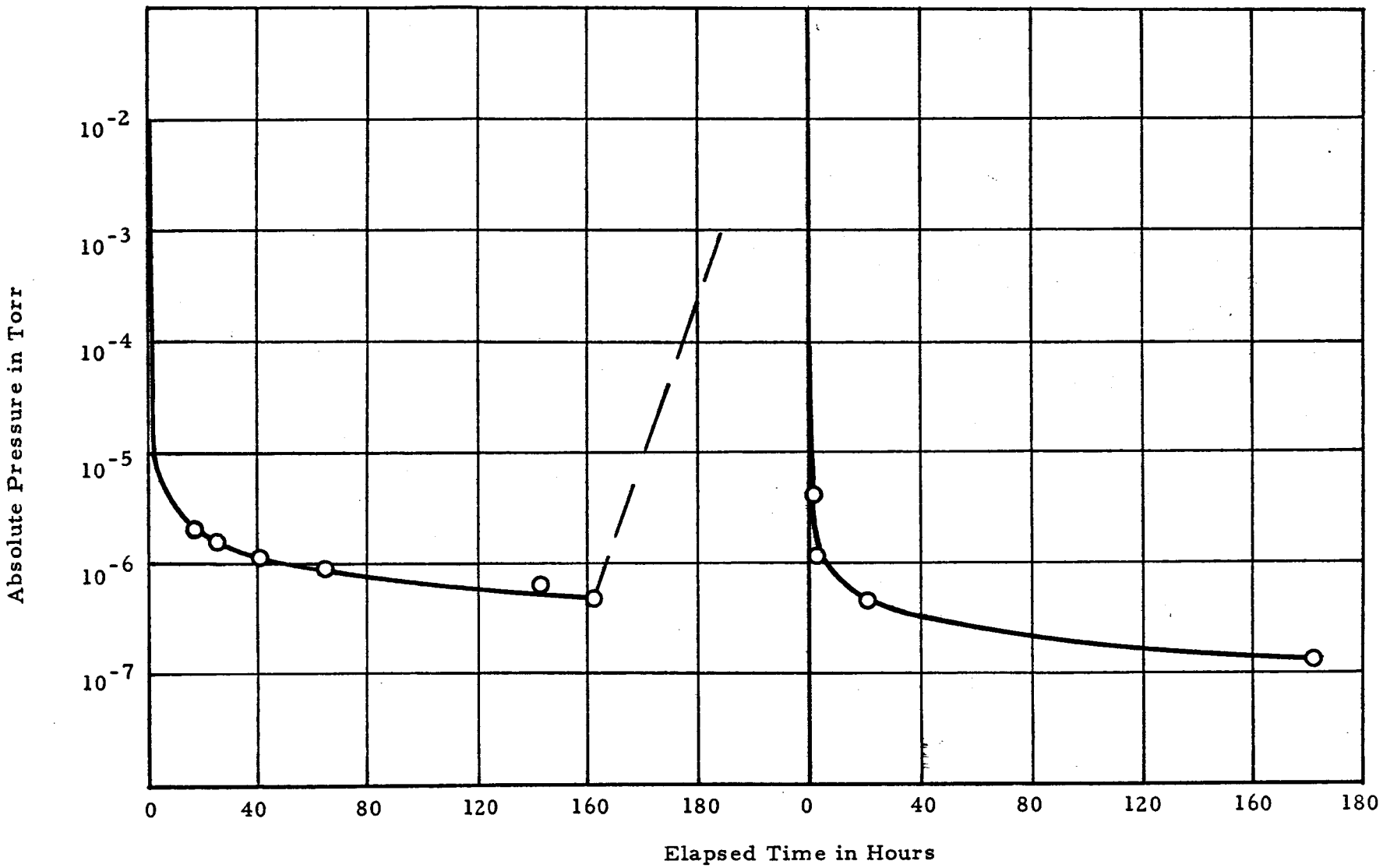

Fig. 42 DRAWDOWN CURVE FOR PENETRATION SAMPLES TO MEASURE IRREVERSIBLE INTERPARTICLE FORCES

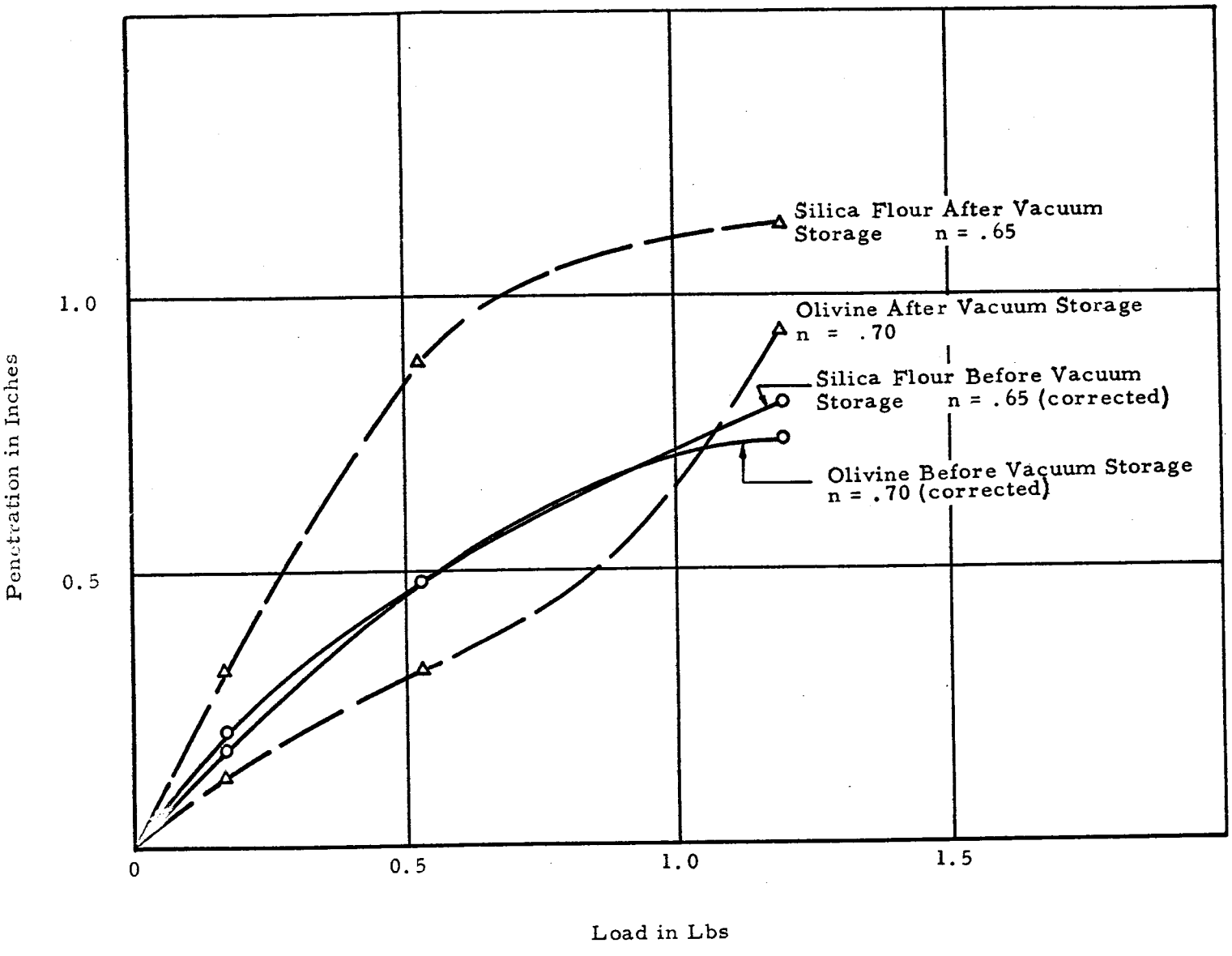

Fig. 43 PENETRATION AS A FUNCTION OF LOAD BEFORE AND AFTER STORAGE IN VACUUM

after exposure to the vacuum, but for the olivine the reverse was true. These results are not consistent with those obtained previously through direct shear tests. The differences in penetration may be due at least in part to experimental error and are not entirely indicative of irreversible effects.

Further studies would be needed to make any definite conclusions in this regard but it may be said that the irreversible effects of vacuum on soil which has been exposed to vacuum levels in the 10^{-7} torr range for the time periods shown in Fig. 42 are not appreciable. It is quite possible, however, that storage of soil for longer periods of time under lower pressure levels (3 or 4 weeks at 10^{-9} torr or lower) would result in the development of interparticle forces which would not disappear upon re-exposure to the atmosphere. Further studies of this nature would aid in the understanding of the previously observed increase in shear strength under vacuum.

X. DISCUSSION OF RESULTS

A. Interparticle Forces

It has been pointed out that the porosity attained by the silica flour samples increased when deposited under ultra high vacuum. It was also pointed out that the resistance to shear displacement as well as the apparent cohesion increased under vacuum. All of these observations indicate the development of attractive interparticle forces on the surfaces of the particles due to vacuum. However, it was noticed that the apparent cohesion of the olivine had a tendency to decrease under ultra high vacuum levels and that the vacuum had little, if any, effect on its resistance to shear displacement. This would indicate either a decrease in attractive interparticle forces or the development of repulsive forces under vacuum. As was also noted previously, the finer grained sample of olivine attained a higher porosity under high vacuum levels (10^{-6} torr and above) than it did under relatively low vacuums (10^{-2} torr), thus indicating an increase in interparticle forces and the development of a flocculent grain structure. It is, therefore, evident that vacuum (above a certain level) causes an increase in interparticle forces in both materials. It also appears that these forces may be either attractive or repulsive.

In a clay-water or colloidal soil system, it is known that both attractive and repulsive forces exist on the particles. The total resultant of these forces may be either attractive or repulsive as shown in Fig. 44 and, as can be seen, will depend greatly on the distance between the particles. Whether condition I or II exists depends upon the electrolyte concentration in the pore water (36).

Although Fig. 44 refers to a clay-water system and is not directly applicable to granular soils, conditions similar to those illustrated could very well have existed in both the silica flour and the olivine. The gravitational forces on the particles in coarse grained soils are quite large relative to those in the silica and olivine samples. Hence, interparticle forces which might have no effect on coarse grained soil could be sufficient to influence the behavior of these fine grained materials. In addition, the specific surface area of silt and clay sized soils is considerably greater than it is for coarse grained soils and, consequently the activity between the soil grains is also greater.

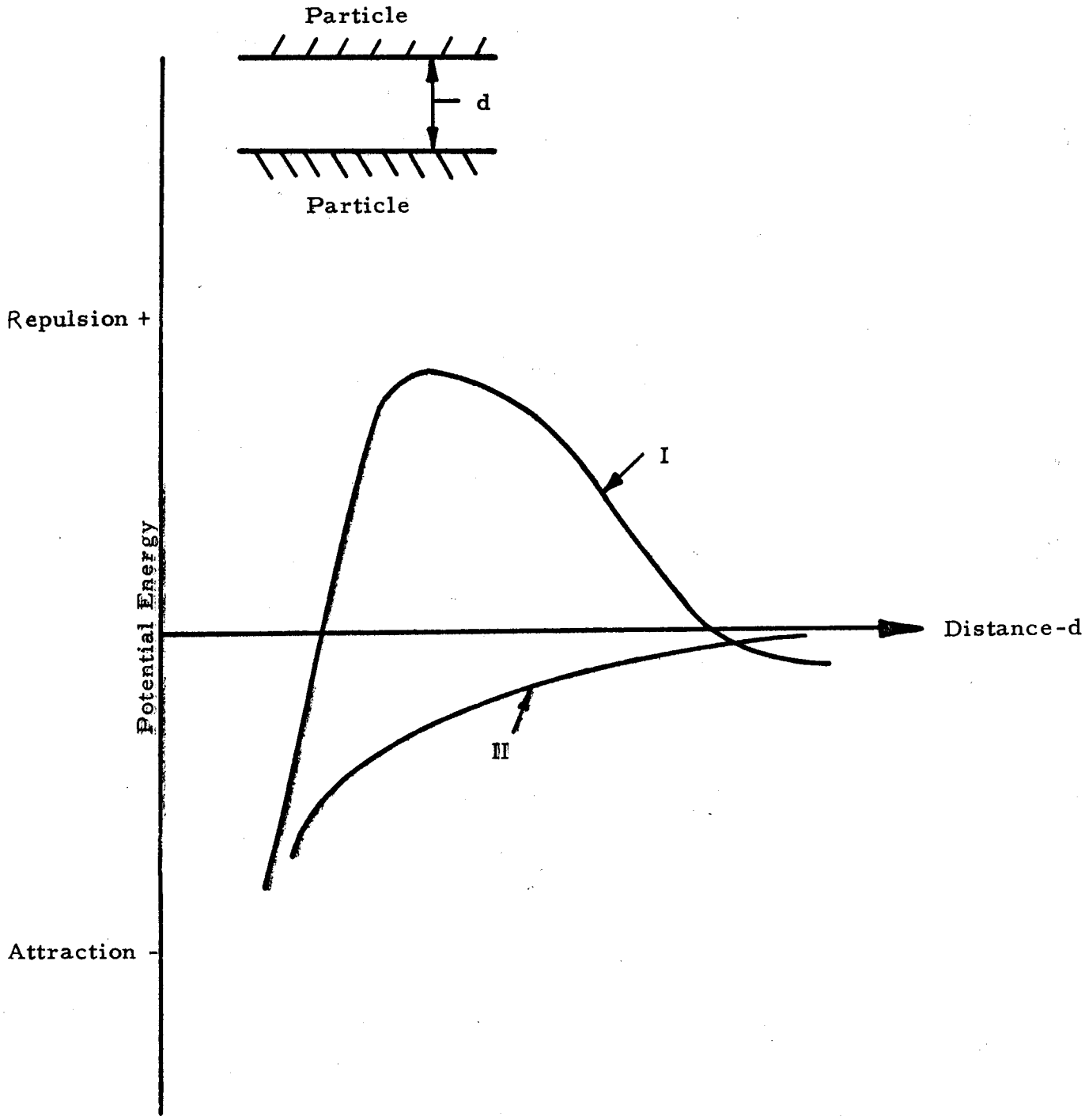

Fig. 44 ENERGY CURVES FOR IDEALIZED COLLOID MODEL (36)

It is also possible that broken bonds in the molecular structure of the crystals could result from the comminution of the rock giving rise to attractive forces. These broken bonds, however, would have a tendency to neutralize themselves and, hence, would not be expected to have significant effects in the soil types used in this investigation.

The surface forces that would be expected to have existed on the soil grains would then be van der Waals forces, which are attractive in nature, and electrostatic forces, which are repulsive. Under atmospheric conditions, adsorbed gas layers on the particles provided a separation between particles of sufficient magnitude to cause the surface forces to be small relative to the gravitational forces. The relatively high porosities of the soil deposited in the atmosphere may be due to bonds created by surface tensions in hygroscopic moisture. Only relatively low vacuums are required to remove the major portion of this moisture and reduce these bonds. Higher vacuum levels begin to remove adsorbed gas layers permitting closer proximity of the soil grains. This causes the surface forces to increase sufficiently to produce particle clustering, and accounts for the observed increasing porosity with increasing vacuum and the increased cohesion under vacuum in the silica flour.

The decrease of cohesion in the olivine, however, may not be accounted for so easily. It was observed during the performance of the experiments that the olivine exhibited considerably different outgassing characteristics than did the silica flour. The length of the required drawdown period to achieve comparable vacuum levels was much greater for the olivine than for the silica. Thus, there appeared to be a considerable difference in the amount of adsorbed water vapor on the olivine particles. The difference in the properties of the two soils under vacuum may then be accounted for in a manner analagous to the varying electrolyte content in the pore fluid reflected in curves I and II in Fig. 44. It is possible that the interparticle forces which were developed in the olivine could have been similar to those shown in curve I (Fig. 44) and could have been attractive or repulsive depending on the amount of adsorbed gas removed, whereas those developed in the silica were always attractive as shown by Curve II. This would account for a decrease in apparent cohesion at pressure levels low enough to remove a sufficient portion of the adsorbed gas

so that the distances between the particles were such that the forces were repulsive. More complete outgassing of the soil would remove an even greater amount of adsorbed gases and the forces developed would be attractive.

In the investigations on porosity the soil sample was undoubtedly outgassed more completely than in the direct shear tests. In the latter case the soil was confined and consequently, the rate at which gas was removed from the soil pores was undoubtedly less. In addition, a certain amount of adsorbed gas was removed in the porosity experiments as the soil was being deposited in vacuum. Although the amount of outgassing during the time in which the particles fell was relatively small, collisions between the particles produced some mechanical removal of adsorbed gas. Thus, the soil after deposition probably had a lower true environmental pressure than did the soil in the direct shear tests corresponding to the same chamber pressure. This would account for the observed clustering of the deposited olivine grains (which indicated the development of attractive forces) and the decrease in apparent cohesion in the shear tests (which indicated the development of repulsive forces) at comparable vacuum levels in the chamber.

Another contributing factor may be the existence of water films on the olivine under atmospheric conditions, which were sufficient to cause measureable values of the apparent cohesion. The removal of these water films under vacuum would then result in a decrease in cohesion if relatively large interparticle forces were not developed. This explanation however, would not account for the fact that vacuum levels of 10^{-6} torr, which would presumably remove this water, did not decrease the cohesion appreciably.

In the silica flour experiments then, the observed clustering of the particles, the relatively high porosity attained by deposition under vacuum, the increase in resistance to shear displacement, and the increase in the apparent cohesion make it quite evident that the interparticle forces which were developed were always attractive. The quite different behavior of the olivine indicates rather definitely that the mineralogical composition of the soil has a pronounced effect on the properties of the material under vacuum.

B. Intergranular Friction

The observed increase in the angle of internal friction was to be expected.

This may also be attributed to the removal of adsorbed gas layers which act as a lubricant. However, the relatively small increase in internal friction corresponding to a rather substantial increase in apparent cohesion indicates that the amount of gas that it is necessary to remove in a very fine grained soil to develop appreciable interparticle forces is relatively small.

C. Temperature Effects

The increase in shear strength with temperature as noted previously might also have been predicted. At elevated temperatures more adsorbed gas is removed due to the activity of the gas molecules. Upon cooling to room temperature, some gas will be condensed on the particles and, hence, the shear strength would be expected to be greater at higher temperatures. However, it should be noted that data at high temperature was obtained in only one experiment which is not sufficient verification of the theory.

D. Bearing Capacity

The results of the bearing capacity experiments are also in accord with the previous discussion of interparticle forces. As was noted by Roddy, et. al. (23) the dynamic bearing capacity of soil may increase or decrease under low vacuum levels depending on the void ratio. However, at ultra high vacuum levels an accompanying small increase in the apparent cohesion will cause a large increase in the bearing capacity. The same is true to a lesser degree for an increase in the angle of internal friction.

XI. CONCLUSIONS

Considerably more data than was obtained in the present investigation would be necessary to gain a thorough understanding of the mechanics of soil behavior under lunar environmental conditions. Nevertheless, some definite conclusions can be drawn on the basis of the data obtained regarding the effect of vacuum on the behavior of soil. These may be summarized as follows:

1) In recording the level of vacuum to which a soil specimen was subjected it was observed that the vacuum which existed in the soil pores was substantially less than that measured in the enclosing vacuum chamber.

2) The porosity attained by soil when deposited under relatively low vacuum levels (pressures from 1 to 1000μ Hg) was always less than when deposited in atmosphere.

3) Coarser grained soil of the same composition always attained lower porosities when deposited in atmosphere than did finer grained soils.

4) Due to the absence of frictional air resistance, the rebound of the soil grains during deposition in vacuum was greater than in atmosphere resulting in a decrease in the angle of repose of the soil in vacuum.

5) The removal of adsorbed gas layers on the particles under high and ultra-high vacuum levels produced a substantial change in interparticle forces. These changes were attractive or repulsive depending on the mineralogical composition of the soil and the environmental pressure. Although not conclusively demonstrated by experiment it is believed that at sufficiently high vacuum levels the interparticle forces would be attractive regardless of the soil composition. It is believed that these forces accounted for the following soil behavior in the manner described:

(a) As a result of clustering of the particles and the ability of the soil grains to achieve and maintain a flocculent grain structure, the porosity attained by soil deposited under ultra-high vacuums was greater than that attained at low vacuum levels and in some instances was as high or higher than that attained in atmosphere.

(b) The apparent cohesion of the soil may increase or decrease due to an

increase in vacuum, depending upon whether the interparticle forces are attractive or repulsive. The cohesion of the silica flour increased but in the case of olivine it appeared to decrease.

(c) Adhesion between the soil and metals increased under vacuum allowing soil deposits to accumulate on the vertical walls of the vacuum chamber and apparatus.

6) Because of the removal of adsorbed gas from the particle surfaces in a vacuum the accompanying reduction in lubrication produced some increase in the angle of internal friction of the soil. The internal friction, however, was affected to a lesser degree than was the apparent cohesion.

7) A decrease in the environmental pressure caused an increase in the resistance of the silica flour to shear displacement but it could not be said, on the basis of the limited data obtained, that there was any definite increase for olivine.

8) The increase in cohesion together with a lesser increase in internal friction resulted in a substantially greater static bearing capacity of both soils in vacuum than in atmosphere.

9) The removal of pore air pressures under both low and high vacuum levels had the effects of causing all stresses induced in the soil to appear immediately as effective stresses.

10) The absolute size of the soil container as well as the ratio of size of bearing plate to size of container used in bearing capacity experiments can have a pronounced effect on the penetration resistance of the soil.

11) An increase in the environmental temperature at very-high vacuum levels appeared to cause a marked increase in the shear strength of the soil.

12) The interparticle forces developed at very-high vacuum levels for the relatively short periods at which the soil was kept under vacuum disappeared upon exposure of the soil to the atmosphere.

Conclusions 11 and 12 listed above are based on very few tests. They should, therefore, be considered merely as indications rather than definite conclusions. An extension of the program covered by this report has already

been initiated and as part of this program it is planned to explore much more fully these and some of the other effects at which insufficient data was obtained.

BIBLIOGRAPHY

1. Barabashov, N. P., Bronshten, V.A., et.al., "The Moon", Literatury House of Physics-Mathematical Literature, Moscow, 1960.
2. Urey, H. C., "The Origin and Nature of the Moon", Endeavor, p. 87, April 1960.
3. Moore, P., "Some Lunar Crater Problems", Sky and Telescope, p. 201, March 1956.
4. Gilbert, G. K., Bull. Phil. Soc., Vol. 12, p. 241, Washington, 1893.
5. Gold, T., Mon. Not. R. Astr. Soc., Vol. 115, p. 585, 1955.
6. Shoemaker, Eugene M., "Exploration of the Moon's Surface", American Scientist, Vol. 50, No. 1, p. 99, March 1962.
7. Kuiper, G. P., "The Surface of the Moon", Chapt. 15 in Space Science, ed. Le Galley, D. P., John Wiley and Sons, New York, 1963.
8. Troitskiy, V. S., "Nature and Physical State of the Upper Stratum of the Moon", Astronomicheskiy Zhurnal, Vol. 39, No. 1, pp. 73-78, April 5, 1962.
9. Hapke, B. W., "Photometric and Other Laboratory Studies Relating to the Lunar Surface", Lunar Surface Materials Conference, Boston, Mass., May, 1963.
10. Salisbury, J. W., Glaser, P.E., Stein, B.A., and Vonnegut, B., "Adhesive Behavior of Silicate Powders in Ultra High Vacuum", A.G.U. Meeting, Washington, D. C., April 1963.
11. Fielder, G. J., Brit. Astr. Assn., Vol. 67, p. 8, 1957.
12. Weil, N. A., "Probable Soil Conditions on the Moon and Terrestrial Planets", First International Conference on the Mechanics of Soil-Vehicle Systems, Turin, Italy, June 1961.

13. Fielder, G., "The Physical Nature of the Surface of the Moon", J. Brit. Interplan. Soc., Vol. 17, p. 57, 1959-60.

14. Buettner, K.J.K., Davis, M.H., Kern, J.W., and Lamar, D.L., "Studies of the Physical Properties of the Moon and Planets", Quarterly Technical Progress Report (7), AR-15-JPL, NASA No. N62-11806, The Rand Corporation, Santa Monica, California, April 1962.

15. Muncey, R. W., "Properties of the Lunar Surface as Revealed by Thermal Radiation", Aust. J. Phys., Vol. 16, No. 1, 1963.

16. Ryan, J. A., "The Case Against Thermal Fracturing at the Lunar Surface", J. Geophys. Res., Vol. 67, No. 6, pp. 2549-2558, June 1962.

17. Grannis, P.D., "Electrostatic Erosion Mechanisms on the Moon", Journal of Geophysical Research, Vol. 64, No. 12, December 1962.

18. Salisbury, J.W., "Lunar Surface Characteristics", Automotive Eng. Congress, Soc. Auto. Eng., Detroit, Michigan, January 1963.

19. Gault, D.E., Shoemaker, E.M. and Moore, H.J., "Spray Ejected from the Lunar Surface by Meteoroid Impact", NASA TN D-1767, April 1963.

20. Opik, E. J., "Surface Properties of the Moon", Progress in the Astronautical Sciences, Vol. 1, North Holland Publishing Company, Amsterdam, 1962.

21. Opik, E. J. and Singer, S. F., "Density of the Lunar Atmosphere", Science, Vol. 133, May 1961.

22. Geer, R. L., "Impact Studies on Lunar Dust Models at Various Vacuums", Tech. Rep. No. ASD TR 61-595, Wright-Patterson A.F.B., Ohio, January 1962.

23. Roddy, D. J., Rittenhouse, J.B. and Scott, R.F., "Dynamic Penetration Studies in Crushed Rock Under Atmospheric and Vacuum Conditions", Technical Report No. 32-242, Jet Propulsion Laboratory, Pasadena, California, April 6, 1962.

24. Weide, D.L., "The Behavior of a Lunar Soil Model in Vacuum", ASTIA AD No. 290608, September 1962.

25. Halajian, J.D., "Laboratory Investigation of 'Moon-Soils' ", IAS National Summer Meeting, IAS Paper No. 62-123, Los Angeles, California, 1962.

26. Rowe, R.D. and Selig, E. T., "Penetration Studies of Simulated Lunar Dust", Seventh Symposium on Ballistic Missile and Aerospace Tech., August 1962.

27. Sjaastad, G.D., "An Experimental Study in Lunar Soil Mechanics", Lunar Surface Materials Conference, Boston, Massachusetts, May 1963.

28. Jaffe, L. D. and Rittenhouse, J.B., "Behavior of Materials in Space Environments", Tech. Report No. 32-150, Jet Propulsion Laboratories.

29. Stein, B.A. and Rostoker, D., "Investigation of Soil Behavior Under High Vacuum", Lunar Surface Materials Conference, Boston, Massachusetts, May 1963.

30. Kopal, Z., "Internal Structure of the Moon", Lunar Missions Meeting, American Rocket Society, Cleveland, Ohio, July 1962.

31. Ramdohr, P., "The Opaque Minerals in Stony Meteorites", J. Geophysical Research, Vol. 68, No. 7, April 1963.

32. Hapke, Bruce W., "Experiments Relating to the Lunar Surface", 2nd Preliminary Report, Center for Radiophysics and Space Research, Cornell University, Ithaca, New York, July 1962.

33. Urey, H.C., "Composition of the Moon's Surface", Z. Physik, Chem. Neue Folge, Bd. 16, Simon-Gedenkheft, S. 346-347, 1958.

34. MacDonald, G.J.F., "The Moon and its Interior", Astronautics, July 1962.

35. Roscoe, K.H., "An Apparatus for the Application of Simple Shear to Soil Samples", Proc. 3rd International Conference on Soil Mechanics, 1:186-191, 1953.

36. Trollope, D.H. and Chan, C.K., "Soil Structure and the Step-Strain Phenomenon", Journal of the Soil Mechanics and Foundations Division, Proceedings ASCE, Vol. 2, April 1960.

37. Firsoff, V.A., "Dissipation of Planetary Atmospheres", Science, 130, 1337, 1959.

38. Martin, R. T., "Water Vapor Adsorption Behavior of Kaolinite After High Vacuum Storage", Lunar Surface Materials Conference, Boston, Massachusetts, May 1963.

39. Yong, R., "A Study of Settlement Characteristics of Model Footings on Silt", Proceedings of the First Pan American Conference of Soil Mechanics and Foundation Engineering, September 1959.

40. Broner, M.A. and Lander, G.A., "How Bad is the Moon Environment?", Space Aeronautics, p. 92, April, 1962.

41. Brown, H., "The Density and Mass Distribution of Meteoritic Bodies in the Neighborhood of the Earth's Orbit", Proceedings, First International Space Science Symposium, Nice, January 1960.

42. Buettner, K.J.K., "The Moon's First Decimeter", Memorandum RM-3263-JPL, Jet Propulsion Laboratory, September 1962.

43. Eimer, M., "Measuring Lunar Properties from a Soft-Lander", Astronautics, July 1962.

44. Halajian, J.D., "Vehicle-Soil Mechanics on the Moon", Automotive Eng. Congress, Soc. Auto. Eng., Detroit, Michigan, January 1963.

45. Head, V.P., "A Lunar Surface Model for Engineering Purposes", Lunar Missions Meeting, American Rocket Society, Cleveland, Ohio, July 1962.

46. Lawrence, L. Jr. and Lett, P.W., "Characterization of Lunar Surfaces and Concepts of Manned Lunar Roving Vehicles", Automotive Eng. Congress, Soc. Auto. Eng., Detroit, Michigan, January 1963.

47. McCartney, E.J., "Navigational Environment on the Moon", Sperry Eng. Rev., Vol. 15, No. 1, Summer, 1962.

48. Palmore, J.I., "Lunar Impact Probe", J. American Rocket Society, p. 1066, August 1961.

49. Pohn, H., Murray, B.C. and Brown, H., "New Applications of Lunar Shadow Studies", Pub. of Astr. Soc. of Pac., Vol. 74, No. 436, April 1962.

50. Ryan, J.A., "Some Predictions as to the Possible Nature and Behavior of the Lunar Soil", 1st International Conference on the Mech. of Soil-Vehicle Systems, Turin, Italy, June 1961.

51. Urey, H.C., "Origin of the Moon's Surface Features-I", Sky and Telescope, Vol. 1, p. 108, January 1956.

52. Urey, H.C., "Origin of the Moon's Surface Features-II", Sky and Telescope, p. 161, February 1956.

53. Vey, E., "Studies of Lunar Soil Mechanics", 1st, 2nd and 3rd Quarterly Reports, NASA Contract No. NASr-65(02), 1962-63.

54. Watson, K., Murray, B. and Brown, H., "On the Possible Presence of Ice on the Moon", J. Geophys. Res., Vol. 66, No. 5, p. 1598, 1961.

55. Watson, K., Murray, B.C., and Brown, H., "The Behavior of Volatiles on the Lunar Surface", J. Geophys. Res., Vol. 66, No. 9, September 1961.

56. Weil, N.A., Selig, E. T. and Vey, E., "Studies of Lunar Soil Mechanics", ARF Research Proposal No. 62-655K, February 15, 1962.

57. Weil, N. A., Discussion of Paper "Some Predictions as to the Possible Nature and Behavior of the Lunar Soil", by J.A. Ryan, First International Conference on the Mechanics of Soil-Vehicle Systems, Turin, Italy, June 1961.

APPENDIX

VACUUM FACILITIES

APPENDIX
VACUUM FACILITIES

The vacuum systems used in this study were of two types, ion pumped systems and oil diffusion pumped systems. The studies of the irreversible effects of vacuum utilized the ion pumped systems shown in Figs. A-1 and A-2 but because of the need for greater pumping speed the other experiments were performed in the oil diffusion pumped systems shown in Figs. A-3 and A-4. The experiments on the porosity at vacuum levels between 10^{-3} and 10^{-6} torr and the bearing capacity experiments were performed in the very-high vacuum system with the remainder of the experiments on porosity and the direct shear tests being performed in the ultra-high vacuum system. A more complete description is given below.

A. 140 liter/second Ion Pump System (Fig. A-1)

This system consists of a fully bakeable, all metal sealed, 12in. dia. by 12 in. high, stainless steel chamber, and a 140 liter per second ion pump. The chamber is equipped with several ports for the incorporation of feed through devices, gages, and other equipment. This system is capable of attaining a pressure of 1×10^{-10} torr.

B. 400 liter/second Ion Pump System (Fig. A-2)

An 18 in. dia. x 30 in. high fully bakeable chamber with all metal seals and several lead through ports is pumped with a 400 liter/sec. ion pump. This system is roughed down by a 5 cfm forepump through a liquid nitrogen trap. Included is a leak detector with an average sensitivity of 1×10^{-11} std. cc/sec. of air. Vacuum levels of 1×10^{-10} torr have also been reached with this system.

C. Ultra-High Vacuum Diffusion Pump System (Fig. A-3)

This system consists of a 24 in. dia. by 30 in. long polished stainless steel chamber. The access door is sealed with a refrigerated 'O' ring. The chamber is bakeable and equipped with mechanical and electrical feed throughs, and is pumped by a four inch diffusion pump with a cold cap, water baffle, and a liquid nitrogen trap. The chamber is roughed down quickly with a 100 cfm rotary piston single stage pump; an 8 cfm compound

holding pump is then used to hold the diffusion pump. Vacuum levels in the 10^{-10} torr range have been acieved in this system with small soil samples in the chamber under a modest bakeout (150° F for 48 hrs). A more intensive bakeout would undoubtedly improve this performance.

Backstreaming is minimized by a 90° elbow in the foreline in addition to the liquid nitrogen trap. Polyphenol ether diffusion pump oil is also used because of its improved backstreaming characteristics. In a separate program, the backstreaming in similar systems was investigated. The amount of oil present in the chamber at vacuum levels of 10^{-8} torr was too small to be measured.

D. Very-High Vacuum Diffusion Pump System (Fig. A-4)

A number of bell jar type chambers are available for use with this system. The chamber used in the current investigation is similar to the one shown in Fig. A-4 but with a mechanical (translational) feed through on the top and several electrical feed throughs. The system is pumped with a six inch diffusion pump through a liquid nitrogen trap. It is roughed down with a 15 cfm compound pump and held with a 5 cfm single stage pump. Vacuum levels in the 10^{-7} torr range can readily be attained.

E. Gages

The vacuum levels in the systems were monitored by Bayert-Alpert ionization gages for pressure levels below 10^{-4} torr. The gages used were the following:

(1) NRC Nottingham gage and control unit with a range of 10^{-4} to 10^{-10} torr.

(2) Varian nude gage and envelope gage with control unit in the range of 10^{-4} to 10^{-11} torr.

For pressures above 10^{-4} torr, Alphatron ionization gages and thermocouple gages were used.

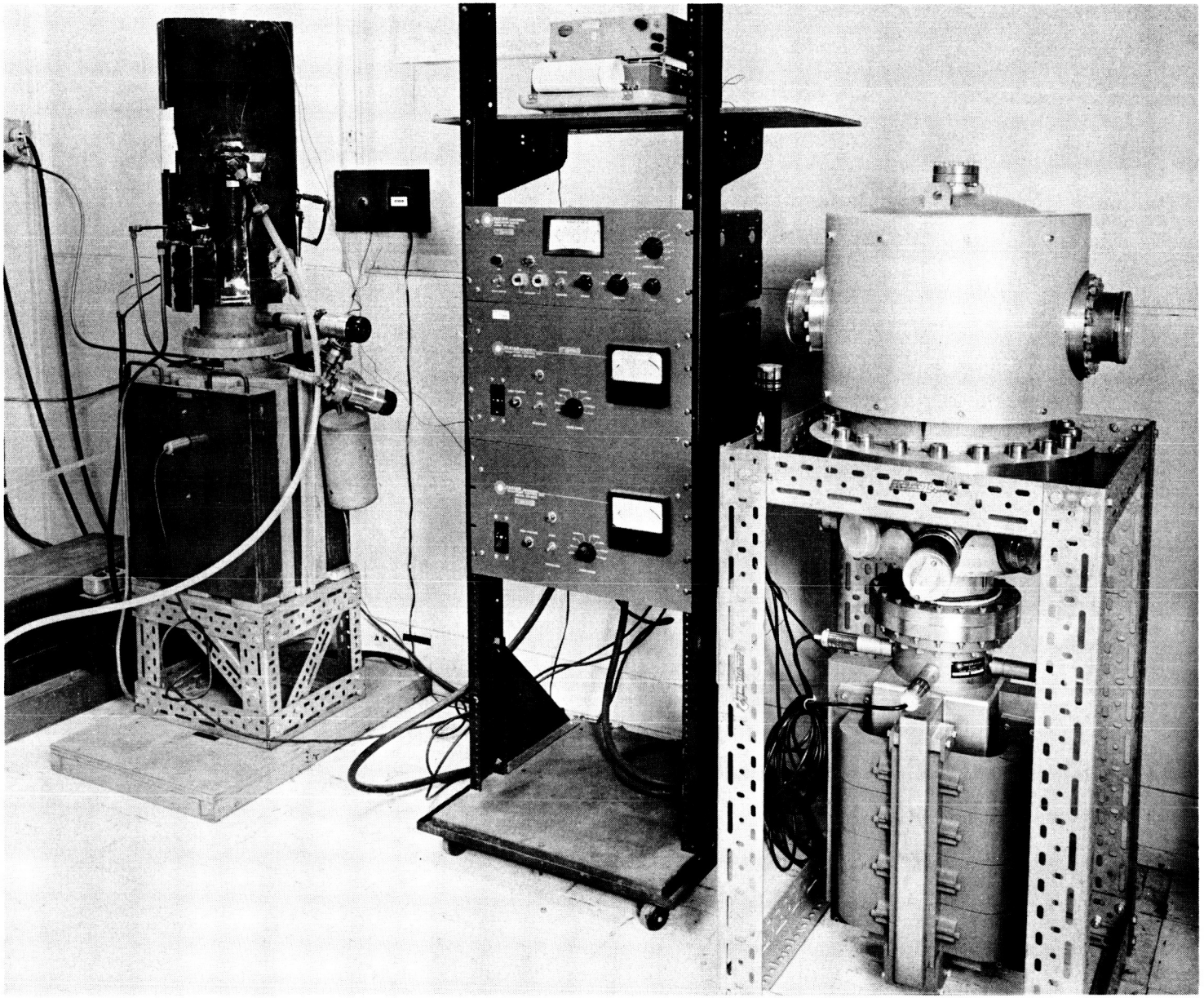

Fig. A-1 140 LITER/SEC. ION PUMP SYSTEM

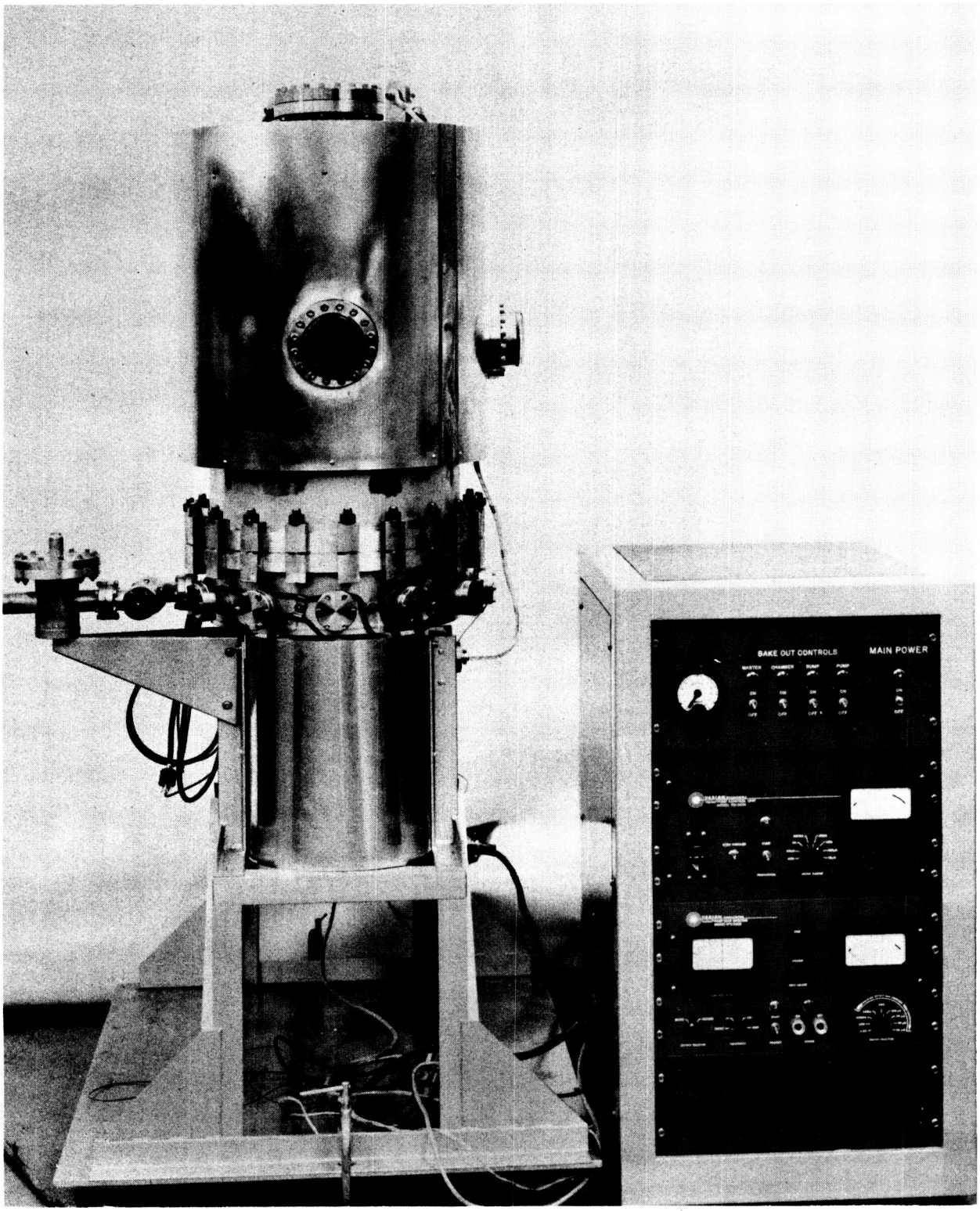

Fig. A-2 400 LITER/SEC. ION PUMP SYSTEM

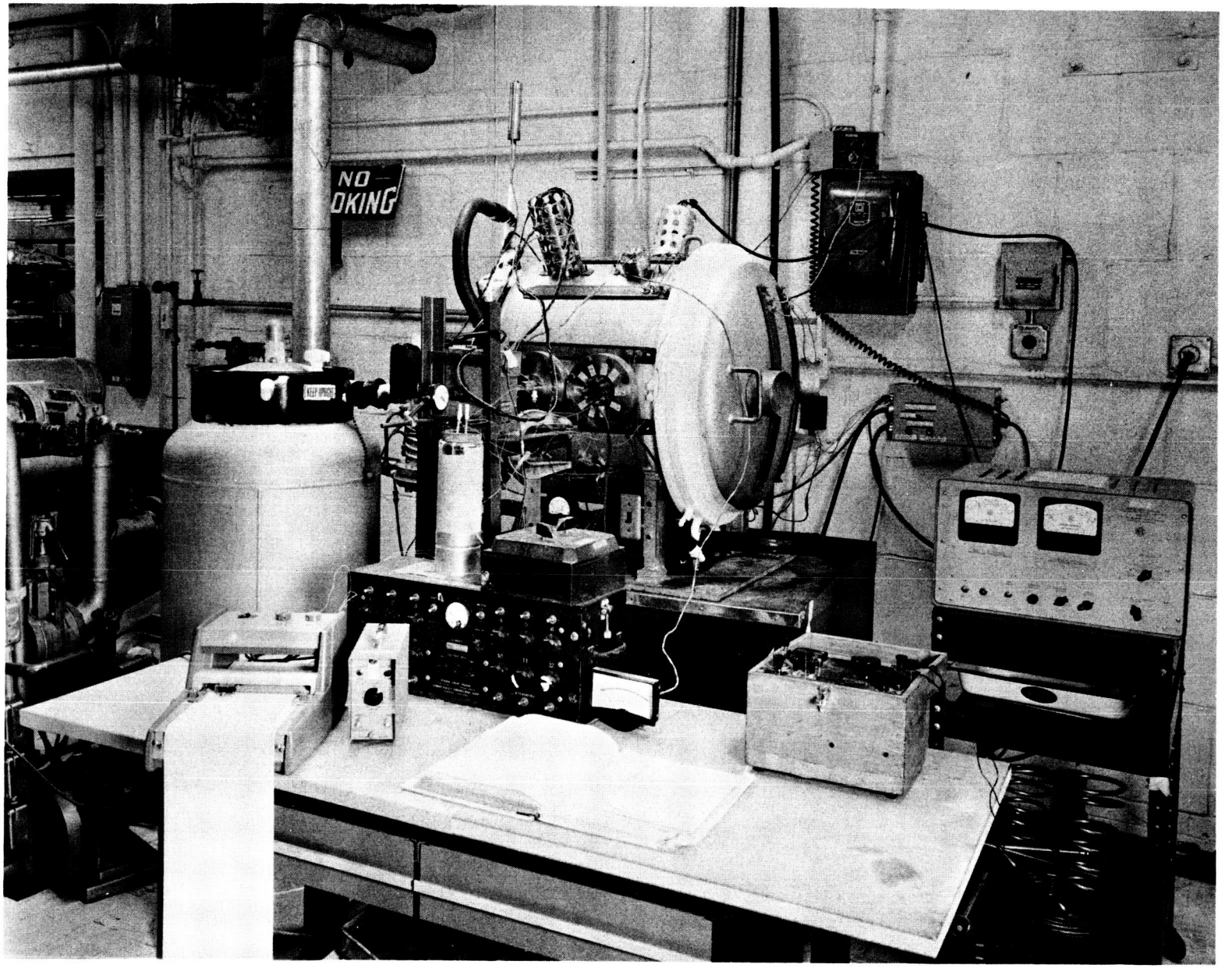

Fig. A-3 ULTRA-HIGH VACUUM DIFFUSION PUMP SYSTEM

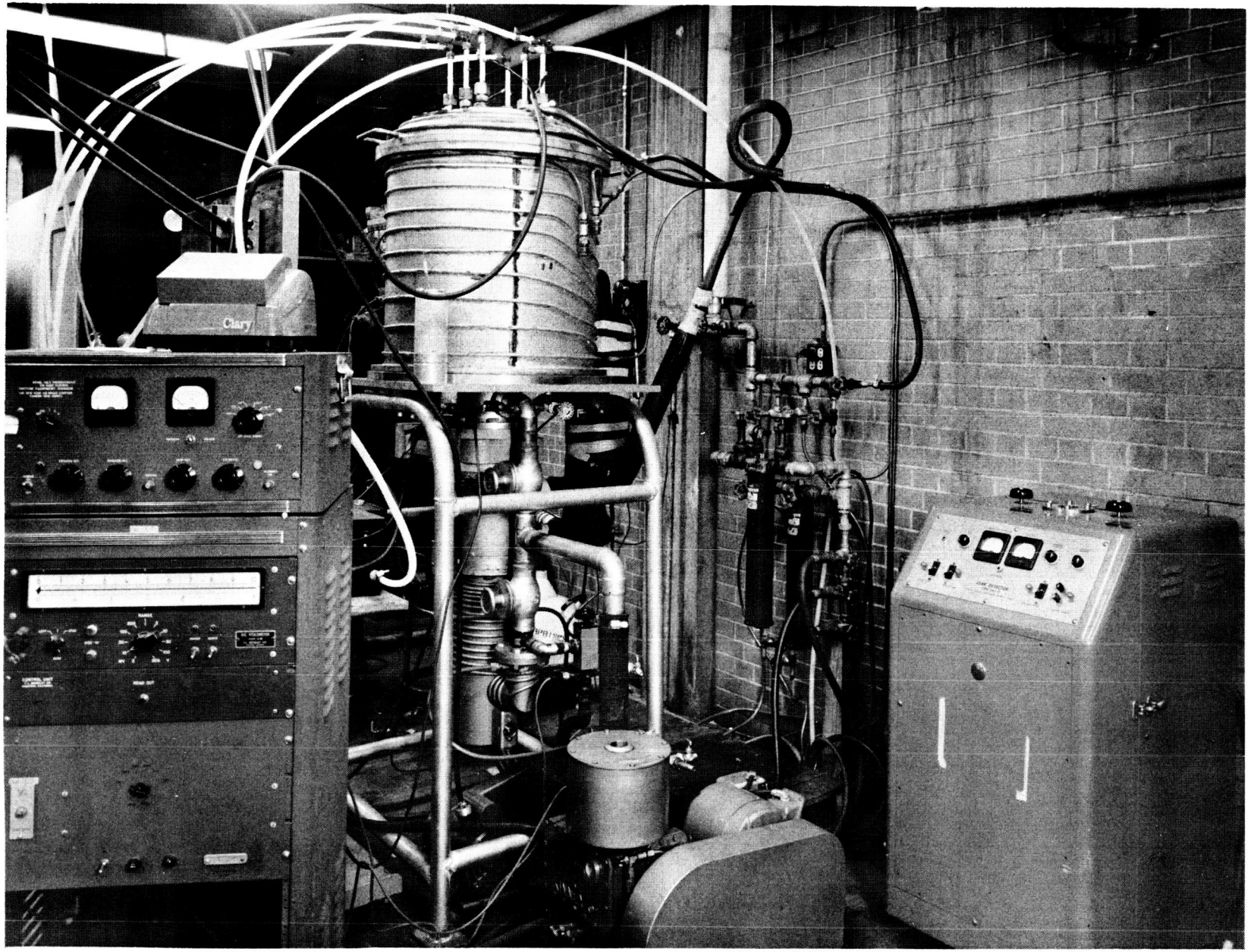

Fig. A-4 VERY-HIGH VACUUM DIFFUSION PUMP SYSTEM